Syrian Arab Republic

Ministry of Higher Education

Syrian Virtual University

ماجستير التأهيل والتخصص في المعلوماتية الحيوية BIS

Broad Neutralization Effects of Monoclonal Antibodies Targeting the Stem Helix of MERS-CoV: A Computational Study using AutoDOCK Vina, HADDOCK and PyMOL Analysis

A thesis submitted in partial fulfillment of the requirements for the degree of Master in Bioinformatics

By Ph. Shaza Al Frijat

shaza_179464

Supervisor

Prof. Dr. Bassem Assfour

2023-2024

Dedication and Acknowledgements

To Maen, my beloved husband and the stronghold of my heart. Your unwavering support, boundless love, and unshakeable trust have been my guiding force. This thesis is a reflection of the strength you've infused into my journey.

To my beloved son, Elisha - the beacon of my life and the source of calm. Thank you for being my constant inspiration and guiding light.

With heartfelt thanks and immense gratitude, to Dr. Bassem, whose assistance, profound insight, guidance, and remarkable scientific contributions have been truly invaluable.

To Dr. Wael, whose invaluable insight and assistance in technical matters have been truly appreciated.

To my brother, Zed, my guiding light, my soul and to my sisters, Suad and Suhad, my pillars of strength, for their constant being by my side and unwavering support during challenging times.

To my father and mother, for their boundless love, unwavering support, and enduring trust.

To my beloved nephews and nieces, Majd, Maen, Naya, Shahd, Ghazal, Bana, Faraj, Zeina, Mouna and Zein, who fill my life with joy and love.

To my second family, Antoinette, Sulaf, Michael, and Nibal, whose warm and compassionate presence, aiding me in caring for baby Elisha. Their kindness and support have been invaluable

To Haidar, Nail, Lubna, Tarek, Hiba, Ghazal, Kawkab, Nidal, and Hala, for their loving presence and constant concern

To all my dear friends, your presence has filled this journey with joy, making each moment memorable and purposeful. Your friendship has been a steady source of inspiration and comfort. A special mention to Mirna Yazji and Hamsa Dawara

To Dr. Hana Alahmad and Dr. Sulaf Farhat, for their invaluable scientific guidance and advice

To Shahd and Kenana, for their presence and love, whose support and advice pushed me forward to continue.

To the sweetest Raghad

To Shahd, for her constant being by my side, and her assistance in the layout, design, and references.

I extend my utmost gratitude to Professor Dr. Bassem Assfour, Professor Dr. Majd AlJamali, Professor Dr. Lama Youssef, Professor Dr Abdul-Qader Abbady and Dr. Mohammad for their invaluable commitment to imparting knowledge and fostering education. Their generosity in sharing knowledge has been instrumental in shaping my academic journey.

Abstract

The emergence of SARS-CoV-2 VOCs, and other zoonotic coronaviruses with pandemic potential, research efforts focus on vaccines and antibodies targeting the most conserved regions of the spike protein. Middle East Respiratory Syndrome Coronavirus (MERS-CoV) continue to pose significant global health threats. Across the coronavirus family, the receptor binding domain is poorly conserved, and so therapeutics that target the receptor binding function have low potential as a pan-coronavirus solution. An alternative relatively conserved target on the coronavirus spike is the stem helix in S2 region, which does harbor neutralizing epitopes and therefore is of interest to generate vaccines effective against pan-beta-coronaviruses.

Monoclonal antibodies (mAbs) possessing broad neutralization capabilities against HCoVs offer a promising avenue for treatment, as there is currently no vaccine or treatment approved against MERS-CoV. This thesis leverages computational methodologies, notably Autodock Vina and HADDOCK, to explore the neutralizing effects of broad neutralizing antibodies (bnAbs) targeting the stem helix of MERS-CoV and SARS-CoV-2. Through method optimization and validation against experimental data, the study aims to efficiently identify potential drug candidates among bnAbs. This approach promises to reduce resource expenditure and streamline subsequent clinical investigations, potentially accelerating targeted therapy development against MERS-CoV while minimizing research costs.

Referencing Zhou et al.'s comprehensive study, which isolated a substantial panel of β-CoV stem-helix bnAbs, structural analyses of these bnAbs unveiled the molecular underpinnings of their broad reactivity. The study determined crystal structures of four bnAbs (CC25.106, CC95.108, CC68.109, and CC99.103) in complex with beta-coronavirus spike stem-helix peptides at resolutions ranging from 1.9 to 2.9

Å. Employing molecular docking simulations via Autodock Vina and HADDOCK2.4, this investigation aims to predict binding modes and affinities of five bnAbs (CC25.106, CC95.108, CC99,103, CC9.113, CC25.36) against the stem helix epitopes of both viruses. Additionally, it explores dynamic behavior and conformational changes of these complexes through molecular dynamics simulations.

The analysis integrates PyMOL visualization to elucidate and interpret binding modes, emphasizing crucial residue interactions governing binding specificity, affinity, and stability of bnAb-stem helix complexes. The synthesis of computational outcomes with experimental data and existing literature aims to enhance the reliability and relevance of findings. By elucidating the molecular mechanisms governing bnAb interactions with conserved MERS-CoV epitopes, this study seeks to contribute to the development of broad-spectrum antiviral strategies targeting coronaviruses. Evaluated across both viruses, the assessment of five distinct bnAbs reveals comparable neutralization potency against SARS-CoV-2 and heightened efficacy against replication-competent MERS-CoV. Notably, while CC25.106 displayed superior performance in combating beta-coronavirus disease, CC9.113 emerged as a promising therapeutic candidate due to its favorable binding characteristics. Despite inherent limitations, this study underscores CC9.113's potential for therapeutic development against coronaviruses, advocating for further exploration across a broader spectrum of bnAbs to streamline future therapeutic initiatives.

Summary

Background

MERS-CoV, a severe respiratory virus identified in 2012 within the coronavirus family, primarily spreads through contact with infected dromedary camels, causing high-fatality respiratory illness. Recent cases, originating in the Arabian Peninsula, stem from zoonotic transmission. The virus has a 2 to 10-day incubation period, leading to pneumonia, acute respiratory distress syndrome, and multiorgan failure, especially in older adults. No specific drugs target MERS-CoV; treatment focuses on symptom management, hydration, and supportive care. Control measures include early diagnosis, suspected case isolation, and public health awareness. Coronaviruses, featuring spike glycoproteins like the Receptor Binding Domain (RBD) and S2 subunit, are crucial for viral entry. Antibodies targeting RBD show promise, but variations pose challenges. Focusing on the conserved S2 subunit and stem-helix region offers broader targeting. Stem-helix broadly neutralizing antibodies (bnAbs) exhibit cross-reactivity against coronaviruses, including SARS-CoV-2 and SARS-CoV-1. Research on bnAbs provides insights into molecular features, neutralizing mechanisms, and structural recognition, aiding vaccine development. Understanding bnAbs contributes significantly to effective therapeutics and preventive measures against emerging coronaviruses.

Aim of study

This work aims to employ computational methods to assess the neutralizing potential of select broadly neutralizing antibodies (bnAbs) against the MERS stem helix. The study involves conducting docking simulations on previously examined complexes to validate and compare outcomes. Furthermore, it includes docking experiments of bnAbs with SARS-CoV-2 to substantiate the hypothesized broad neutralization ability of these monoclonal antibodies against different coronaviruses.

Methods

This study employed molecular docking programs, namely AutoDock Vina and HADDOCK 2.4, to investigate the interactions between five selected broad neutralizing antibodies (bnAbs) and the stem helices of both SARS-CoV-2 and MERS-CoV. The computational analysis was complemented by utilizing PyMOL for result visualization.

Results

Analysis of HADDOCK scores and affinity scores for the interactions between selected bnAbs and SARS-CoV-2/MERS-CoV stem helices revealed CC25.106 and CC9.113 as potent candidates. While CC25.106 demonstrated strong HADDOCK scores and established experimental broad neutralization efficacy, a comparative analysis indicates CC9.113 as a promising candidate due to its favorable affinity scores and potential therapeutic efficacy against both coronaviruses. Evaluation of RMSD, Z-scores, and interacting residues supported CC25.106's effectiveness against HCoV stem helices. Despite the absence of experimental data, CC9.113 showcased promising characteristics, indicating its potential as a therapeutic agent against coronaviruses.

Conclusions

CC9.113's Therapeutic Potential: Findings suggest CC9.113's promising role as a therapeutic candidate due to its favorable interactions and binding characteristics. Further experimental validation is recommended to confirm its potential in therapeutic development against coronaviruses. The study's limitations, focusing on two bnAbs due to time constraints and limited access to docking programs, highlight the need for broader comparative analyses in future investigations. Expanding comparisons can enhance accuracy, minimizing resource usage in therapeutic development against coronaviruses.

Keywords

MERS-CoV, bnAbs, CC9.113, AutoDock Vina, HADDOCK2.4.

Table of Contents

Table of Figures

Table of Figures

Table of Figures

List of Tables

List of Abbreviations

Abbreviation	Name
MERS-CoV	Middle East Respiratory Syndrome Coronavirus
β-CoV	Beta-coronaviruses
SARS-CoV-2	Severe acute respiratory syndrome-related virus of the genus Beta-coronavirus
S protein	Spike protein
DPP4	Dipeptidyl peptidase 4
CD26	Clusterof Differentiations 26
ORFs	Open reading frames
E protein	Envelope protein
M protein	Membrane protein
N protein	Nucleocapsid protein
PreF	Pre-fusion
RBDs	Receptor-binding domains
PostF	Post-fusion
HR	Heptad repeats
Cryo-EM	Cryo-electron microscopy
NTD	N-terminal domain
CTD	C-terminal domain
6-HB	Six-helix bundle
IFN	Type I interferon
PRRs	Pattern recognition receptors

ssRNA	Single-stranded RNA
TRIM25	Triple motif protein 25
RIG-I	Retinoic acid-inducible gene I
ARDS	Acute respiratory distress syndrome
CP	Convalescent plasma
IVIG	Intravenous immunoglobulin
mAbs	Monoclonal antibodies
Tc	Trans-chromosomic
HFNC	China utilized high-flow nasal cannula
HCoV	Human Coronaviruses
ML-CoVs	MERS-like CoVs
bnmAbs	Broadly neutralizing monoclonal antibodies
nAb	Neutralizing antibody
VOCs	Variants of Concern
TM	Transmembrane
FP	Fusion peptide
HV	Hypervariable loops
CDRs	Complementarity-determining regions
SH	Stem Helix
EC50	Half maximal effective concentration
IC50	Half-maximal inhibitory concentration
HADDOCK	High Ambiguity Driven protein-protein DOCKing
CNS	Crystallography and NMR System
AI	Artificial intelligence

APBS	Adaptive Poisson-Boltzmann Solver
PDB	Protein Data Bank
FV	Fragment variable
RMSD	Root Mean Square Deviation
l.b.	Lowest bound
u.b.	Upper bound

CHAPTER I
INTRODUCTION

Introduction

MERS-CoV (Middle East Respiratory Syndrome Coronavirus) is an enveloped virus that expresses a positive-sense single-stranded RNA. MERS-CoV, like all coronaviruses, is a spherical or pleomorphic in shape with spike proteins on its surface. These spike proteins resemble the crown-like appearance of the virus, hence the name "corona."[1,2,3,4]

Beta-coronaviruses (β-CoV) that infect humans exhibits significant genome diversity.[5] MERS-CoV, categorized within the lineage C beta-coronaviruses,[5] is the second reported example of a zoonotic coronavirus that results in severe respiratory infection with high mortality rate in humans after SARS-CoV-2. [6]

MERS-CoV is the sixth known human coronavirus initially detected in Saudi Arabia in 2012. Currently, the virus continues to infect humans with high rates of morbidity and mortality. [4,7,8] MERS is a lethal coronavirus (CoVs) that have caused dreadful epidemic or pandemic in a large region or globally. [8] Human infections with MERS-CoV have been reported in at least 27 countries. [4,7]

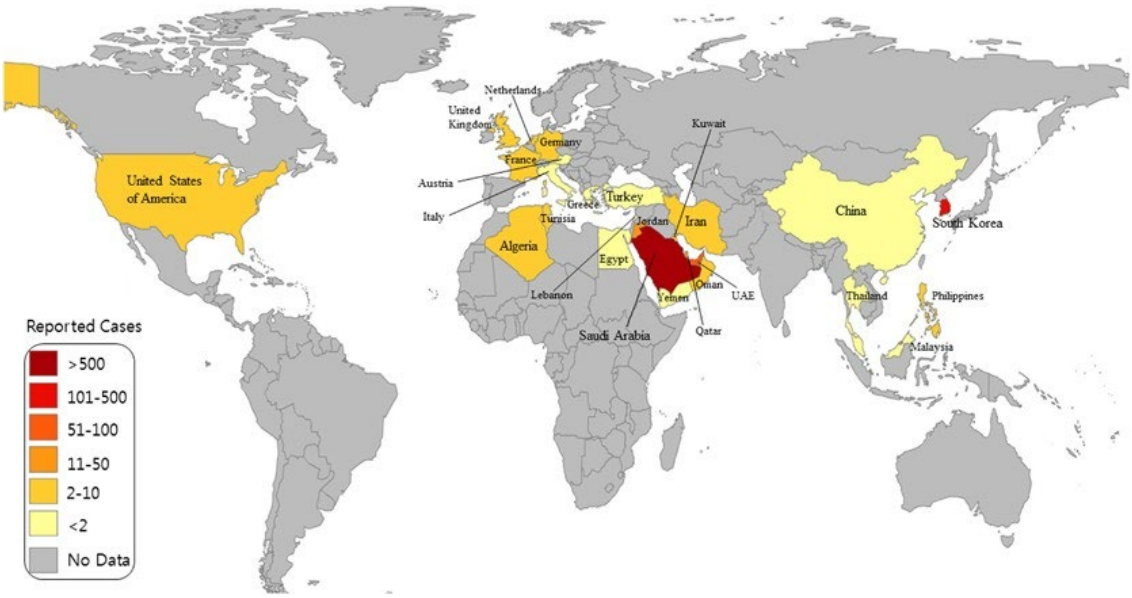

Figure 0-1 Global distribution map of Middle East respiratory syndrome coronavirus (MERS-CoV)[56]

New MERS-CoV cases are still being reported especially in the Arabian Peninsula, Qatar and Saudi Arabia. [9,10,11,12] This is partly due to the continuous zoonotic introduction of this virus to the human population in this region by dromedaries. The dromedary camel is the only animal species that has been reported to transmit this virus to humans. [10,11,12]

Although MERS-CoV is less transmissible than SARS-CoV-2, but the fatality rate (~35%) is much higher than that of SARS-CoV-2. Most surprisingly coinfection of SARS-CoV-2 and MERS-CoV in some patients could result in the emergence of a new β-CoV clade, e.g. SARS-CoV-3 or MERS-CoV-2. It was susbected to occur from genetic recombination between SARS-CoV-2 and MERS-CoV, resulting in a high transmission rate like SARS-CoV-2 and a high MERS-CoV-like case-fatality rate [9].

Between 13 September 2022 to 12 August 2023, the Ministry of Health of KSA reported three additional cases of Middle East respiratory syndrome coronavirus (MERS-CoV), with two associated deaths. The cases were reported from Riyadh, Asser, and Makkah Al Mukarramah regions. [10,11,12] All three cases were non-health-care workers, had symptoms like fever, cough, and shortness of breath, and had comorbidities. Two of the three cases had a history of contact with dromedary camels and all of them had a history of consuming raw camel milk in the 14 days prior to the onset of symptoms [12].

MERS-CoV is a zoonotic virus, studies have shown that humans are infected through direct or indirect contact with infected dromedary camels, with the exact route of transmission remains unclear.[13] It primarily spreads among humans via the consumption of the animal's meat or milk, leading to considerable illness and mortality. It may replicate in the upper respiratory tract and lungs of dromedary camels, leading to upper respiratory tract infections. [14,15,16]

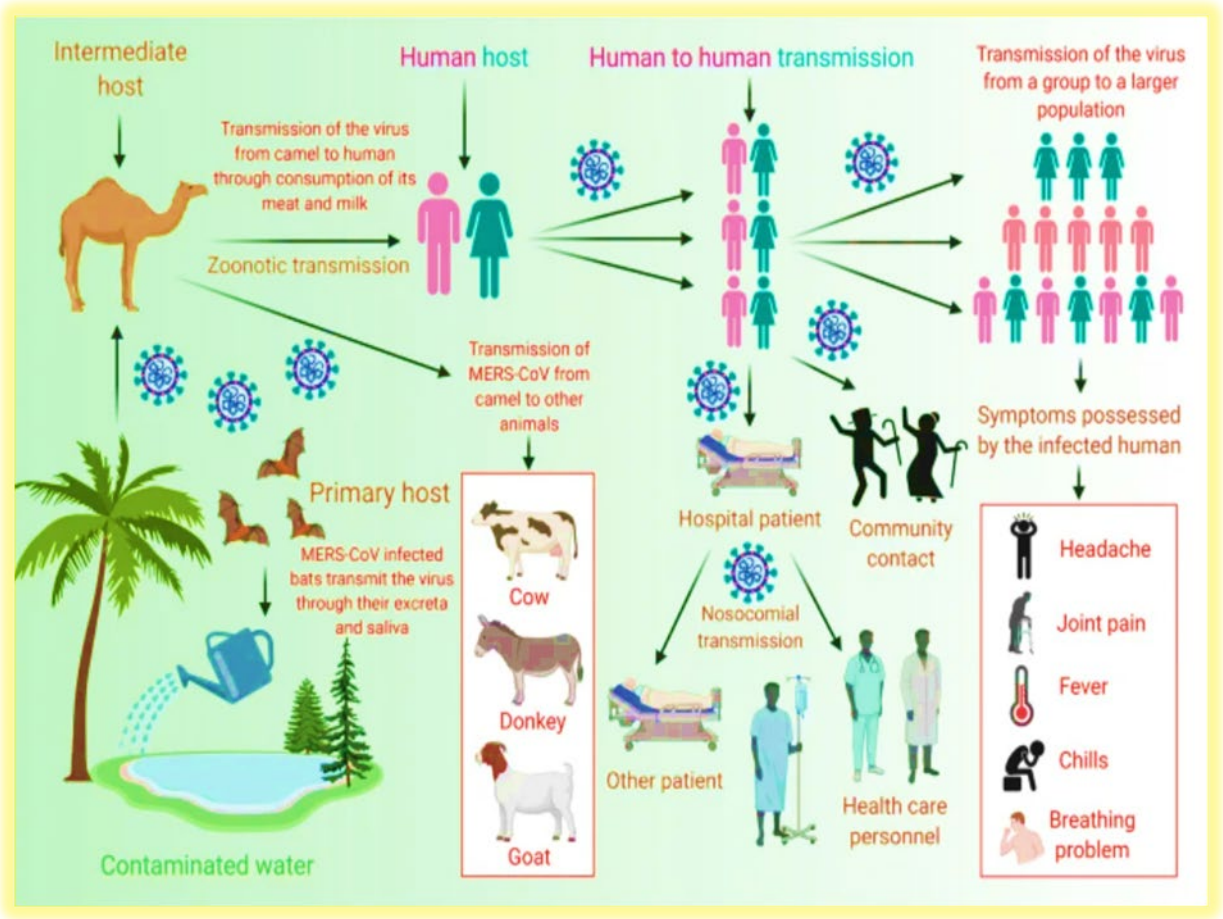

Figure 0-2 Schematic depiction of the transmission pattern of MERS-CoV and symptoms possessed by infected individual[58]

Recent research suggests a potential airborne transmission of MERS-CoV, through three main transmission routes (long-range airborne, close contact, and fomite). Human-to-human transmission of MERS commonly occurs in unprotected contact in healthcare settings and close household contacts of infected individuals, through exposure to respiratory droplets carrying the virus, often released when an infected person coughs or sneezes. [15,16,17]

CHAPTER II

BACKGROUND & LITERATURE REVIEWS

I. Background and Literature Reviews

II.1.Entering Mechanism of MERS

Understanding how MERS-CoV enters human cells is crucial for developing effective treatments. The virus operates by evading the body's natural antiviral immune response as part of its pathogenic activity. [18]

Coronavirus (CoV) infection initiates when the viral particle recognizes a host cell receptor and merges its membrane with the host cell membrane, mainly occurring in the lower respiratory tract. The entry of MERS-CoV, involving receptor binding and membrane fusion, is regulated by the viral spike (S) protein. [19,20,21,22]

The exterior of coronavirus virions is decorated with a sizable trimeric spike (S) glycoprotein responsible for facilitating cell entry. In the case of MERS-CoV, the S glycoprotein begins as a single-chain precursor and undergoes cleavage by furin-like host proteases, resulting in the formation of the S1 and S2 subunits. The mature S protein exists as a homotrimer composed of non-covalently linked S1 and S2 subunits. Within this structure, a trimer of S1 acts as a fusion-suppressive cap situated atop a trimer of S2 subunits. [20,21,22]

Recently, DPP4 (dipeptidyl peptidase 4), also known as T-cell activation antigen CD26, was identified as the cellular receptor for MERS-CoV. When the MERS-CoV spike protein engages with CD26, [22,26,27,28,48] a large irreversible conformational change of S2 mediates fusion of the viral and host-cell membranes, initiating the infection process. [20,21,22]

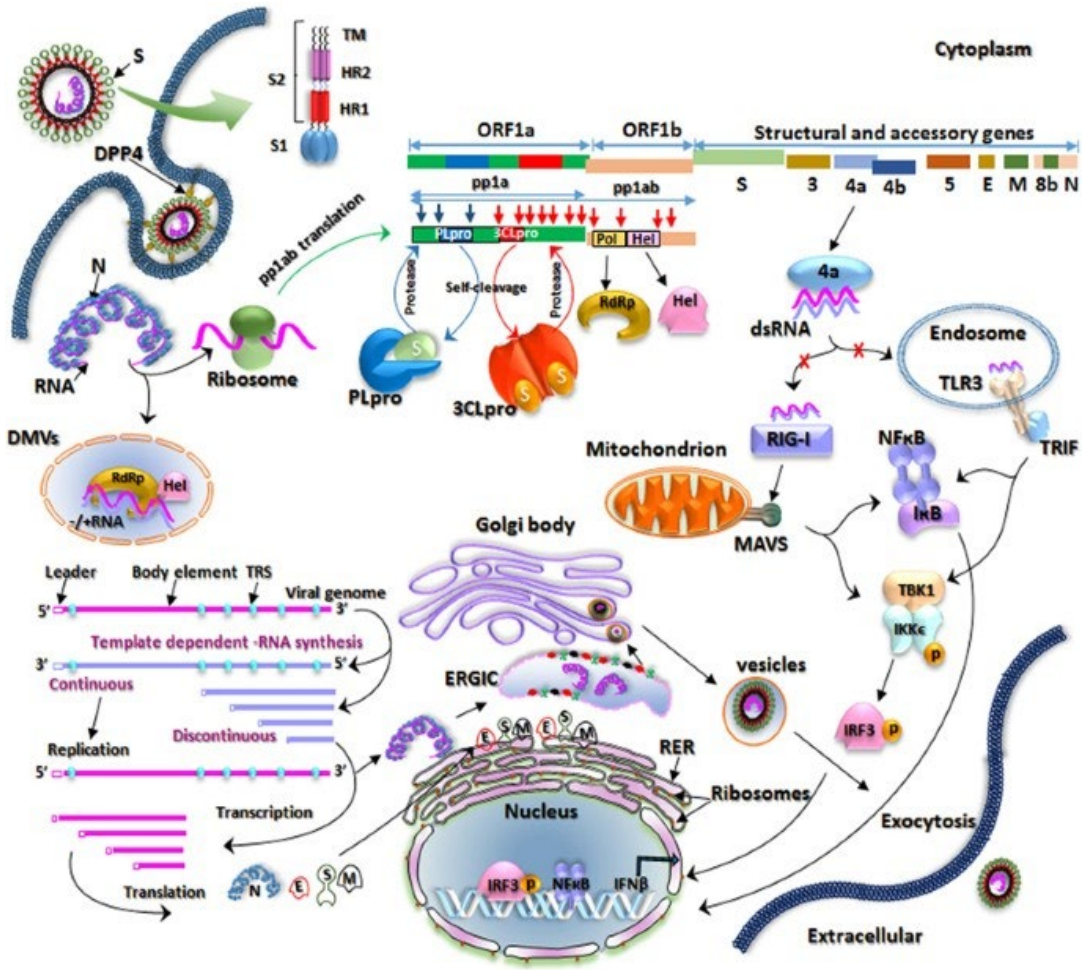

Figure I-1 Schematic of the replication cycle of Middle East respiratory syndrome coronavirus (MERS-CoV)[57]

CD26 marks the third peptidase recognized as a functional receptor for coronaviruses. It's a type-II transmembrane glycoprotein found abundantly in non-ciliated bronchial epithelium, kidney, small intestine, liver, parotid gland, and even in the testis and prostate. Notably, MERS-CoV can utilize the evolutionarily conserved DPP4 protein from various species, prominently identified in bats. [22,26,27,28]

Upon attachment of MERS-CoV, the virus's envelope merges with the cell membrane, releasing its genetic material into the host cell. The viral RNA undergoes replication and translation within the host cell, generating new viral particles. These

newly formed viruses have the capability to infect nearby cells, consequently propagating the infection [19]

II.2. Structure of MERS-CoV

The genome of MERS-CoV consists of a single, positive-stranded RNA that encodes a minimum of 10 open reading frames (ORFs). These ORFs are translated into four primary viral structural proteins: the spike (S) protein, envelope (E) protein, membrane (M) protein, and nucleocapsid (N) protein. [20,25] Additionally, it encodes numerous accessory proteins, such as 3, 4a, 4b, 5, and 8b, whose origins and functions remain unknown. [25]

The E protein resides mainly within the intracellular membranes of the virus and serves a significant function in viral assembly, budding, and intracellular movement. Research by Surya et al. in 2013 indicated that coronavirus E proteins typically 76–109 amino acids and are expected to contain at least one α-helical transmembrane region. Subsequently, it was determined that the E protein consists of a total of 82 amino acid residues.

The M protein, part of the viral envelope, contributes to virus assembly and morphogenesis by interacting with other viral proteins.

The S, M, and E proteins are integrated into the rough endoplasmic reticulum membrane and are transported toward the endoplasmic reticulum-Golgi region. There, they engage with the N proteins, forming viral particles. This interaction ultimately disrupts the fusion of cellular and viral membranes. Consequently, the development of fusion peptides could hold substantial promise in peptide-based therapeutic approaches. [20]

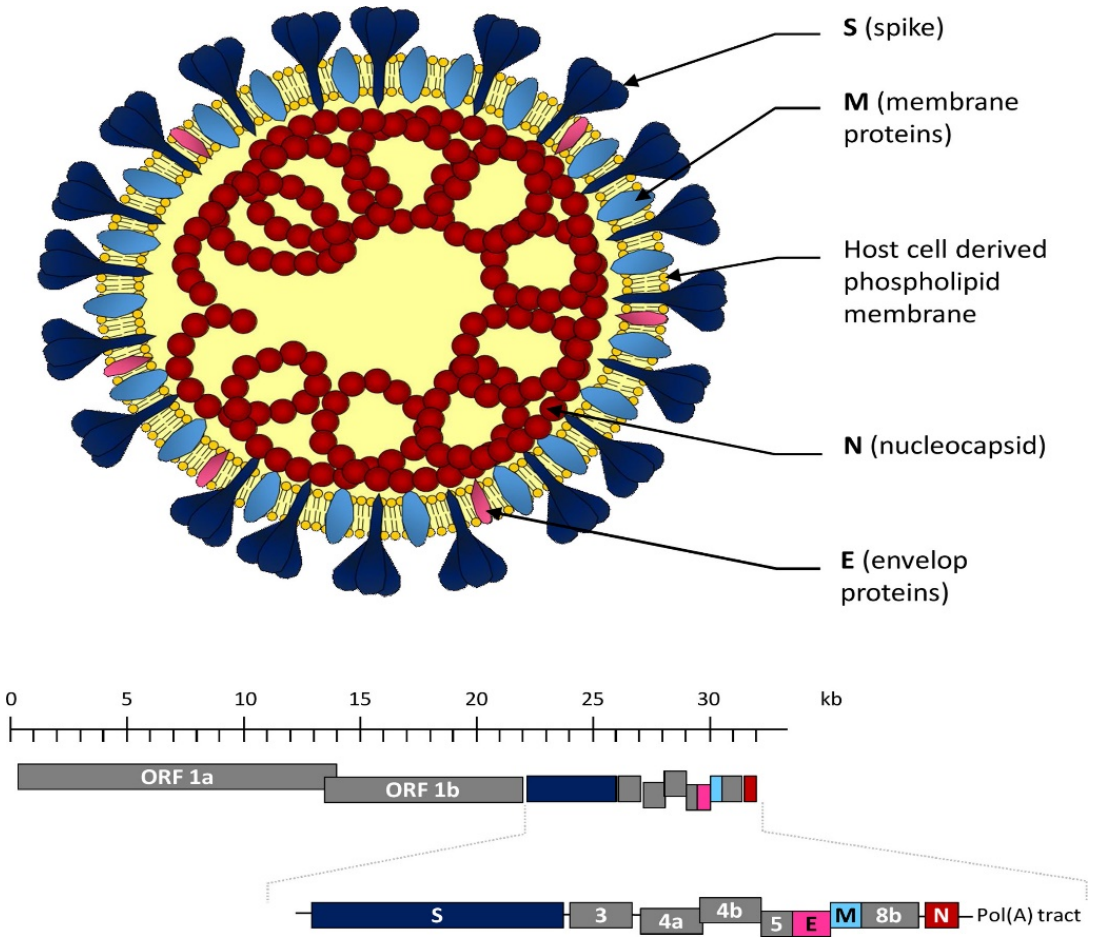

Figure I-2 Structure and genomic organization of MERS-CoV[59]

The spike (S) protein of MERS-CoV is a type I transmembrane glycoprotein situated on the virus envelope's surface, forming spikes in a trimeric arrangement. These spikes create the distinctive appearance of the virus. [1,20,22, 24] On the viral surface, the S protein takes on a mushroom-shaped pre-fusion (PreF) conformation, with S1 receptor-binding domains (RBDs) positioned farthest from the viral membrane. To bind to host receptors, these RBDs undergo conformational alterations, assisted by protease cleavage events. These changes allow the metastable S2 domain to undergo a refolding process, transitioning into a low-energy, rod-shaped coiled-coil structure known as the post-fusion (PostF) S conformation. The structures of both preF and postF

S represent the initial and final conformations of the S protein, orchestrating the sequence leading to membrane fusion. [5,29,30,31,32]

The S protein of MERS-CoV is integral to virus entry and infection. This protein, consisting of 1353 amino acids, forms trimers that create the spikes or peplomers on the enveloped coronavirus particle's surface. It is characterized by heavy glycosylation, featuring a substantial extracellular domain and a relatively short cytoplasmic terminal. [1,22,24]

The S protein plays a pivotal role in CoV tropism and disease severity by facilitating viral entry, binding, and fusion. Proteolysis occurs between the S1 and S2 segments, crucial for these functions. [20,22,24,35] Various host proteases have the capability to cleave the S protein of MERS-CoV. For instance, furin contributes in two distinct steps during the activation process of cleavage in infection. Initially, furin targets the R751/S752 position, cleaving the S protein during its biosynthesis. Subsequently, after viral entry, furin further digests S2 to S2′ at the R887/S888 position, located adjacent to the fusion peptide. [35]

The S1 subunit of the S protein is tasked with binding to the cellular receptor (DPP4) via its receptor-binding domain (RBD) region. This critical interaction facilitates viral entry into host cells. Conversely, the S2 subunit encompasses two regions known as heptad repeats 1 and 2 (HR1 and HR2), which combine to form a complex termed the fusion core. This structural arrangement serves as a fundamental architecture for membrane fusion processes involved in viral entry. [5,20,22,24,29,30,31,32]

Cryo-electron microscopy (cryo-EM) examinations of different β-coronaviruses have unveiled a four-domain structure within the S1 subunit. This architecture comprises an N-terminal domain (NTD), a C-terminal domain (CTD),

along with subdomains I and II, delineated as internal and external subdomains, respectively. [20,21,22]

Among CoVs, the internal subdomains tend to maintain a relatively conserved structure. However, the external subdomains exhibit substantial variability across CoVs. These external subdomains primarily engage in receptor binding, leading to the utilization of different receptors among CoVs due to these variations. [1]

In the case of most β-coronaviruses, including MERS-CoV, the S1-CTD is employed for binding to their respective functional receptors. [20,21,22] The S1 proteins of MERS-CoV exhibit dynamic structural changes, oscillating between open and closed conformations. Within this dynamic behavior, each of the three S1-CTDs can take on either a compact "down" conformation, concealing the receptor-binding surface, or an "up" conformation, which facilitates interaction with host-cell receptors. Researchers hypothesize an equilibrium between these conformations, where binding to the receptor favors the "up" conformation of all three CTDs. This results in an unstable three CTD "up" arrangement, triggering the dissociation of S1 and prompting the refolding of S2. [20,21,22]

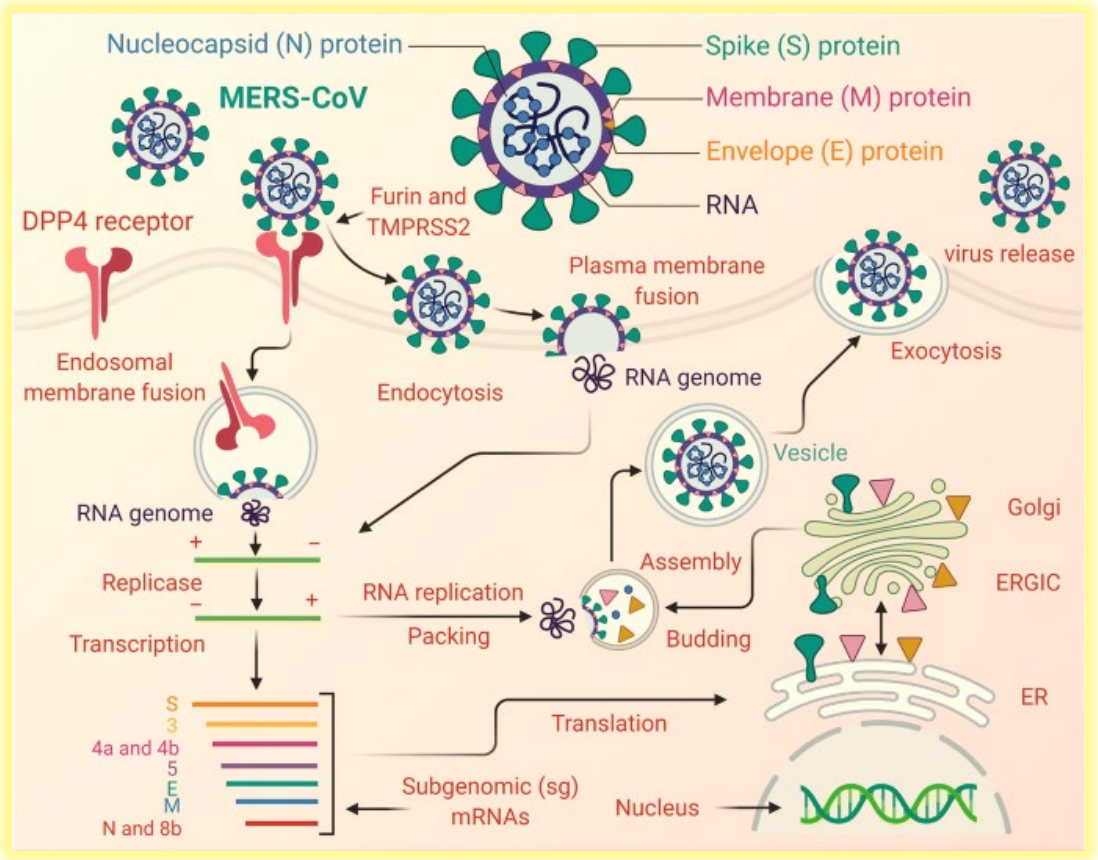

Figure I-3 Schematic illustration of the genomic structure and the life cycle of the MERS-CoV[60]

In the S2 subunit, the heptad repeat 1 (HR1) region undergoes a homo-trimeric assembly, revealing three significantly conserved hydrophobic grooves on its surface. These grooves serve as binding sites for heptad repeat 2 (HR2). As part of the fusion process, this interaction leads to the formation of a six-helix bundle (6-HB) core structure. This 6-HB structure plays a critical role by facilitating the convergence of viral and cellular membranes, bringing them into close proximity. This proximity is essential for the fusion of the viral and cellular membranes, enabling viral entry into the host cell. [21]

II.3. Immuno-response

The body's immune system reacts to the infection by initiating an immune response, which, in some cases, can become overly active, leading to severe symptoms. Type I interferon (IFN) serves as the primary defense against viruses, playing a pivotal role in initiating the host's antiviral responses. When a virus infects the body, the innate immune system is activated through specific proteins known as pattern recognition receptors (PRRs). These receptors can identify viral components like single-stranded RNA (ssRNA). Consequently, the innate immune system triggers the release of cytokines, which act as signaling molecules coordinating the immune response. This response helps impede the virus's replication within the body. [38]

N protein of CoV can hinder the production of type I interferon (IFN) through various mechanisms. It interferes with the interaction between two crucial proteins, triple motif protein 25 (TRIM25) and retinoic acid-inducible gene I (RIG-I). Additionally, it binds to the E3 ubiquitin ligase of TRIM25. This binding activity disrupts the ubiquitination process, preventing the activation of RIG-I mediated by TRIM25. Ultimately, this interference with the TRIM25-RIG-I interaction and the inhibition of ubiquitination impede the activation of RIG-I, resulting in the inhibition of IFN production. This indicates that the N protein of CoV plays a regulatory role in the host's immune response against the virus by controlling the production of IFN. [1]

MERS-CoV infiltrates and replicates within macrophages, leading to the induction of MHC-I, MHC-II, and co-stimulation-related genes.[39] This activates the adaptive immune system, particularly involving T cells and B cells, which play vital roles in combating the infection. Cytotoxic T cells among T cells assist in eliminating infected cells, while B cells produce antibodies capable of neutralizing the virus. CD4+ T cells are crucial for virus-specific antibody production by activating B cells in a T-

dependent manner. Meanwhile, CD8+ T cells function as cytotoxic agents, targeting and eliminating virus-infected cells. For diagnosing MERS-CoV infection, the detection of specific antibodies against the virus in human serum is confirmatory. However, these antibodies typically become detectable around days 14–21 post-infection. Their concentrations increase over time and can persist for more than 18 months. The long-term antibody response varies based on the severity of the infection, highlighting the importance of understanding the potency and duration of the adaptive immune response to MERS-CoV infection. [39,40]

Absolutely, humoral immune responses are intricate, encompassing diverse arrays of polyclonal antibody species. These antibodies differ in their isotypes, which dictate their functional properties, target epitope specificity, and affinity for the specific antigens they recognize. This diversity in the humoral response allows for a broad and adaptable immune defense against a variety of pathogens and antigens. [41]

Understanding the immune response mechanism triggered by MERS-CoV infection is pivotal for developing effective vaccine candidates. An ideal vaccine should robustly stimulate both cellular and humoral immunity. Creating vaccines that enhance both arms of the immune system will be crucial in providing comprehensive protection against MERS-CoV. [39,40]

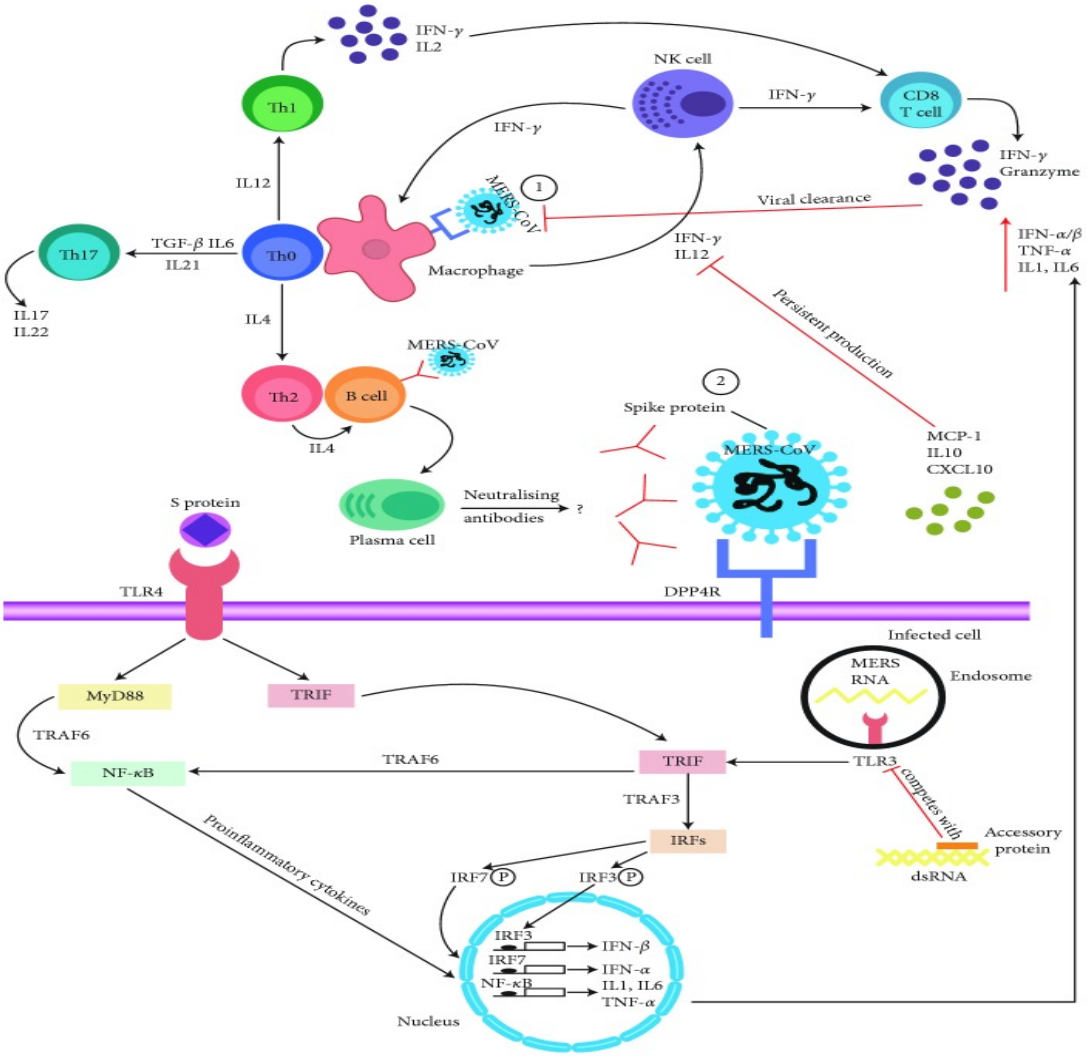

Figure I-4 The proposed schematic representation of the immune response to MERS-CoV infection and how the invading virus is processed during an infection.[59]

II.4. Symptoms and Therapy

Absolutely, MERS-CoV remains a significant public health concern, particularly in the Middle East. The absence of effective antiviral medications or approved vaccines against MERS-CoV heightens the worrisome nature of this threat. The ongoing lack of specific therapeutics or preventive measures underscores the importance of continued research and development efforts to address this persistent health risk. [2]

Indeed, one of the primary challenges posed by MERS-CoV infection is the absence of distinct clinical features that would allow for easy differentiation from other viral respiratory illnesses. This lack of specificity, coupled with the precautions taken to prevent potential secondary spread of MERS-CoV, can lead to medical complications. Prolonged and challenging isolation measures aimed at preventing transmission can hinder timely and essential complementary testing, often creating difficulties in appropriate patient management while awaiting PCR test results. This scenario may lead to medical confusion and suboptimal care for the patient. [33]

The incubation period for MERS typically spans from 2 to 10 days, with an average duration of 5 to 6 days. In fatal cases, death usually occurs around 11.5 days after the onset of symptoms. MERS-CoV infections tend to be more prevalent in men, and over half of the reported cases involve individuals aged 50 years or older. [35]

The clinical manifestation of MERS-CoV infection was initially characterized as severe, often leading to pneumonia accompanied by acute respiratory distress syndrome (ARDS), septic shock, and multiorgan failure, ultimately resulting in fatalities. [12,33,34,35] This severe presentation was notably prominent in elderly individuals (over 65 years old) and patients with pre-existing chronic conditions such as cardiovascular disease, respiratory ailments, kidney issues, diabetes, acquired or congenital immune disorders, and cancer. [35] Around one-third of patients develop pneumonia, while approximately 20% progress to ARDS. [12,33,34]. In suspected cases, individuals exhibiting acute respiratory illness along with chest radiographs indicating pneumonia and ARDS were considered likely candidates for MERS-CoV infection. [36]

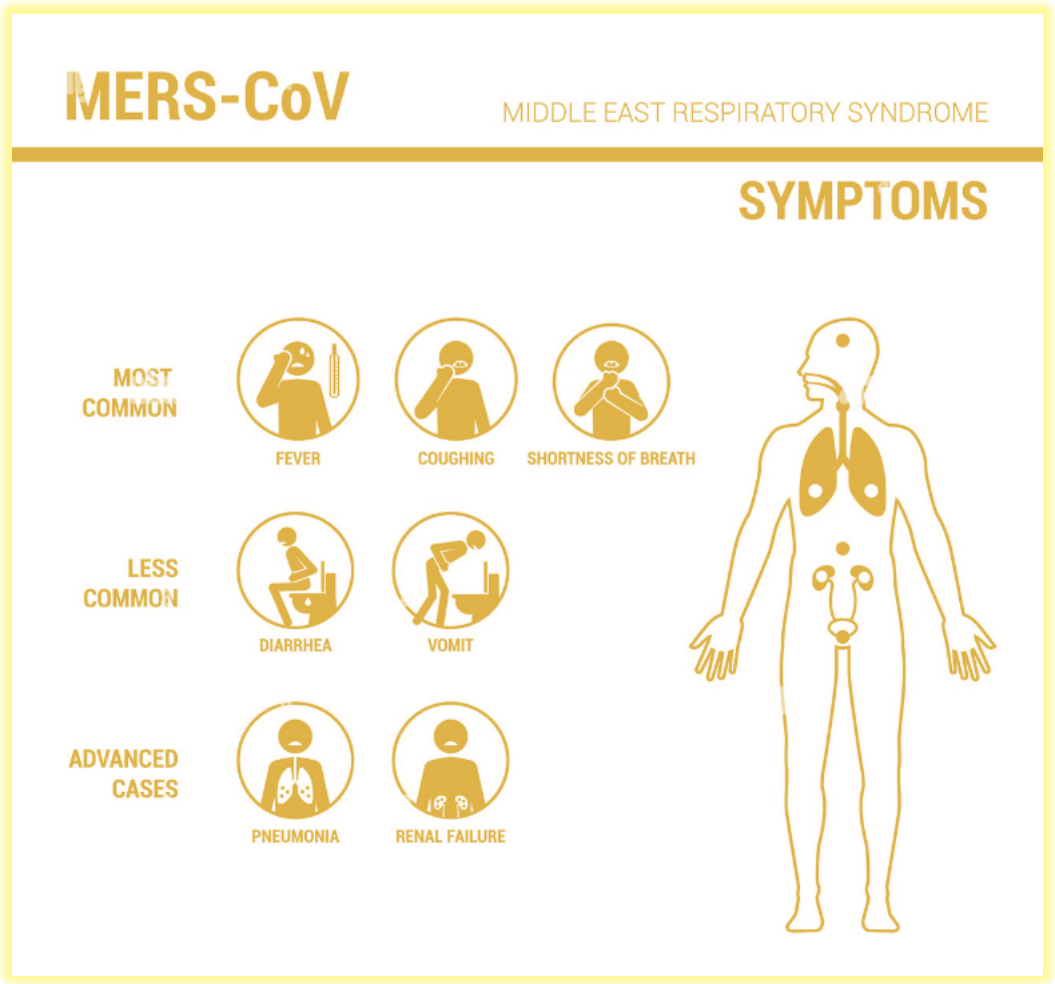

Figure I-5 MERS CoV symptoms medical infographic

Subsequently, reports surfaced indicating that some patients exhibited mild flu-like symptoms or remained asymptomatic after exposure to MERS-CoV (ranging from 2 to 14 days post-exposure), accounting for 14% to 80% of cases. [12,33,34,35] The most prevalent clinical symptoms include fever exceeding 38°C, cough, headaches, muscle and joint pains, breathing difficulties, and shortness of breath. Gastrointestinal symptoms like abdominal pains, vomiting, and diarrhea were less frequently observed. [35] The emergence of MERS-CoV as a cause of severe respiratory illness underscores the urgent need for developing effective therapeutic and preventive measures against MERS-CoV infection. Presently, there are no specific drugs available to target MERS-CoV. [4]

The future trajectory of MERS-CoV remains uncertain, making it challenging to predict whether it will fade away or persist as a threat to human populations. However, the development of efficient vaccines for both host animals and humans could significantly impact the course of MERS-CoV, potentially shifting the balance from a potentially pandemic situation to the eventual elimination of MERS-CoV. [33] Moreover, understanding the epidemiological and viral factors contributing to the emergence of MERS-CoV in the Middle East poses challenges. The high seropositivity rate of African dromedary camels' contrasts with the absence of a similar disease in local human populations, making it difficult to comprehend the dynamics behind the transmission and potential spill-over to humans. [33]

The treatment approach for Middle East Respiratory Syndrome (MERS) primarily revolves around symptom management. This involves administering medications to alleviate fever and pain, ensuring proper hydration, and maintaining electrolyte balance. Isolation of infected individuals is crucial to prevent disease transmission.

For severe cases requiring hospitalization, supportive care is provided, which includes oxygen therapy and mechanical ventilation for those experiencing severe respiratory distress. Intravenous fluids may be given to maintain adequate hydration levels.

In cases where secondary bacterial infections arise alongside MERS, antibiotics may be prescribed if there's suspicion or confirmation of bacterial involvement.

The use of corticosteroids in MERS treatment remains controversial. While they might assist in reducing inflammation, their potential to suppress the immune response necessitates careful consideration.

It's crucial to recognize that MERS, while less contagious, holds a higher fatality rate compared to some other coronaviruses, with a mortality rate of up to 36%. Therefore, public health measures and heightened awareness, particularly early diagnosis and isolation of suspected cases, are pivotal components in controlling its spread. [12]

Figure I-6 Information for those travelling to the Middle East - MERS-CoV[60]

Various therapeutic approaches have been explored for MERS treatment, including convalescent plasma (CP), intravenous immunoglobulin (IVIG), monoclonal antibodies, and repurposing existing clinically approved drugs. However, these therapeutic options often come with drawbacks or limitations, indicating the need for alternative approaches. The pursuit of effective therapeutic treatments for MERS highlights the pressing necessity for additional treatment modalities. Research continues to explore novel approaches to address the limitations of existing therapies and develop more effective treatments against MERS-CoV infection. [20]:

* High-throughput screening of compounds and small molecules has proven beneficial for researchers in evaluating extensive drug libraries regarding their in vitro antiviral activity against novel targets, including MERS-CoV. The repurposing approach offers significant advantages by saving time and reducing the costs typically associated with developing entirely new drugs. Several repurposed drugs have demonstrated potential antiviral effects against MERS-CoV. Examples of these drugs, showcasing validated activity against coronaviruses, include ribavirin, hexachlorophene, nitazoxanide, and homo-harringtonine. These findings underscore the potential for repurposed medications to serve as effective treatments against MERS-CoV infection. [20]
* Convalescent plasma (CP) and whole blood therapy have emerged as potential treatments for infectious diseases like MERS. CP involves using whole blood or plasma obtained from individuals who have recovered from viral diseases, and it has been employed as a treatment during outbreaks. [20] CP therapy becomes a primary treatment option in scenarios where the human population lacks pathogen-specific immunity, and available treatment options are limited. This therapy holds promise, especially for the elderly, immune-suppressed individuals like cancer or transplant patients, where vaccination might not elicit adequate protective antibody responses. [20,37] Additionally, it could benefit populations with underlying health conditions where vaccination isn't feasible. [37] In contrast to vaccines and monoclonal antibodies (mAbs), CP therapy requires minimal development and relies on a standard infrastructure for blood collection. This characteristic allows for swift deployment, even in settings with limited resources, especially in developing nations where alternative mAb-based therapies might be cost-prohibitive. This aspect highlights the potential of CP therapy to be rapidly implemented, particularly in

regions with fewer resources, which constitute a significant portion of the global population. [37]

* Intravenous immunoglobulin (IVIG) is a serum-derived blood product primarily utilized in treating various autoimmune and inflammatory conditions. Although extensively used in managing several diseases such as heart failure, mycobacterial infections, epilepsy, Alzheimer's, among others, there is currently no evidence suggesting IVIG's efficacy against MERS. However, Luke et al. conducted a study where trans-chromosomic (Tc) bovines were engineered to produce human polyclonal immunoglobulin G antibodies. These antibodies demonstrated the ability to neutralize MERS-CoV in both in vitro assays and animal models. This study's implications suggest a potential method for producing therapeutic immunoglobulins to prevent and/or treat MERS-CoV infections and potentially other emerging infectious diseases. This innovative approach holds promise in developing therapeutic strategies against such viral infections. [20]

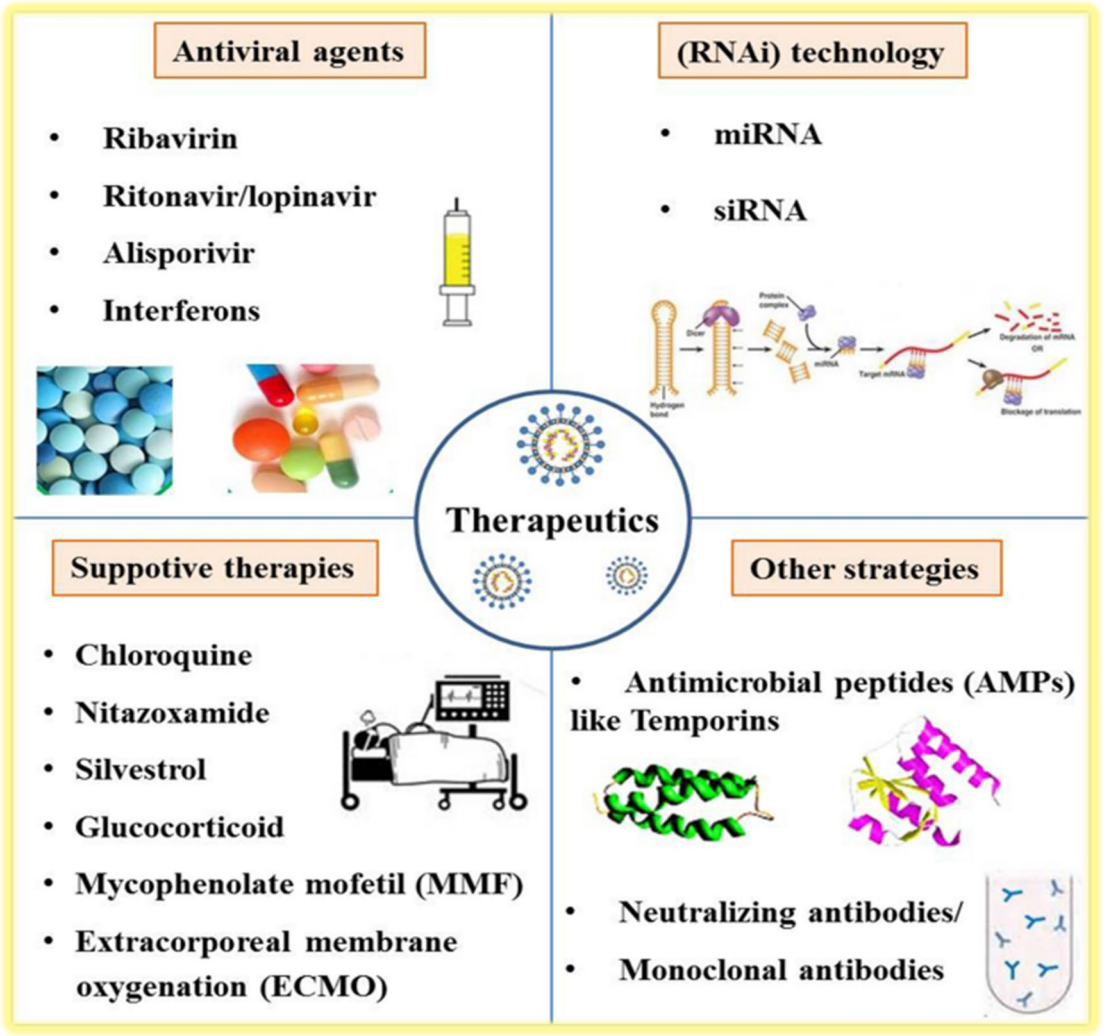

Figure I-7 Therapeutic strategies available against MERS-CoV [62]

* Various therapeutic strategies aimed at impeding MERS-CoV's entry into cells and inhibiting virus-cell membrane fusion have been explored. These include cathespin inhibitors, TMPRSS2 inhibitors, furin inhibitors, kinase inhibitors, and IFITM proteins, among others. These approaches target different stages of the virus's entry and fusion process to impede its ability to infect cells. Additionally, a study conducted in China utilized high-flow nasal cannula (HFNC) therapy in treating a patient with MERS. HFNC therapy is a respiratory support method that delivers heated and humidified oxygen at higher flow rates than conventional oxygen therapy. Its use in managing MERS highlights the exploration of various supportive

therapies to aid in the treatment of respiratory distress associated with the infection. [20]

* Within the coronavirus family, the receptor binding domain (RBD) exhibits poor conservation across different strains. Consequently, therapeutics targeting the receptor binding function face challenges in offering a broad solution against various coronaviruses. [4,22] In contrast, the HR (heptad repeat) region within the S2 subunit demonstrates higher conservation among different Human Coronaviruses (HCoVs). This HR region plays a critical role in HCoV infections by facilitating the formation of the 6-helix bundle (6-HB), a structure essential for mediating viral fusion. Targeting this more conserved HR region presents a potential avenue for developing therapies that could have broader efficacy against multiple coronaviruses. [4]. The interaction between the HR1 and HR2 regions in coronaviruses is conserved, involving specific residues within these helices. Peptides derived from the HR2 region of various enveloped viruses have exhibited the ability to competitively bind viral HR1, effectively inhibiting viral infection. This suggests that targeting the HR1 region could be a promising strategy for developing fusion inhibitors against highly pathogenic Human Coronaviruses (HCoVs) like MERS. Peptides are small fragments of proteins typically comprising of 2–50 amino acid residues. These peptides achieve viral inhibition through various modes of actions, including direct binding to virions or host cell-surface receptors, blocking viral entry, interfering enzymatic activity to inhibit intracellular replication, and indirectly modulating immune responses. [4] Compared to conventional small molecule drugs, peptide synthesis can be initiated and modified rapidly. Peptides' chemical nature endows them with high specificity and efficacy at very low concentrations, often in nanomolar or picomolar ranges. [4] Over the last two decades, numerous studies

have synthesized a wide array of anti-viral peptides targeting the membrane fusion step, particularly the HR regions in the S2 subunit. These fusion inhibitors hold promise for translation into therapeutic peptides. However, peptides derived from HR1 (targeting HR2) have shown limited activity, possibly due to their tendency to self-aggregate. Despite this, many peptides designed to counter MERS-CoV have exhibited potent anti-CoV activity, showing IC50 values in the micromolar concentration range. Continued research in this area offers hope for the development of effective peptide-based therapeutics against coronaviruses like MERS. [8]

* Monoclonal Antibodies mAb: The presence of MERS-like CoVs (ML-CoVs) represents a significant concern for global public health. Despite laboratory and clinical trials, there is currently no commercially available vaccine for MERS-CoV. [21][39] The ongoing threat posed by MERS-CoV and the potential emergence of similar coronaviruses underscores the urgency in developing effective preventive measures such as vaccines. While research efforts have delved into vaccine development and some progress has been made in laboratory and clinical settings, the absence of a licensed vaccine emphasizes the continuing need for further research to address this pressing health concern. Zoonotic coronaviruses have demonstrated a remarkable capacity to breach species barriers and swiftly infect humans, as observed with the emergence of new Human Coronaviruses (HCoVs). This unpredictability highlights the challenge in solely targeting a single HCoV with a specific drug, as newly emerging HCoVs might render such treatments ineffective. [4] Given the absence of a broad-spectrum anti-HCoV drug available for clinical use, it becomes crucial to identify a common or conserved target site among existing HCoVs. Such an approach could potentially pave the way for developing therapeutics effective against multiple HCoVs, thereby addressing the rapid and

unpredictable nature of zoonotic coronaviruses. Identifying conserved regions or targets could offer a more universal solution against these viruses and aid in combatting future emerging HCoVs. [4] Establishing multiple Human Coronavirus (HCoV) S-mediated cell-cell fusion assays has been instrumental in identifying a pan-HCoV fusion inhibition target site. These assays aimed to determine the cross-inhibitory spectrum between HR1Ps and HR2Ps, derived from the HR1 and HR2 regions, respectively, of various HCoVs. By utilizing these assays, researchers sought to understand the inhibitory potential of HR1Ps and HR2Ps from different HCoVs against each other. This approach helps in identifying potential targets for fusion inhibition that could work across multiple HCoVs, thus aiming to develop a potential pan-HCoV inhibitor effective against infections caused by various HCoVs in the human respiratory tract. This strategy offers a promising pathway towards developing broad-spectrum therapeutics targeting a wide range of Human Coronaviruses. [4] creating safe and efficacious MERS vaccines that induce broad-spectrum immune responses is crucial. These vaccines should aim to enhance protective efficacy not only against multiple strains of MERS-CoV but also against MERS-like coronaviruses that have the potential to cause pandemics. [4] Developing such vaccines requires novel strategies that can evoke robust immune responses capable of recognizing and neutralizing various strains of MERS-CoV and related coronaviruses. An effective vaccine strategy would ideally encompass a comprehensive understanding of the diverse genetic variations among different strains while eliciting a broad and durable immune response. This approach could potentially provide cross-protection against a wide range of MERS-related viruses, contributing to global preparedness against potential outbreaks. [21] Various monoclonal antibodies (mAbs) have been tested and have exhibited promising anti-

MERS-CoV activity in laboratory settings (in vitro studies). These mAbs are specifically designed to target and neutralize MERS-CoV, showing potential in inhibiting the virus's ability to infect and replicate in cell cultures. While these in vitro findings are encouraging, further research, including preclinical and clinical studies, is necessary to assess the efficacy, safety, and therapeutic potential of these monoclonal antibodies in living organisms, particularly in humans. This rigorous evaluation process is crucial to determine their effectiveness as potential treatments against MERS-CoV infection. [33] Antibody responses, particularly the production of neutralizing antibodies, play a pivotal role in effectively treating MERS-CoV infections in humans. The increased use of monoclonal antibodies (mAbs) as therapeutics can be attributed to their exceptional specificity and high affinity for their target antigens, along with their adaptable structure, allowing for engineering modifications. [45] Following the identification of MERS-CoV, potent neutralizing monoclonal antibodies were swiftly isolated. Multiple technological platforms, including phage or yeast display of antibody libraries, animal immunization, and direct isolation from survivors of MERS-CoV infection, facilitated this isolation process. The development of monoclonal antibodies capable of retaining neutralizing activity against various coronavirus lineages and concerning variants is crucial for preparing against potential future pandemics. These broadly neutralizing monoclonal antibodies (bnmAbs) have the potential to serve as therapeutics. Moreover, they can contribute to the rational design of vaccines that aim to induce the production of bnmAbs in vaccinated individuals. This approach holds promise in providing a broader and more robust immune response against multiple strains and variants of coronaviruses, aiding in the mitigation of future outbreaks. [45] Coronaviruses feature surface spike glycoproteins, known as predominant antigens

that trigger the antibody response.[1] These antibodies have the potential to target spike proteins, hindering the virus from entering host cells. Consequently, developing monoclonal antibodies directed at these proteins is favored for protection, as opposed to vaccine preparation, which demands extensive time and laborious efforts [21,39,42] The HR1 and HR2 regions within the S2 subunit combine to form a six-helix bundle fusion core, acting as a pivot to bring the viral and host cell membranes closer together. This six-helix bundle (6-HB) structure plays a crucial role in the fusion process, facilitating the close proximity required for viral fusion and entry. Hence, the S protein stands out as a key target for the development of specific drugs. Particularly, the S1 RBD (receptor-binding domain) proves to be a highly effective target site. Antibodies directed at the RBD or vaccines based on the RBD have previously demonstrated potent antiviral activity, effectively blocking the virus from binding to host receptors and showcasing protective effects. [4] The receptor-binding domain (RBD) situated within the S1 subunit holds the primary neutralizing epitopes, making it a focal point for developing initial COVID-19 vaccines. These vaccines aimed to induce a robust neutralizing antibody (nAb) response by targeting this specific domain, crucial for neutralizing the virus and conferring immune protection against COVID-19 [9,21,43] Studies examining the structure have shown that the epitopes of these antibodies coincide with the DPP4-binding surface, establishing a structural foundation for their neutralizing properties. [20] Monoclonal and polyclonal antibodies targeting DPP4 have demonstrated the ability to hinder MERS-CoV infection in primary human bronchial epithelial cells and Huh-7 cells. [20The majority of neutralizing antibodies against MERS-CoV focus on the receptor-binding subdomain, coinciding with the DPP4 binding surface. These antibodies exhibit a common aspect of neutralization by competing directly

with the cellular receptor DPP4 to bind to the receptor-binding domain (RBD). This competition for binding to RBD is a key mechanism through which these antibodies neutralize the virus. [45,46,47] Adney and colleagues conducted a research study assessing the effectiveness of a MERS-CoV S1 subunit vaccine with adjuvants. Their findings revealed reduced and delayed viral shedding in dromedary camels and provided complete protection for alpacas against MERS-CoV infection. [21] Other studies also support these findings, indicating that the protective effectiveness of MERS vaccines aligns positively with the levels of neutralizing antibodies present in the serum. [21] Earlier studies have demonstrated that the Receptor Binding Domain (RBD) found in the SARS-CoV-2 S protein can effectively impede SARS-CoV-2 infection and is capable of generating robust neutralizing antibodies, offering protection against SARS-CoV-2 infection. [20] Given that MERS-CoV belongs to the same beta-coronavirus genus as SARS-CoV-2, there's an expectation that the RBD of MERS-CoV could similarly exhibit effectiveness in obstructing MERS-CoV infection. This suggests the potential for inducing neutralizing antibody responses against MERS-CoV infection in vaccinated animals through the utilization of the MERS-CoV RBD. [26] A recent study has identified and characterized a collection of seven human neutralizing antibodies (nAbs) and two monoclonal antibodies (mAbs). These specific antibodies are potent inhibitors targeting the Receptor Binding Domain (RBD) and demonstrate robust neutralizing activity against MERS-CoV. [20] Moreover, another study successfully developed two potential antibodies which exhibited efficacy in animal models infected with MERS-CoV. Despite their effectiveness, it's worth noting that producing monoclonal antibodies is a time-consuming and challenging process [20] Mutations, particularly within and around the Receptor Binding Site (RBS) of coronaviruses, have the

potential to create viral variants resistant to neutralization by commonly induced classes of antibodies. These variants, known as Variants of Concern (VOCs), can evolve without significantly compromising viral fitness. This phenomenon poses a challenge to the efficacy of existing antibodies in combating these mutated strains [9,43] On another note, the S2 subunit within the Human Coronavirus (HCoV) S protein consists of various segments, including the fusion peptide (FP), heptad repeat 1 (HR1), central helix (CH), connector domain (CD), stem helix (SH), heptad repeat 2 (HR2), and transmembrane anchor (TM) [5]. The S2 domain facilitates the fusion of the viral envelope with the host cell membrane. Following proteolytic cleavage at the S2′ site just before the fusion peptide (FP), the FP is exposed, allowing for its insertion into the host cell membrane and subsequent fusion [44]. Despite being generally less potent than antibodies directed at the RBD, the S2 domain is relatively more conserved. This conservation suggests that epitopes within the S2 domain may serve as optimal targets for the development of Broadly Neutralizing Monoclonal Antibodies (bnmAbs) effective against diverse existing and future emerging coronaviruses. [5,9] Studies have shown that monoclonal antibodies designed to target the Receptor Binding Domain (RBD) of the SARS-CoV-2 did not effectively recognize the corresponding region in the SARS-CoV-2. This observation underscores the limited cross-reactivity within this specific region between these coronaviruses. Conversely, the membrane fusion domain, particularly within the S protein, is one of the most conserved areas among coronaviruses. Consequently, focusing on targeting the membrane fusion process might offer a higher likelihood of success across different coronaviruses in potential future outbreaks. This broader targeting strategy could potentially offer more cross-functional efficacy against a spectrum of coronavirus strains [22] With the emergence of Variants of Concern

(VOCs) within SARS-CoV-2 and the continual threat posed by zoonotic coronaviruses with pandemic potential, current research endeavors are concentrated on vaccines and antibodies that focus on the most conserved regions within the spike protein. Researchers are targeting the more conserved facets of the Receptor Binding Domain (RBD) with numerous neutralizing antibodies (nAbs). Stem-helix broadly neutralizing antibodies (bnAbs) have spotlighted the potential offered by conserved bnAb S2 epitopes. These conserved sites within the S2 epitopes might hold promise for the development of vaccines against a broad spectrum of beta-coronaviruses. Nonetheless, the development of a comprehensive panel of stem-helix bnAbs is still necessary to understand the shared molecular features of antibodies targeting this specific site. [45]

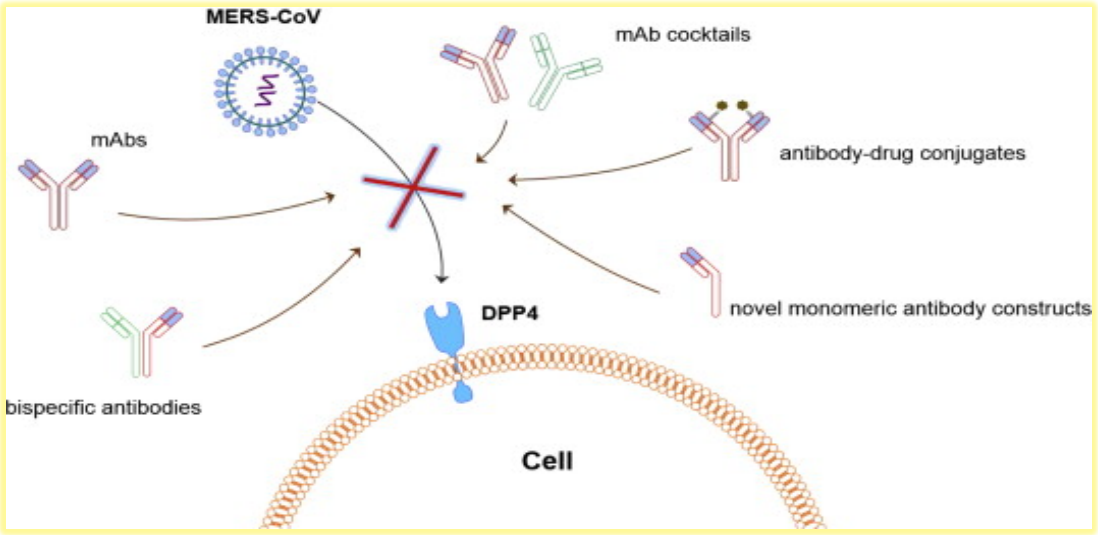

Figure I-8 Schematic illustration of the inhibition of MERS-CoV cell entry by neutralizing mAbs, mAb cocktails, bispecific antibodies, antibody-durg conjugates, and novel monomeric antibody constructs.[62]

II.5. Reference Study: Broadly neutralizing anti-S2 antibodies protect against all three human beta-coronaviruses that cause deadly disease.

In our reference study, a study conducted by Zhou.p. et al., the largest collection of β-CoV stem-helix broadly neutralizing antibodies (bnAbs) was successfully isolated,

revealing key insights into their shared features and the molecular foundation behind their extensive neutralization of coronaviruses. These S2 stem-helix bnAbs exhibited a high prevalence of antibody germline characteristics that could be leveraged in targeted vaccine development. Moreover, selected bnAbs displayed protection against infection caused by all three major human beta-coronaviruses—SARS-CoV-2, SARS-CoV-1, and MERS-CoV which are known to cause severe diseases. This discovery holds immense promise in developing strategic vaccine approaches to prompt the generation of such broadly neutralizing antibodies. Additionally, it expands the array of options for antibody-driven preventive and therapeutic approaches. The stem helix within the S2 region emerges as a plausible and targetable element for intervention strategies. Notably, a range of anti-SH (stem-helix) neutralizing antibodies, displaying varying degrees of cross-reactivity and cross-neutralizing activity against coronaviruses, have been identified. These antibodies have been either isolated from convalescent COVID-19 patients or induced through immunization in mice. [43]

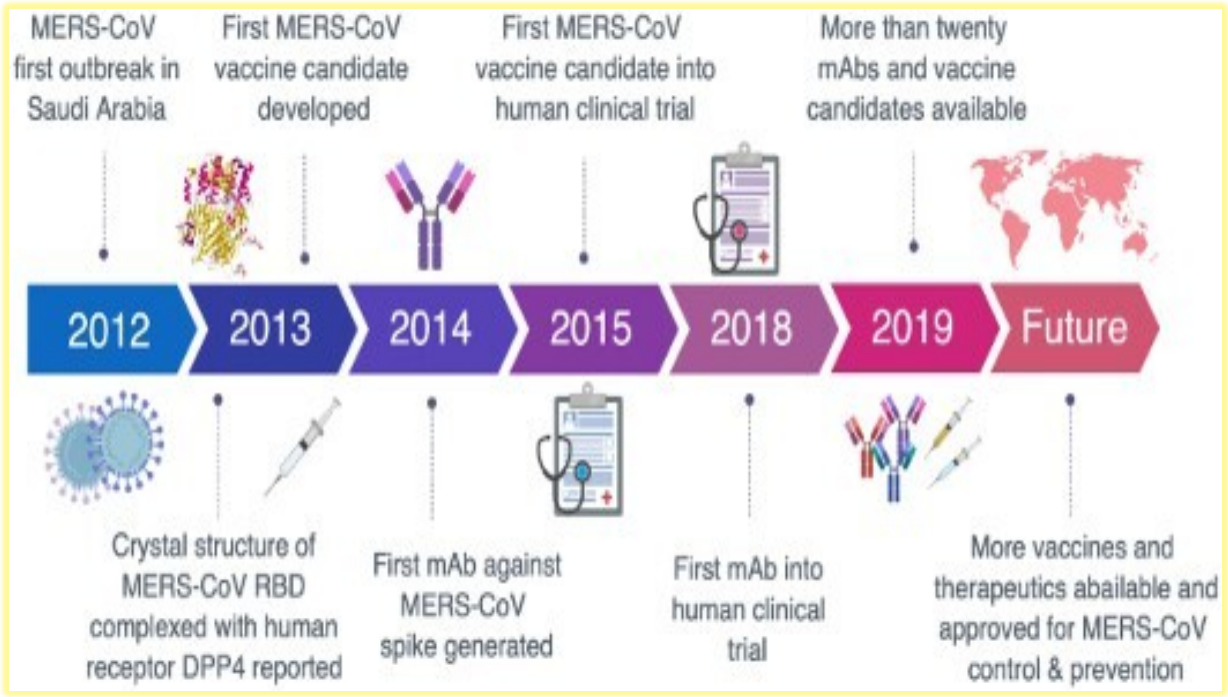

Figure I-9 Antibodies and vaccines against Middle East respiratory syndrome coronavirus[63]

The structural insights into the recognition of beta-coronaviruses by four specific bnAbs (CC25.106, CC95.108, CC68.109, and CC99.103) were obtained through crystal structures, revealing key details at resolutions spanning 1.9 to 2.9 Å.

Monoclonal antibodies (mAbs) have demonstrated prolonged in vivo half-lives and remarkable stability, paving the way for their advancement as immunotherapeutic agents for both the treatment and prevention of MERS-CoV infections. Notably, RBD-specific neutralizing mAbs and fusion inhibitory HR2 peptides have exhibited high efficacy in inhibiting MERS-CoV entry. However, these agents target distinct phases of viral entry: while RBD-specific neutralizing mAbs hinder viral attachment to the cell surface receptor, HR2 peptides impede viral fusion with the host cell membranes. Considering their complementary modes of action in combating MERS-CoV, combining neutralizing mAbs with HR2 peptides holds promise for a potential synergistic effect against MERS-CoV infection. This combination could potentially

enhance therapeutic efficacy by simultaneously impeding different stages of the viral entry process. [43]

CHAPTER III

METHODS & MATERIALS

II. Methods and Materials

MERS-CoV, a zoonotic virus, poses a significant global public health risk. Therefore, it's crucial to create an efficient treatment plan against it. Immuno-informatics and computational biology tools offer a quicker and more cost-efficient way to design potential therapies for MERS-CoV. [49]

Several treatment approaches have been linked to better clinical outcomes for MERS [50] In recent decades, monoclonal antibodies (mAbs) have emerged as a vital and swiftly expanding category of therapeutic substances, finding use across diverse disease fields. They stand among the top-selling and rapidly advancing therapies on the market, with applications spanning various significant medical conditions, including infectious diseases. [51]

Monoclonal antibodies (mAbs) show promise in preventing and treating newly emerged variants of concern (VOC) and infections originating from animals. Specifically, mAbs that target the stem helix of HCOV have been employed in treatments. [50] Numerous studies and experiments indicate that broadly neutralizing antibodies (bnAbs) are the most effective therapeutic agents against MERS-CoV. In our present research, we utilized molecular docking to assess how select bnAbs could neutralize the MERS stem helix. Understanding the structural foundation of antibody-antigen interactions is essential in designing effective biological drugs centered on antibodies.

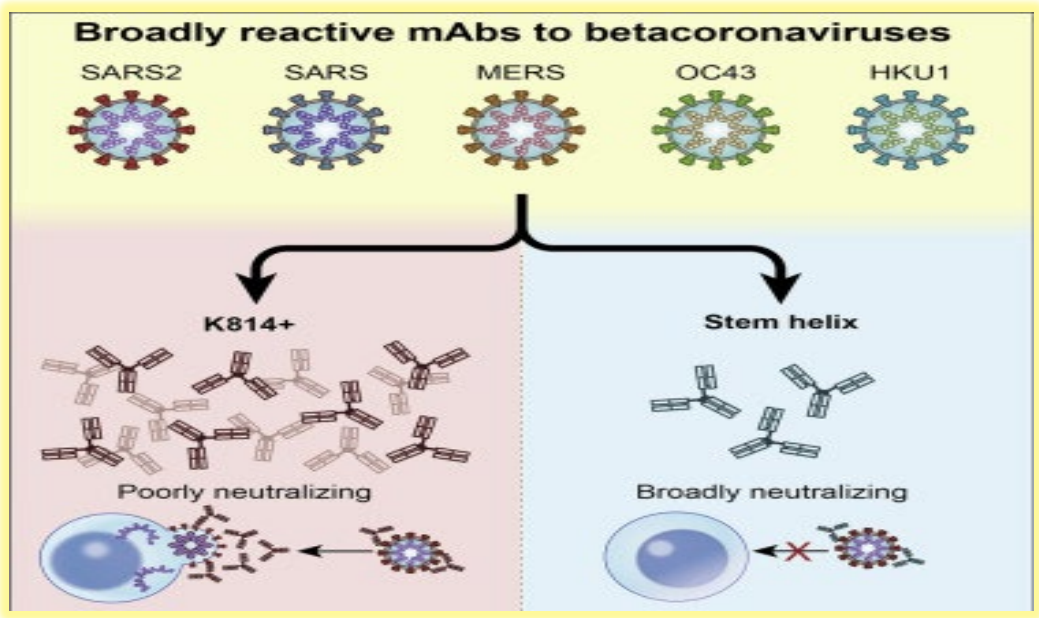

Figure II-1 Broadly neutralizing mAbs use IGHV1-46 and target conserved residues on the stem helix [64]

Antibodies exhibit a Y-shaped structure, typically formed by two identical pairs of polypeptide chains known as light and heavy chains. Based on their variability in structure and sequence, distinct variable and constant domains can be identified. Specifically, the light chain contains one variable and one constant domain, while the heavy chain comprises one variable and three or more constant domains. The variable domain consists of a conserved framework housing six hypervariable loops (HV loops), three from each chain, forming the complementarity-determining regions (CDRs). These regions, especially the HV loops, play a pivotal role in antigen recognition and specificity. [52]

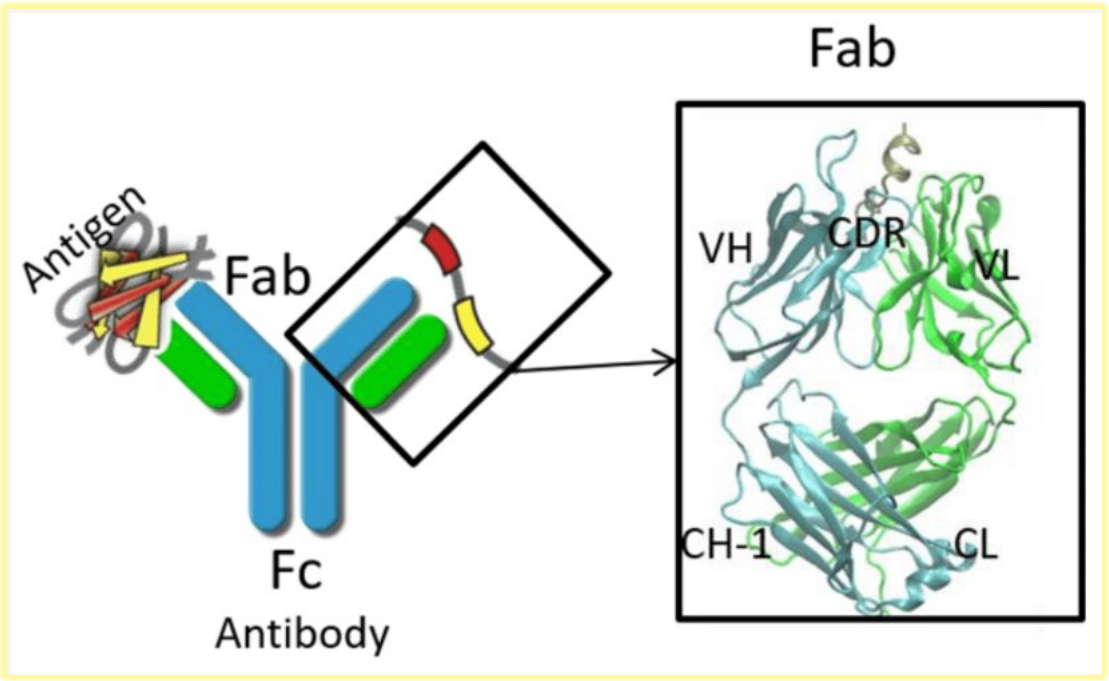

Figure II-2 Schematic representation of an antibody with Fab region and Fc region.[65]

In the realm of research, computational methods like molecular docking offer a rapid and valuable alternative to experimentally characterizing the structures of these antibody-antigen complexes. [52] Accurately predicting the structures of antibody-antigen complexes and using this knowledge for structure-based antibody design remain significant hurdles in computational biology. These challenges have far-reaching implications in areas such as biotherapeutics, immunity, and vaccine development. [53] While antibody recognition of antigens mainly occurs within the complementarity-determining regions (CDR) loops, modeling antibody-antigen interactions presents a distinct computational challenge. Despite this challenge, the vital role of antibody-antigen recognition in therapeutics and disease has driven the development of numerous predictive docking algorithms tailored for these complex interactions. Consequently, docking has emerged as an increasingly crucial tool in pharmaceutical research. [53]

The docking process involves two basic steps: prediction of the ligand conformation as well as its position and orientation within these sites (usually referred to as pose) and assessment of the binding affinity. These two steps are related to sampling methods and scoring schemes, respectively. [55]

III.1. Data collection

Performing molecular docking between the stem helix of MERS-CoV or SARS-CoV-2 and five distinct bnAbs using HADDOCK and AutoDock Vina sounds like an insightful study. It's notable that four of these bnAbs were chosen from a panel established in Zhou. P. et al.'s research. This specific panel of β-CoV spike stem-helix bnAbs was created by utilizing SARS-CoV-2 and MERS-CoV S proteins as baits. They isolated 40 stem-helix mAbs from 10 COVID-19 convalescent donors by targeting antigen-specific single B cells. This approach could provide valuable insights into the interactions between these antibodies and the viral stem helices. [43]

The scrutiny involved in this study aimed to ascertain the interaction and orientation between the two molecules, elucidating the precise binding between the antigen and the antibodies, as detailed in reference [54]. This analysis likely focused on understanding the specific binding mechanisms and configurations between the antigen, either the MERS-CoV or SARS-CoV-2 stem helix, and the five distinct bnAbs, shedding light on their interaction patterns.

The selected bnAbs, CC25.106, CC95.108, and CC99.103, were obtained from Zhou. P. et al.'s research, where their crystal structures were determined in association with beta-coronavirus spike stem-helix peptides. These structures, available at resolutions between 1.9 to 2.9 Å, were retrieved from the RCSB Protein Data Bank using accession codes 8DGU, 8DGV, and 8DGW. The aim was to comprehensively understand how these antibodies recognize beta-coronaviruses at a structural level.

CC9.113, also from Zhou. P. et al.'s study, lacked experimental structural data but was selected based on favorable EC50 and IC50 values. The concepts of IC50 and EC50 are fundamental to pharmacology. The EC50 is the concentration of a drug that gives half-maximal response. The IC50 is the concentration of an inhibitor where the response (or binding) is reduced by half.

To bridge this gap, its structure was predicted using the AlphaFold 2 server, providing an estimation of its molecular configuration.

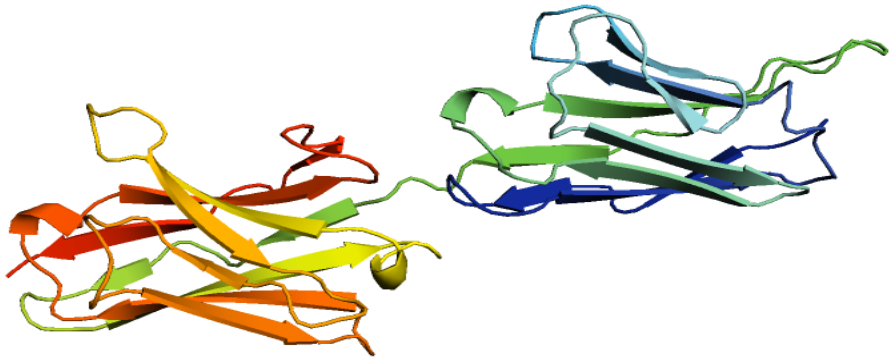

Figure II-3 CC9.113 structure predicted by AlphaFold2 and visualized by PyMOL

CC25.36, sourced from Song, G.'s research, had its crystal structure determined while binding to the RBD (Receptor Binding Domain) of SARS-CoV-2. The process involved cloning HC and LC variable regions into expression vectors, followed by determining the CC25.36/RBD/CV38–142 complex's crystal structure using X-ray techniques. Despite efforts to access the specific structures with accession codes 8SIQ, 8SIR, 8SIS, 8SIT, 8SDF, 8SDG, and 8SDH from the RCSB Protein Data Bank, they were found as unreleased structures (HPUB: processing complete, entry on hold until publication). Consequently, the structure of CC25.36 was predicted using the AlphaFold 2 server to gain insights into its molecular configuration.

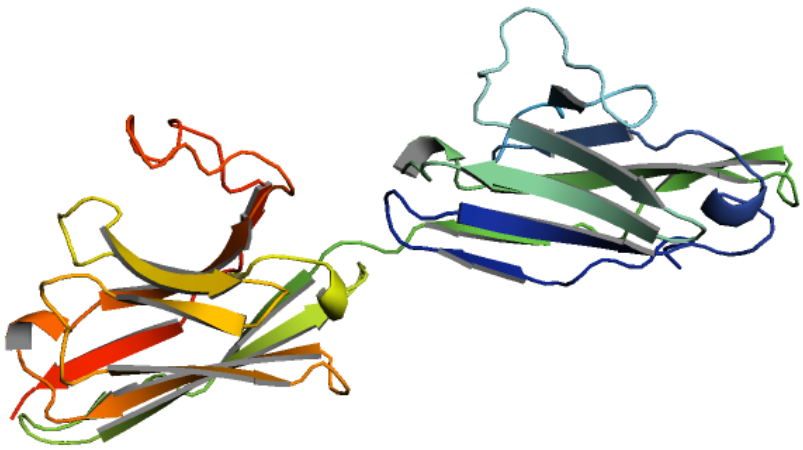

Figure II-4 CC25.36 structure predicted by AlphaFold2 and visualized by PyMOL

III.2. HADDOCK 2.4

The emergence of docking web servers, such as HADDOCK, signifies a growing interest in utilizing these platforms. HADDOCK (High Ambiguity Driven protein-protein DOCKing) [66] is an information-driven flexible docking method designed for modeling biomolecular complexes.

HADDOCK (see: https://www.bonvinlab.org/software/haddock2.4) is a collection of python scripts derived from ARIA (https://aria.pasteur.fr) that harness the power of CNS (Crystallography and NMR System – https://cns-online.org) for structure calculation of molecular complexes. What distinguishes HADDOCK from other docking software is its ability, inherited from CNS, to incorporate experimental data as restraints and use these to guide the docking process alongside traditional energetics and shape complementarity. Moreover, the intimate coupling with CNS endows HADDOCK with the ability to actually produce models of sufficient quality to be archived in the Protein Data Bank.

In a study conducted by Ambrosetti.F et al., investigators explored leveraging information about complementarity-determining regions and binding epitopes to guide the modeling process. They conducted a comparative analysis of four docking software

suites—ClusPro, LightDock, ZDOCK, and HADDOCK—specifically tailored for antibody-antigen modeling. Their study, based on a dataset of 16 complexes, revealed that HADDOCK, incorporating information to steer the docking process, exhibited superior performance. It outperformed other platforms in terms of both success rate and the quality of generated models, regardless of whether information about the epitope on the antigen was available or not. [52]

We will make use of the HADDOCK2.4 webserver, PyMOL, PDB2PQR, APBS, proABC-2 and PDB-tools webserver. These tools collectively enable researchers to perform molecular docking simulations, visualize molecular structures, predict binding sites, validate structures, and conduct various analyses crucial for understanding the interactions between antibodies and antigens at a detailed molecular level.

HADDOCK was designed so that the molecules experience varying degrees of flexibility and different chemical environments, and it can be divided in three different stages, each with a defined goal and characteristics:

- ✓ Randomization of orientations and rigid-body minimization (it0)

In this initial stage, the interacting partners are treated as rigid bodies.

- ✓ Semi-flexible simulated annealing in torsion angle space (it1)

The second stage of the docking protocol introduces flexibility to the interacting partners through a three-step molecular dynamics-based refinement in order to optimize interface packing.

- ✓ Refinement in Cartesian space with explicit solvent (water)

The final stage of the docking protocol immerses the complex in a solvent shell so as to improve the energetics of the interaction. HADDOCK currently supports water (TIP3P model) and DMSO environments.

The following comprehensive breakdown outlines the detailed procedure from structure retrieval to docking and analysis:

✓ Obtaining Structures

- Using PDB Files from Database: Download the .pdb files of the bnAbs (CC99.103, CC25.106 and CC95.108) and CoV stem helix (MERS-CoV spike stem helix peptide and SARS-CoV-2 spike stem helix peptide) separately from the PDB database using codes 8DGV, 8DGU and 8DGW. Employ PyMOL to extract the individual structures of the bnAbs and CoV stem helix from the complex.
- Sequence Retrieval and Structure Prediction:
    - In cases without available experimental data, retrieve the sequences from GenBank. For CC25.36 use the codes GenBank: OM467977.1 to get nucleotide sequence, GenBank: UKB92452.1 light chain fasta sequence and GenBank: UKB92346.1 heavy chain fasta sequence.
    - For CC9.113 use the codes GenBank: OP699213.1 to get nucleotide sequence, GenBank: WBW48684.1 light chain fasta sequence and GenBank: WBW48644.1 heavy chain fasta sequence.
    - Utilize AlphaFold2 for predicting the 3D structures of the CC9.113 and CC25.36 bnAbs stem helix based on their sequences.

✓ Utilizing PDBTools Web Pipeline:

- Use the PDBTools web interface to upload the .pdb files. Apply the following pipeline:
- Preprocessing: pdb_splitchain
- Main: pdb_delhetatm and pdb_tofasta

✓ Identifying bnAb Paratope:

- Use the generated .fasta files to determine the paratope of bnAb utilizing ProABC2.

✓ Preprocessing bnAb Structure:

- Apply PDB_Tools for preprocessing the bnAb structure:
- pdb_chain to rename all chains as 'A'.
- pdb_reres to renumber the antibody residues uniquely.

✓ Inspecting Structures using PyMOL:

- Visualize the bnAb structure in PyMOL:
- Highlight the predicted paratope. Inspect the predicted binding site. Examine the surface characteristics of the bnAb structure.

✓ HADDOCK2.4 Docking:

- Input data: Input the prepared .pdb files into HADDOCK:
  - Upload the bnAb.pdb file as the protein (Molecule 1).
  - Upload the CoV sh.pdb file as the peptide (Molecule 2).
  - Keep the parameters as default only check on for Fix molecule at its original position during it0?
- Input parameters:
  - Select active residues from the reference study and ProABC2 file.
  - Passive residues (surrounding surface residues) would be automatically defined around the active residues. Keep other parameters as default.
- Docking parameters:
  - Set these parameters as follows:
    - Number of structures for rigid body docking= 10000
    - Number of structures for semi-flexible refinement=400
    - Number of structures for the final refinement=400
    - Number of structures to analyze=400

- Keep all other parameters as default.
- Check COVID-19 related parameters and submit the job.

✓ Results Analysis using PyMOL:

- Analyze the HADDOCK results in PyMOL to visualize the docked complex. Assess the interactions between bnAb and CoV stem helix based on the docking results.

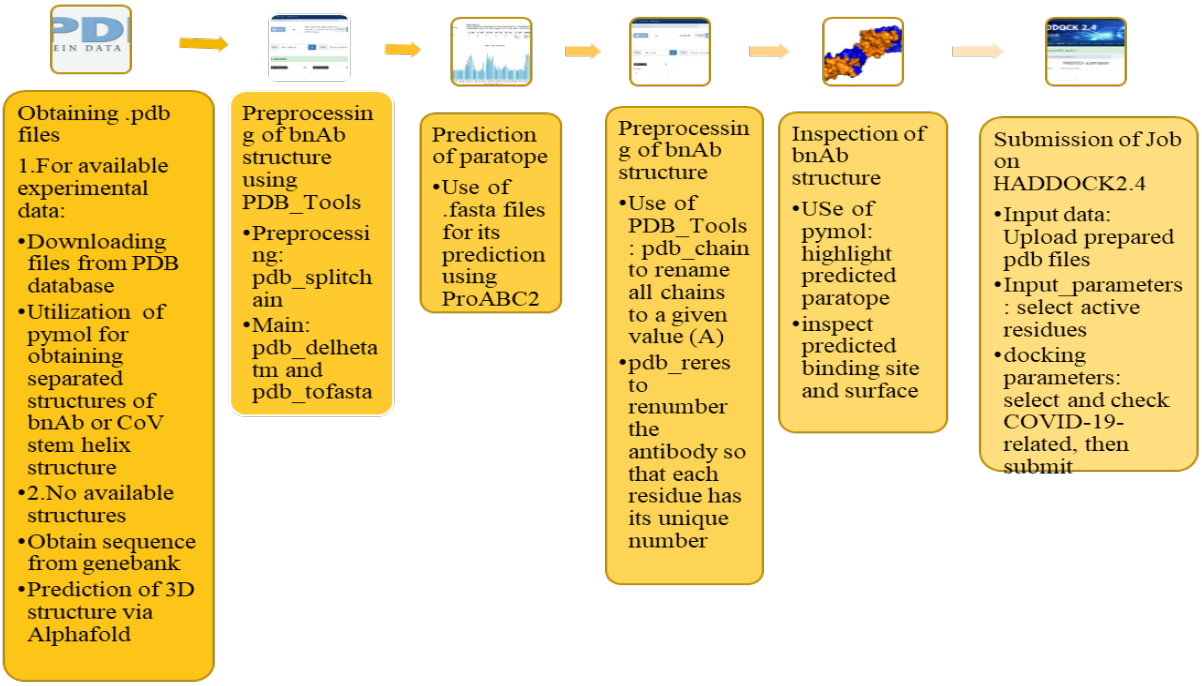

Figure II-5 HADDOCK submission protocol

III.3. AlphaFold2

AlphaFold is an AI system developed by DeepMind that predicts a protein's 3D structure from its amino acid sequence. [67]

III.4. PyMOL

PyMOL is a widely used tool for visualizing and analyzing molecular structures.

Launched over Christmas break in December 1999, PyMOL was originally designed to: (1) visualize multiple conformations of a single structure [trajectories or docked ligand ensembles] (2) interface with external programs, (3) provide professional

strength graphics under both Windows and Unix, (4) prepare publication quality images, and (5) fit into a tight budget

High-Quality Rendering: It provides high-quality graphics and visualization capabilities, allowing users to generate publication-ready images and videos of molecular structures.

Manipulation and Analysis: PyMOL enables users to manipulate, analyze, and annotate molecular structures, highlighting specific regions, bonds, or interactions within the complex structures.

Utilize PyMOL for visualizing and analyzing the docked complexes generated by HADDOCK2.4 and AutoDockVina and visualize the electrostatic interaction, a result from APBS (Adaptive Poisson-Boltzmann Solver). It will allow you to create detailed and high-quality visual representations of these molecular interactions, aiding in the illustration and explanation of binding orientations. [68]

III.5. proABC-2

The proABC-2 server is freely available at: https://wenmr.science.uu.nl/proABC2/.

Understanding the fundamentals of antibody–antigen interactions is a critical step for the rational design and engineering of immunoglobulins. proABC-2 is based on a deep learning framework and shows a high performance with an AUC of 0.96 and an MCC of 0.57. proABC-2 predictions can be used to drive the modeling of antibody–antigen complexes using the information-driven docking approach HADDOCK.

The input is processed to calculate all of the sequence-derived features (germline, canonical structures and length of the HV loops), and these are passed to the CNN to make the predictions. The computation only takes a few seconds. [69]

III.6. PDB-Tools Web

PDB-Tools Web is a user interface for the pdb-tools Python package. The classic Protein Data Bank (PDB) file format is a flat text file that is still used by many structural biology software to represent the spatial coordinates of macromolecular structures. PDB-tools web is a fully configurable, user-friendly web interface for the command-line application pdb-tools. Using the portal users can, in a few clicks, build a complex pipeline which can then be saved (and uploaded) for future use and reproducibility. This pipeline is composed by different processing blocks with atomic tasks on the PDB provided data, to name a few, removing certain atom types, renaming chains, renumbering residues, removing multiple occupancies or detecting gaps among many others. [70] The webserver is available at https://wenmr.science.uu.nl/pdbtools/ and the list of all available processing blocks is described on the online manual at https://wenmr.science.uu.nl/pdbtools/manual.

III.7. PDB2PQR

PDB2PQR simplifies the preparation of structures for continuum solvation calculations and various biomolecular modeling tasks. It streamlines tasks like adding missing atomic coordinates and assigning crucial force field parameters for accurate continuum electrostatics methods, aiding experts and non-experts in conducting electrostatic analyses. Its functions include adding missing heavy atoms, estimating titration states, assigning charges and radii, and producing compatible PQR outputs for multiple computational packages.

https://server.poissonboltzmann.org/

https://pdb2pqr.readthedocs.io/en/latest/

III.8. APBS

Understanding electrostatic interactions is crucial in studying biomolecular processes. With the rapid determination of protein and biopolymer structures,

integrating this knowledge into physical models for drug discovery requires assessing energetic interactions within these molecules and their connections in cellular pathways. Solvation properties and electrostatic interactions, due to their long-range nature and significant charges in biopolymers, hold special importance.

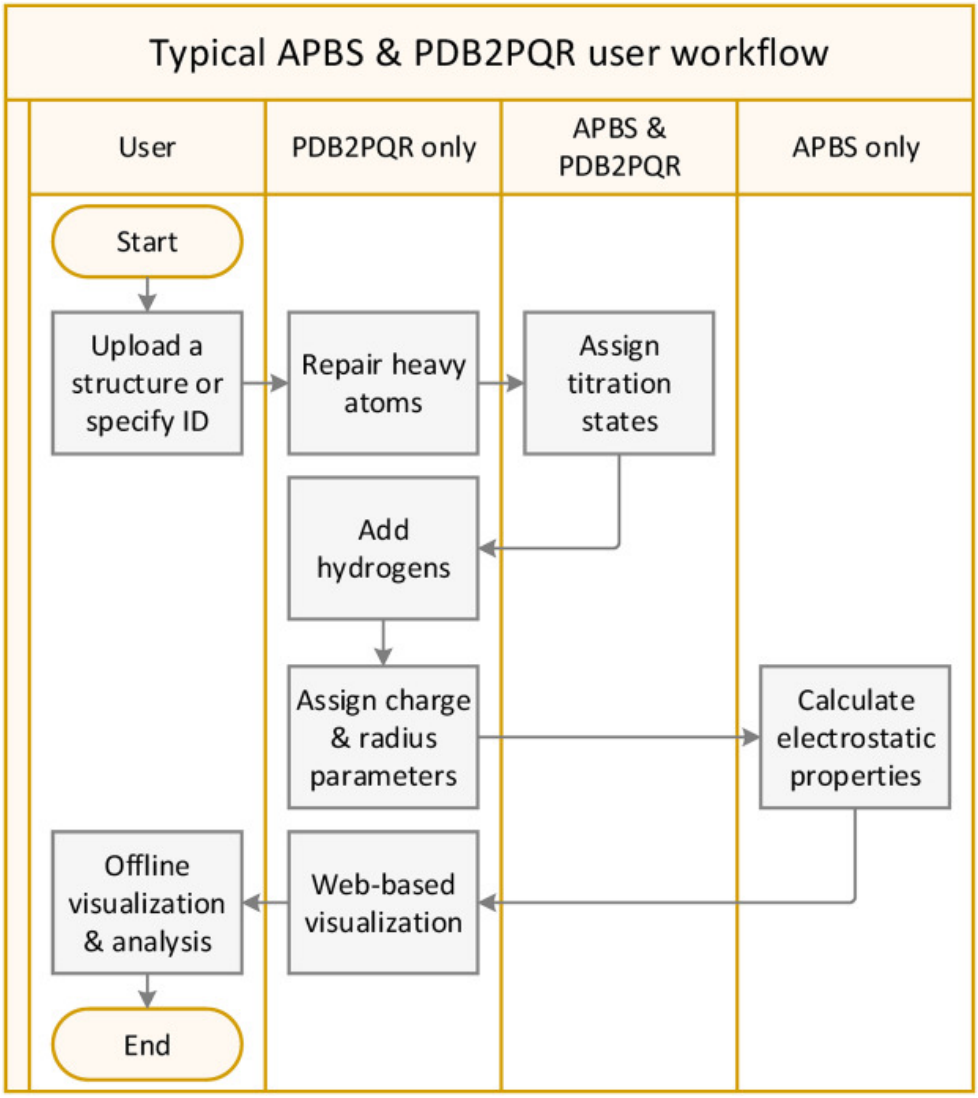

Figure II-6 Workflow for biomolecular electrostatics calculations using the APBS-PDB2PQR software suite.

APBS tackles continuum electrostatic equations for large biomolecular assemblies. Built with modern design principles, it seamlessly interfaces with various computational packages and adapts to evolving methods. Extensive documentation for users and programmers, along with utilities for calculations and analysis, supports the

APBS code. Moreover, its free, open-source license ensures accessibility across the biomedical community.

https://server.poissonboltzmann.org/

https://apbs.readthedocs.io/en/latest/

III.9. AutoDockVina

AutoDock Vina (https://vina.scripps.edu/) is arguably one of the fastest and most widely used open-source docking engines. It was originally designed and implemented by Dr. Oleg Trott (http://olegtrott.com/) in the Molecular Graphics Lab (now CCSB (https://ccsb.scripps.edu/)) at The Scripps Research Institute.

AutoDock Vina facilitates the design and execution of simple and complex docking simulations. The new version provides Python bindings, enabling easier scripting for virtual screening and other advanced applications. [71]

A detailed guide for docking using AutoDock Vina after obtaining the .pdb files for bnAbs and CoV stem helix peptides:

✓ Structure Preparation:

- Use PyMOL to extract the individual structures of the bnAb (selecting only FV) or CoV stem helix

✓ BnAb.pdbqt File Preparation:

- Process the bnAb.pdb file:
- Delete water molecules and heteroatoms, add polar hydrogens, assign Kollman charges, assign AD4 types and finally save the prepared structure as a .pdbqt file.

✓ CoVsh.pdbqt File Preparation:

- Process the CoV stem helix (CoVsh.pdb) file:

- Delete water molecules and heteroatoms, add polar hydrogens, add Gasteiger charges and then save the prepared structure as a .pdbqt file.
- Choose and detect root from the torsion tree.

✓ Grid Generation:

- Determine the diameters of the grid box around the binding site. Create a config.txt file with grid dimensions and other necessary parameters.

✓ Running Autodock Vina:

- Execute Autodock Vina with the prepared .pdbqt files and the configuration file. Allow Autodock Vina to perform the docking calculations.

✓ Results Processing:

- Use vina-split.exe to process and split the results obtained from Autodock Vina.
- Extract and analyze the docking poses and scores generated by Autodock Vina.

✓ Results Analysis calculations using the APBS-PDB2PQR software suite and PyMOL:

- Use APBS to solve properties and electrostatic interactions.
- Utilize PyMOL to visualize and analyze the docking results.
- Inspect the docked conformations of bnAb and CoV stem helix complexes to understand their binding interactions.

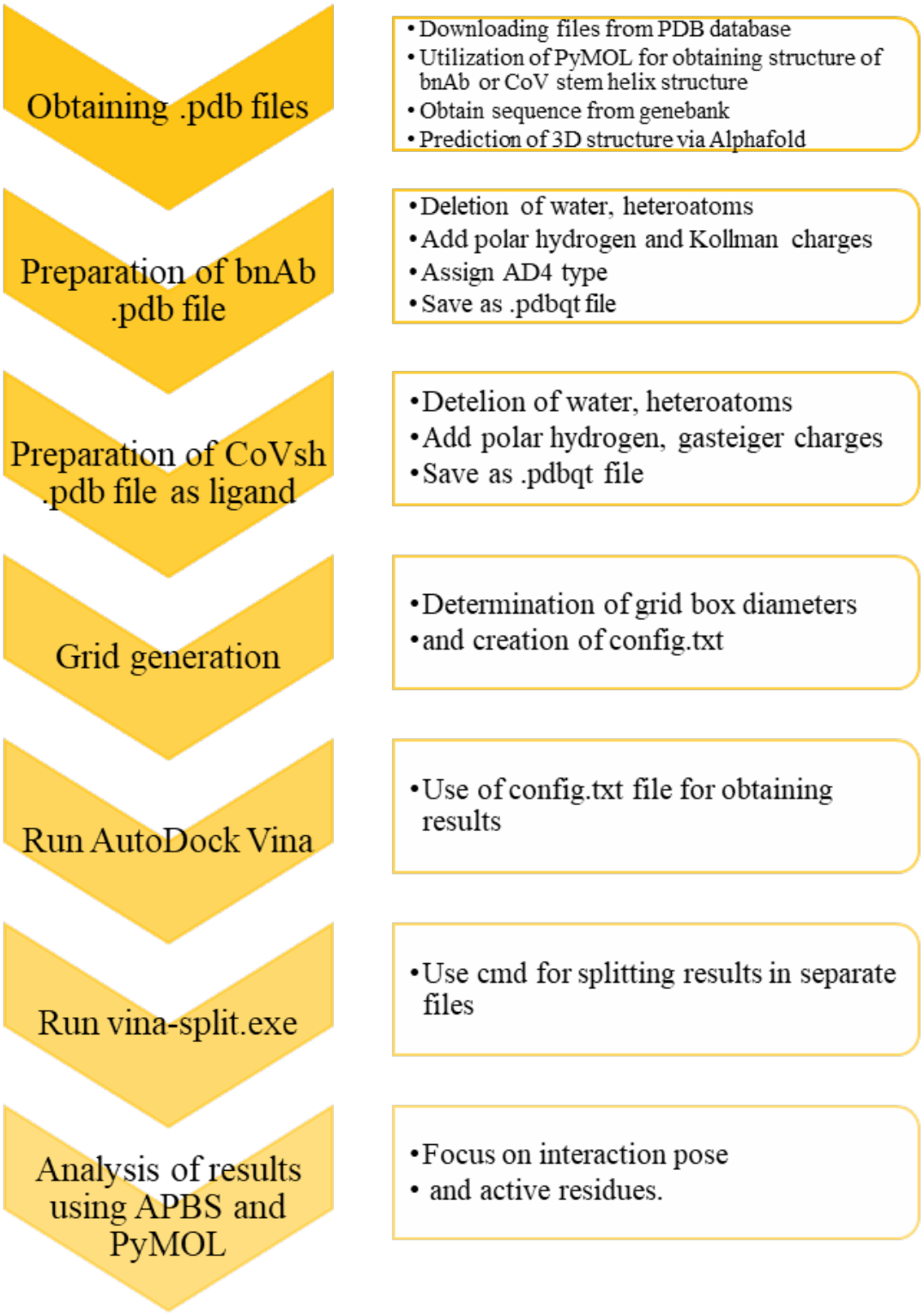

Figure II-7 Autodock Vina Protocol

CHAPTER IV

RESULTS & DISCUSSION

III. Results and Discussion

IV.1. Results

Understanding the binding poses and affinity between an antigen and antibody holds immense significance in computer-aided drug design. During the initial phases of drug discovery projects, obtaining this information commonly involves employing molecular docking methods.

In this case, the molecular docking process was conducted utilizing two distinct software tools: AutoDock Vina and HADDOCK2.4. These software programs are instrumental in predicting and analyzing how molecules interact, thereby revealing potential binding orientations and the strength of interactions between the antigen and antibody. Assessing the performance and outcomes of these tools is essential in determining their accuracy in predicting binding poses and affinity, crucial aspects guiding the discovery and design of effective drugs.

IV.1.1. HADDOCK 2.4

Assessing HADDOCK's performance involves two key aspects: sampling success and scoring success.

Sampling Success: This measures whether HADDOCK generates clusters where the ligand assumes the correct binding pose. These acceptable poses typically exhibit an interface RMSD of less than 2 Å from the crystal structure. While HADDOCK's scoring function helps distinguish between acceptable and unacceptable poses based on energetic stability, it hasn't been proven how consistently this scoring function correctly ranks ligands with similar affinities. Hence, crystal structures remain essential to confirm the most acceptable complexes.

Scoring Success: This evaluation is crucial to determine HADDOCK's overall docking performance. If scoring success is achieved, the top-scoring cluster should represent an acceptable binding pose. In an ideal scenario, total scoring success would eliminate the need for crystal structures to identify clusters replicating the native binding pose.

Both sampling success and scoring success play vital roles in comprehensively assessing HADDOCK's performance in generating accurate protein-ligand complexes without solely relying on crystal structure verification. [72]

Based on the chosen parameters, only the top 400 highest-scoring structures out of the initial 10,000 generated during rigid body minimization proceed to undergo semi-flexible annealing. Subsequently, these same 400 structures advance to the final refinement stage. Consequently, each HADDOCK submission predicts a total of 400 final complexes. The 400 final complexes from the HADDOCK submission undergo assessment through ranking and scoring similar to the evaluation performed during the initial docking protocol. After scoring, these complexes are then clustered together based on their structural similarity. This clustering helps identify groups of complexes that share similar structural characteristics among the selected top-scoring 400 structures.

The HADDOCK scoring function encompasses a linear combination of diverse energies and buried surface area, which varies across the different stages of docking (rigid body (it0), semi-flexible refinement (it1), and explicit solvent refinement (water)).

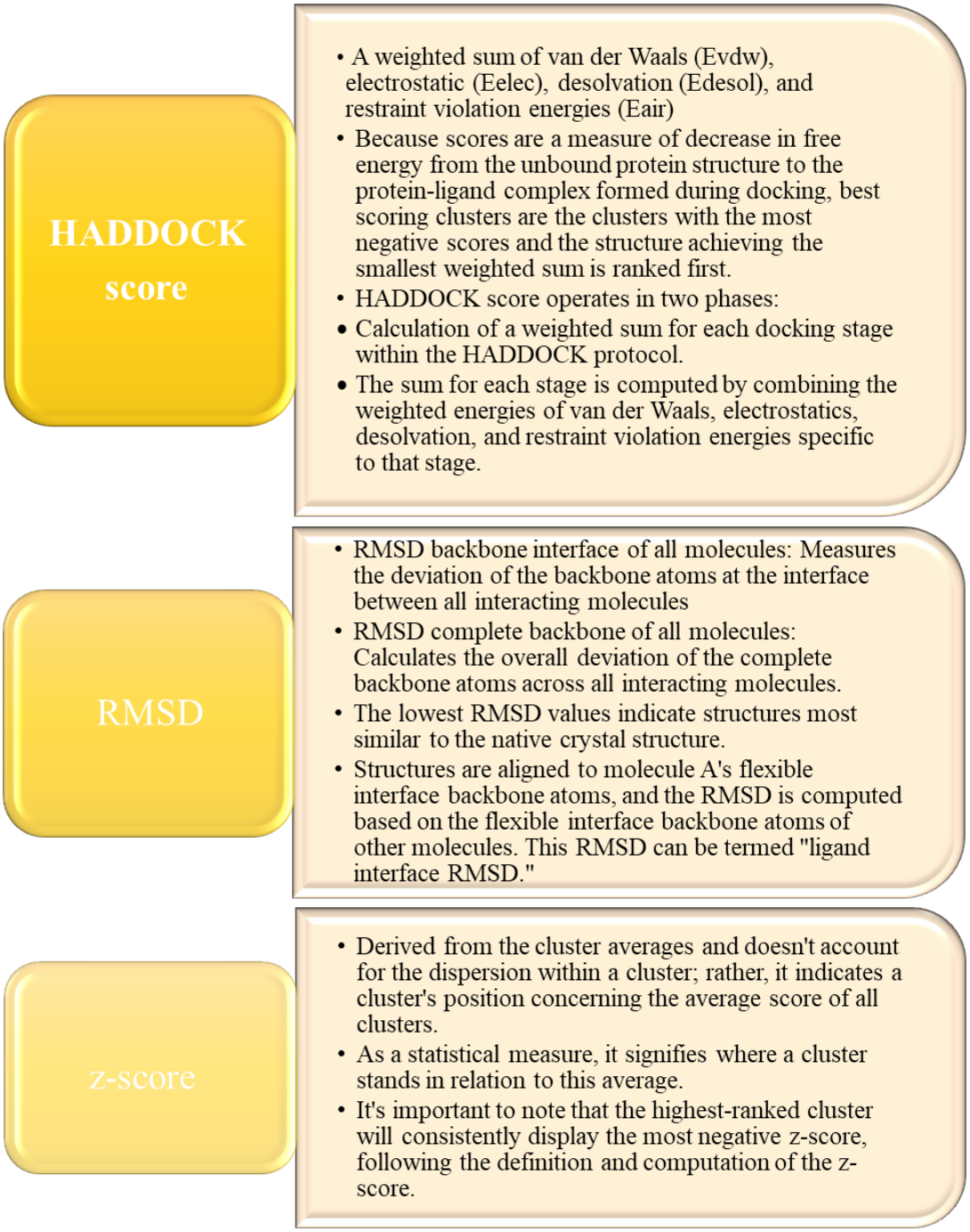

Figure III-1 Docking parameters

Table III-1 HADDOCK Results

Docking Complex	Cluster	HADDOCK score	RMSD [1]	Z-Score
CC25.106 MERS-COV stem helix SH	23 Clusters Cluster2	-75.0 +/-2.2	0.2 +/-0.1	-2.2
CC25.106 SARS-COV-2 stem helix SH	2 Clusters Cluster1	-164.2 +/-1.4	2.3 +/-1.9	-1.0
CC95.108 MERS-COV stem helix SH	10 Clusters Cluster1	-120.6 +/-1.2	0.1 +/-0.1	-2.7
CC95.108 SARS-COV-2 stem helix SH	11 Clusters Cluster2	-79.9+/-3.0	0.3 +/-0.2	-1.7
CC99.103 MERS-COV stem helix SH	18 Clusters Cluster1	-107.8 +/ - 2.7	2.4 +/-1.7	-2.2
CC99.103with SARS-COV-2 stem helix SH	18 Clusters Cluster1	-91.1 +/-4.7	0.2 +/-0.1	-2.8
CC9.113 MERS-COV stem helix SH	10 Clusters Cluster1	-23.2 +/-9.1	1.1 +/-0.6	-1.4
CC9.113 SARS-COV-2 stem helix SH	11 Clusters Cluster1	-15.0 +/-7.1	0.9 +/-0.6	-1.9
CC25.36 MERS-COV stem helix SH	20 Clusters Cluster2	-19.0 +/-6.7	0.6 +/-0.4	-2.2
CC25.36 SARS-COV-2 stem helix SH	14 Clusters Cluster3	6.0 +/-1.8	2.1 +/-0.3	-1.3

[1] from the overall lowest energy structure

IV.1.2. AutoDock Vina

The docking effects were evaluated by the affinity value. The affinity values <−5 kcal/mol represent good binding interaction between bnAbs and CoV stem helix peptide.

In AutoDock results, "Dist from RMSD l.b." typically refers to the distance or deviation of the Root Mean Square Deviation (RMSD) from the lowest bound (l.b.). This parameter helps measure how far the RMSD value of a docked structure is from a reference or the most optimal bound conformation. It indicates the structural variation or similarity of the docked pose concerning a known or expected conformation, often the reference ligand-bound structure.

"Best mode RMSD u.b." in AutoDock results typically denotes the Root Mean Square Deviation (RMSD) of the best or most favorable docking mode from the upper bound (u.b.). This value represents the deviation or difference between the docked pose considered the best mode and a specified upper bound, often a reference or ideal structure. It indicates how closely the best predicted pose aligns with the upper bound or an expected conformation.

The docking conformations were superimposed on the crystal structure. The corresponding binding affinities, Distance from RMSD lowest bound and best mode RMSD upper bound are listed in Table 2

Table III-2 AutoDock Vina results

Docking Complex	Affinity (kcal/mol)	Dist from rmsd l.b.	best mode rmsd u.b.
CC25.106 MERS-COV stem helix SH	-10.8	0.00	0.00
CC25.106 SARS-COV-2 stem helix SH	-21.8	0.00	0.00
CC95.108 MERS-COV stem helix SH	-12.5	0.00	0.00
CC95.108 SARS-COV-2 stem helix SH	-11.1	0.00	0.00
CC99.103 MERS-COV stem helix SH	-17.2	0.00	0.00
CC99.103 SARS-COV-2 stem helix SH	-11.3	0.00	0.00
CC9.113 MERS-COV stem helix SH	-12.3	0.00	0.00
CC9.113 SARS-COV-2 stem helix SH	-12.0	0.00	0.00
CC25.36 MERS-COV stem helix SH	-11.2	0.00	0.00
CC25.36 SARS-COV-2 stem helix SH	-11.1	0.00	0.00

IV.1.3. APBS and PDB2PQR

PDB2PQR software is part of the APBS suite that was developed to assist with the conversion of PDB files to PQR format. The PQR file simply replaces the temperature and occupancy columns of a PDB flat file with the per-atom charge (Q) and radius (R). [23]

PyMOL can display the results of the calculations as an electrostatic potential molecular surface. The potentials are on a [-5,5] red–white–blue color map in units of kJ/mol/e. Color-coded electrostatic surface where red indicates negatively charged regions of the surface, white neutrally charged and blue positively charged one.

IV.1.4. PyMOL

In addition to employing molecular docking tools like AutoDock Vina and HADDOCK2.4, the analysis of their results often involves the utilization of visualization software like PyMOL. PyMOL plays a pivotal role in the post-docking analysis by providing a comprehensive platform to visualize and interpret the generated molecular structures.

Its functionality allows to visually inspect and analyze the predicted binding poses between the antigen and antibody obtained from the docking simulations. PyMOL enables the exploration of complex molecular interactions, facilitating a deeper understanding of the structural aspects governing the binding affinity and interactions between these molecules. This visualization aids in assessing the plausibility and accuracy of the predicted binding modes, offering valuable insights crucial for subsequent steps in drug design and discovery efforts.

The following Tables and Figures display the results analyzed using PyMOL.

Table III-3 MERS' Docking residues

MERS		CC25.106	CC95.108	CC99.103	CC9.113	CC25.36
HADDOCK2.4	H_bond Residues	ASP31 HIS35 LYS52 SER53 ASN56 ARG58 TRP306	TYR33 ARG98	ILE97 TYR233	ARG55 SER77 ARG78 ARG211	PRO14 ASP62 THR78 ARG143 VAL211 TYR214
	Binding site Residues	THR30 ASP31 TYR32 TYR33 HIS35 LYS52 SER53 ASN56 THR57 ARG58 GLY96 VAL98 HIS99 ASN245 ASN246 TRP306 ASP307 ASN309 LEU310	THR3 ASP31 SER32 TYR33 ILE50 LYS52 SER53 ASP96 ARG98 THR243 PHE245 TRP304 ASP305 SER306 THR307	SER31 ASP32 TYR33 ILE50 ASN52 SER55 GLY56 THR57 ARG58 GLY96 ILE97 LEU98 THR99 GLY100 LEU101 ASN232 TYR233 GLY251 THR254 TYR292 GLY293 SER294 SER295 PRO296 PHE298	GLY16 ARG18 SER53 ARG55 ASP61 ARG62 SER64 GLY65 SER66 SER77 ARG78 GLU80 SER141 TRP157 ILE160 SER169 PHE210 ARG211 PRO213	ALA13 PRO14 GLY15 GLN16 ARG17 PRO61 ASP62 PHE64 SER65 ILE77 THR78 GLY79 LEU80 SER142 ARG143 ASN144 TYR161 SER164 ARG208 GLY209 VAL210 VAL211 GLY212 TYR213 TYR214 ASP215 MET216 ASN223 TRP224 LEU225
AutoDock Vina	H_bond Residues	GLU1 GLN37 THR80	LEU4 LYS45 ARG61 GLN105	TYR32 TYR33 SER93 ILE96	TYR88 PHE101	GLY176 SER181 ARG182 ASN194
	Binding site Residues	GLU1 VAL2 GLN3 GLN37 LEU39 PRO40 THR42 PRO44 LYS45 SER56	VAL2 LEU4 THR42 PRO55 SER56 GLY57 ILE58 PRO59 ARG61 GLN79	ASN31 ASP32 TYR33 TYR49 ILE50 ASN52 GLY56 ARG58 TYR91 GLY92	PRO41 GLY42 THR100 PHE101 PRO103	SER128 ARG130 ILE162 SER163 SER154 SER165 GLY166 SER167 GLY176 ARG177

Experimental Results

	PRO59 PHE62 GLN79 THR80 GLY81 GLU83 TYR102 TRP103 GLN109	GLY81 ILE101 PHE102 TRP103 GLY104 GLN105	PRO95 PHE96 GLY99 LEU100		PHE178 SER179 ILE180 SER181 ARG182 ASP183 ASN184 TYR190 LEU191 ASN194 SER195
H_bond Residues	VL ASN51 LYS66 VH TYR33 LYS52 GLY95 and HIS97	VL ASN51 LYS66 VH TYR33 LYS52 GLY95 and HIS97	VL ASN51 LYS66 VH TYR33 LYS52 GLY95 and HIS97	-	-
Binding site Residues	VH ASN56 VH TYR33 ILE50 ARG98/HIS 97 VL TYR32	VH ASN56 VH TYR33 ILE50 ARG98/HIS 97 VL TYR32	VH TYR33 ILE50 VH THR57 GLY95 ILE96 VL TYR32 TYR91 PHE96 VL PRO95 and PRO95a.	-	-

✓ CC25.106 with MERS-COV stem helix SH HADDOCK results:

Hydrogen bonds ASP-31 ASN-1241 2.1A, HIS-35 GLU-1234 2.5A, LYS-52 ASP-1233 2.3A SER-53 GLU1237 2.2A, ASN-56 ASN1225 2.5A, ARG-58 THR-1227 2.4A, TRP-306 THR-1227 2.1A

Binding site Residues: THR30 ASP31 TYR32 TYR33 HIS35 LYS52 SER53 ASN56 THR57 ARG58 GLY96 VAL98 HIS99 ASN245 ASN246 TRP306 ASP307 ASN309 LEU310

Note1 : The Broadly Neutralizing Antibodies (BnAb) are displayed as sticks with a stick radius of 0.1 and colored according to the CHNOS elements. Meanwhile, the stem helix peptide is depicted in a ball-and-stick representation and colored by element as CHNOS.

Note 2: In the provided images, negatively charged regions of the protein are indicated in red, while positively charged regions are highlighted in blue. This color scheme emphasizes the electrostatic properties of the protein, with red indicating regions with an excess of negative charge and blue representing regions with an excess of positive charge. This visual representation helps identify potential charge-charge interactions within a protein's structure, providing insight into its electrostatic properties.

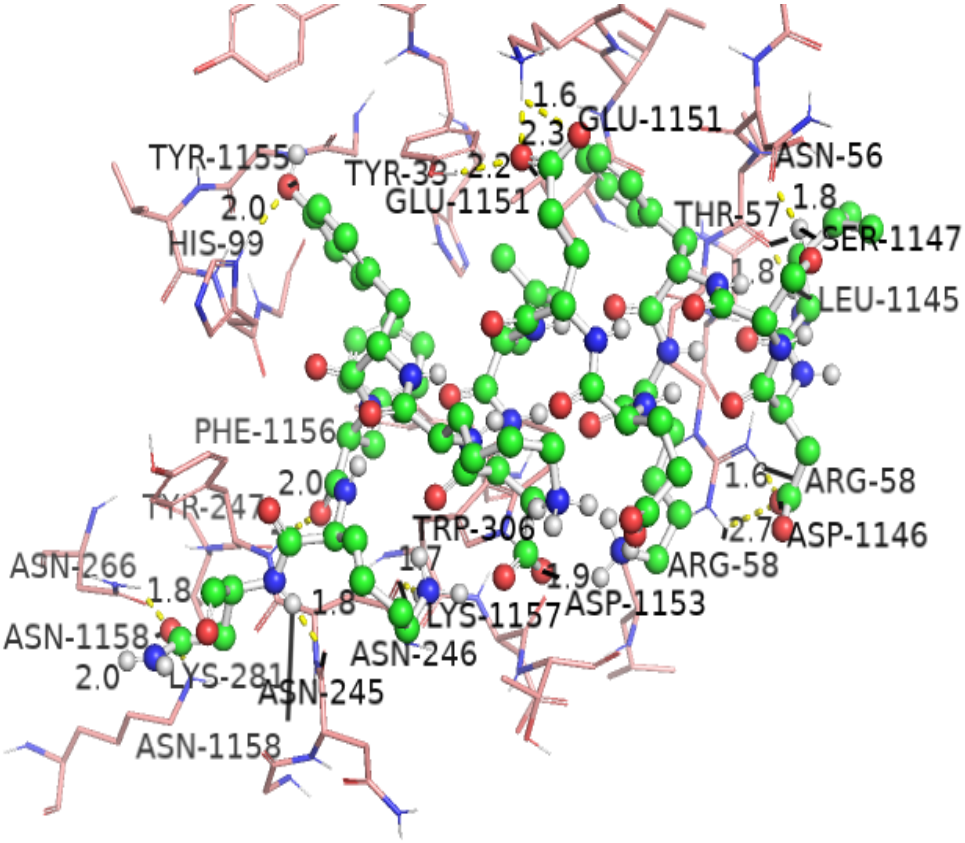

Figure III-2 CC25.106 with MERS-COV stem helix SH HADDOCK H_Bonds visualized by PyMOL

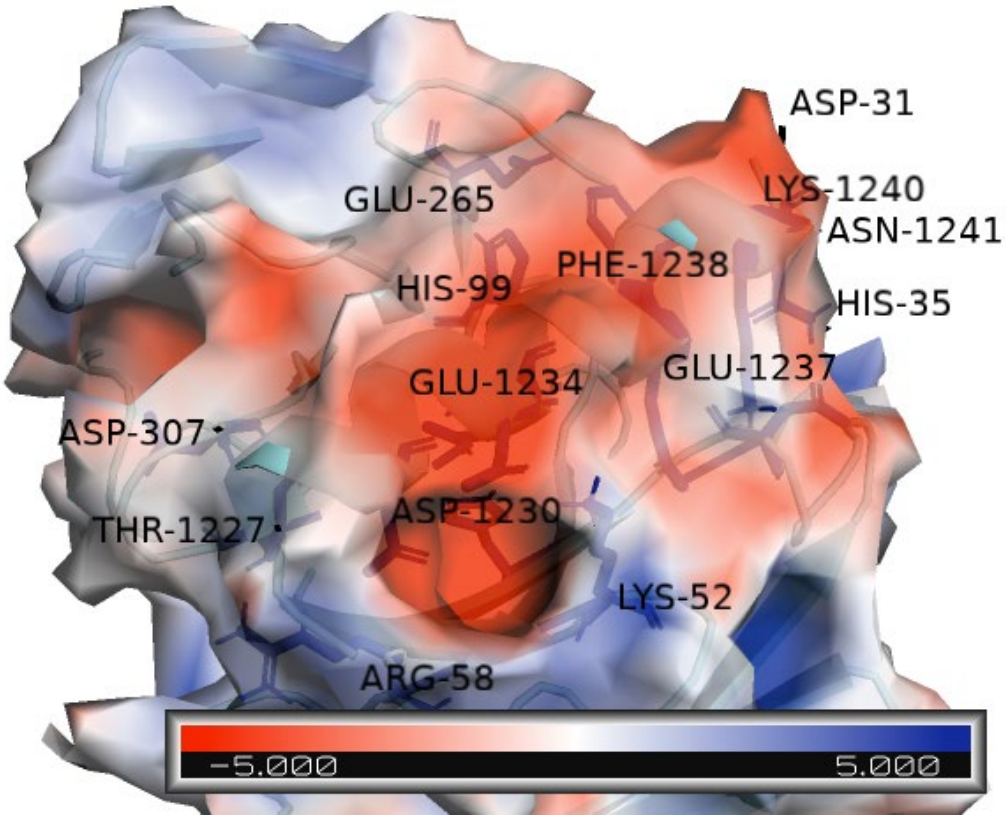

Figure III-3 CC25.106 with MERS-COV stem helix SH HADDOCK electrostatic interaction calculations using the APBS-PDB2PQR software suite, visualized by PyMOL

✓ CC25.106 with MERS-COV stem helix SH AutoDock Vina results:

Hydrogen bonds GLU-1 SER-1226 2.3A, GLN-37 GLU-1234 3.2A, THR-80 GLU-1237 3.1A

binding site Residues: GLU_1, VAL_2, GLN_3, GLN_37, LEU_39, PRO_40, THR_42, PRO_44, LYS_45, SER_56, PRO_59, PHE_62, GLN_79, THR_80, GLY_81, GLU_83, TYR_102, TRP_103, GLN_109

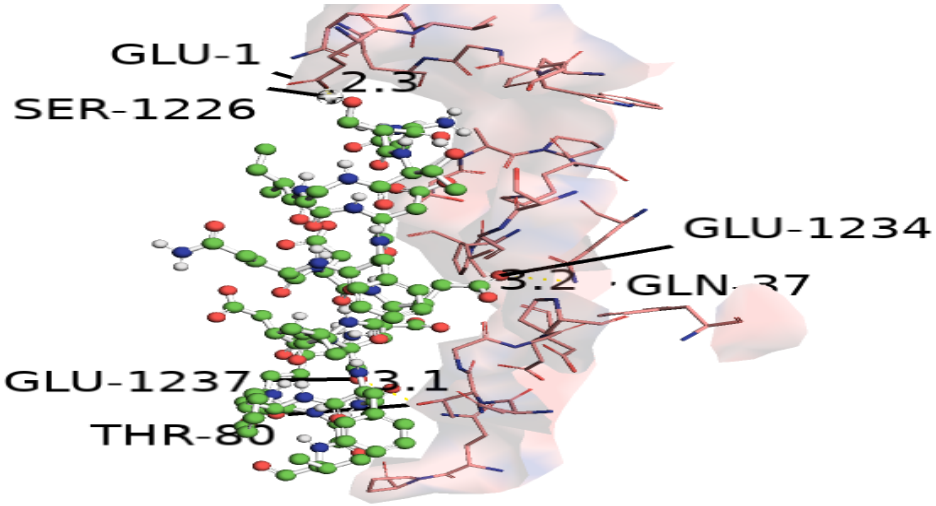

Figure III-4 CC25.106 with MERS-COV stem helix SH AutoDock Vina H_Bonds visualized by PyMOL

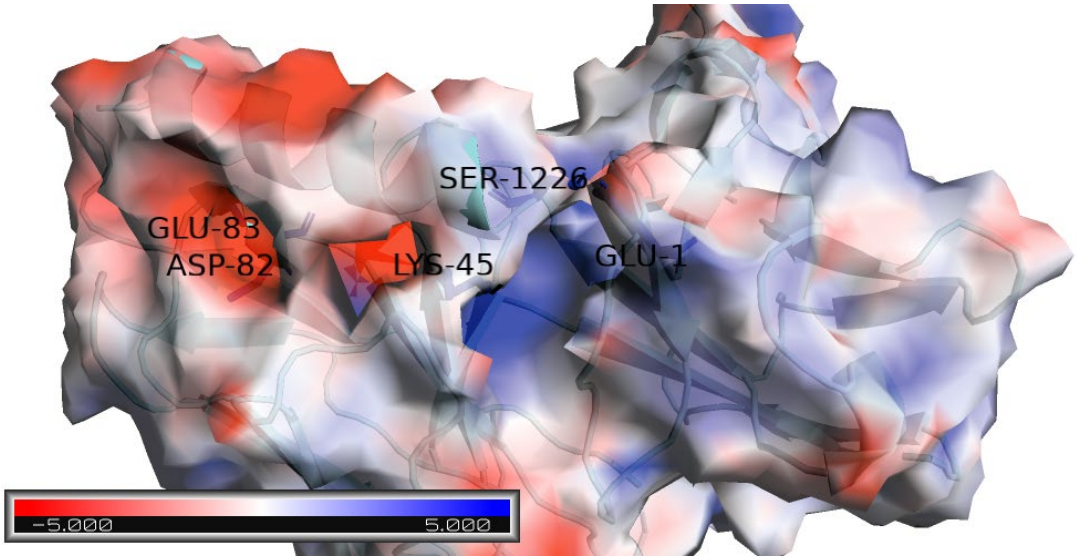

Figure III-5CC25.106 with MERS-COV stem helix SH AutoDock Vina electrostatic interaction calculations using the APBS-PDB2PQR software suite, visualized by PyMOL

✓ CC95.108with MERS-COV stem helix SH HADDOCK results:

2H_Bonds: TYR33 GLU1234 3.3A ARG98 ASP123 3.6A

Binding site Residues: THR3 ASP31 SER32 TYR33 ILE50 LYS52 SER53 ASP96 ARG98 THR243 PHE245 TRP304 ASP305 SER306 THR307

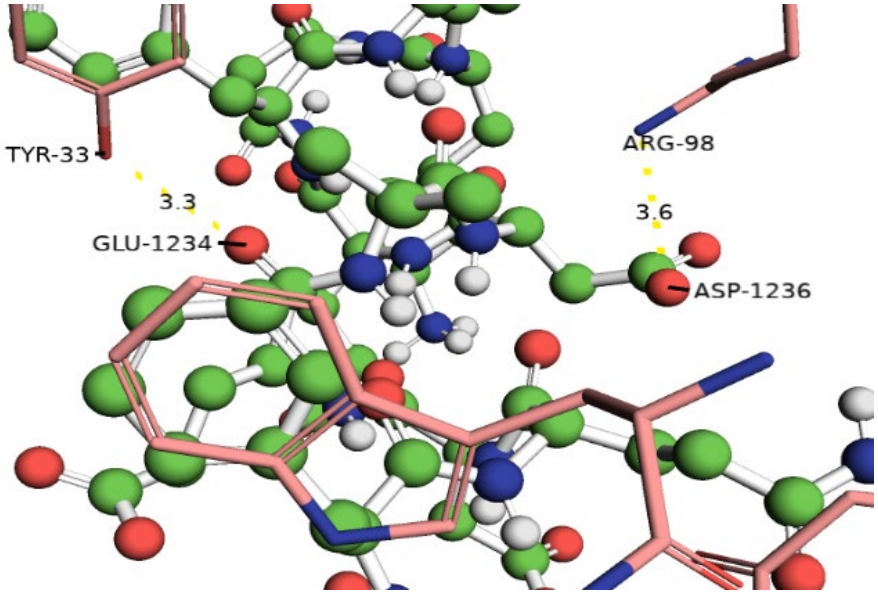

Figure III-6 CC95.108 with MERS-COV stem helix SH HADDOCK H_Bonds visualized by PyMOL

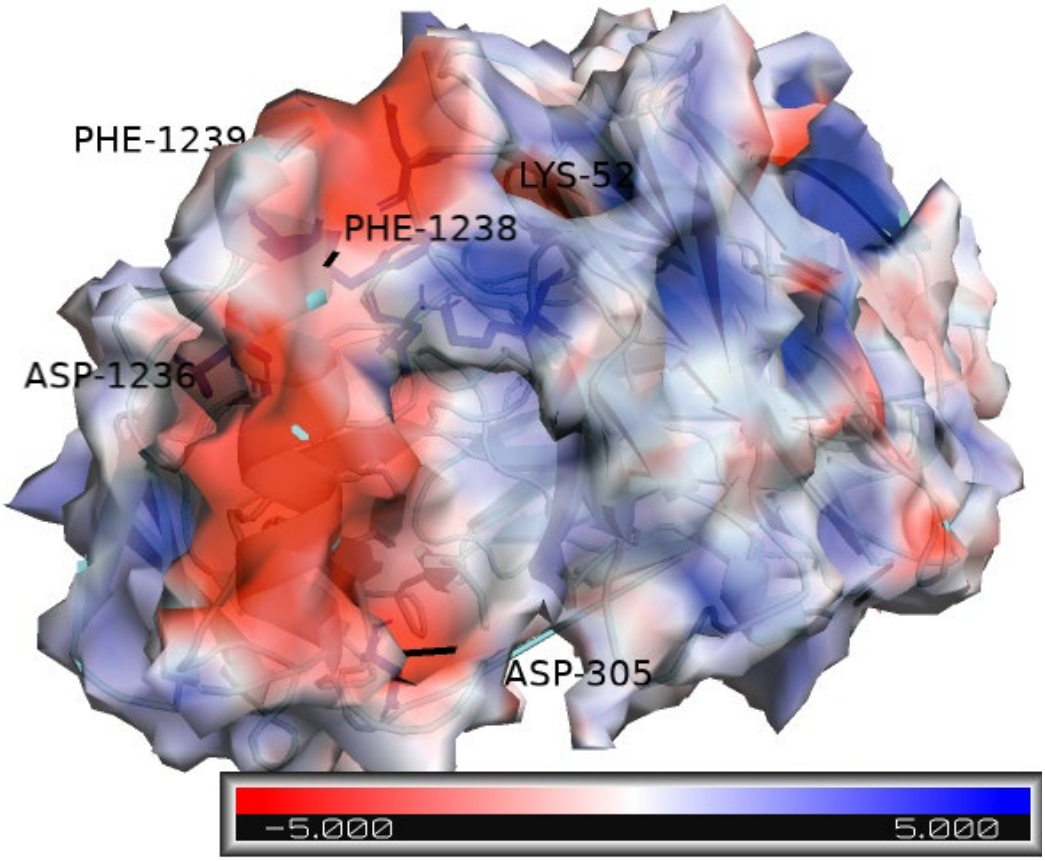

Figure III-7 CC95.108 with MERS-COV stem helix SH HADDOCK electrostatic interaction usingAPBS, visualized by PyMOL

✓ CC95with MERS-COV stem helix SH AutoDock Vina results:

LEU4 THR1227 2.8A LEU4 THR1227 2.5A LYS45 GLU1234 3.0A ARG61 ASN1241 3.2A GLN105 ASN1225 2.4A

Binding site Residues: VAL2 GLN3 LEU4 VAL5 THR42 ALA43 LYS45 LEU46 SER56 GLY57 ILE58 PRO59 ARG61 PHE62 GLN79 TYR91 ILE101 PHE102 TRP103 GLN105 GLY106 THR122

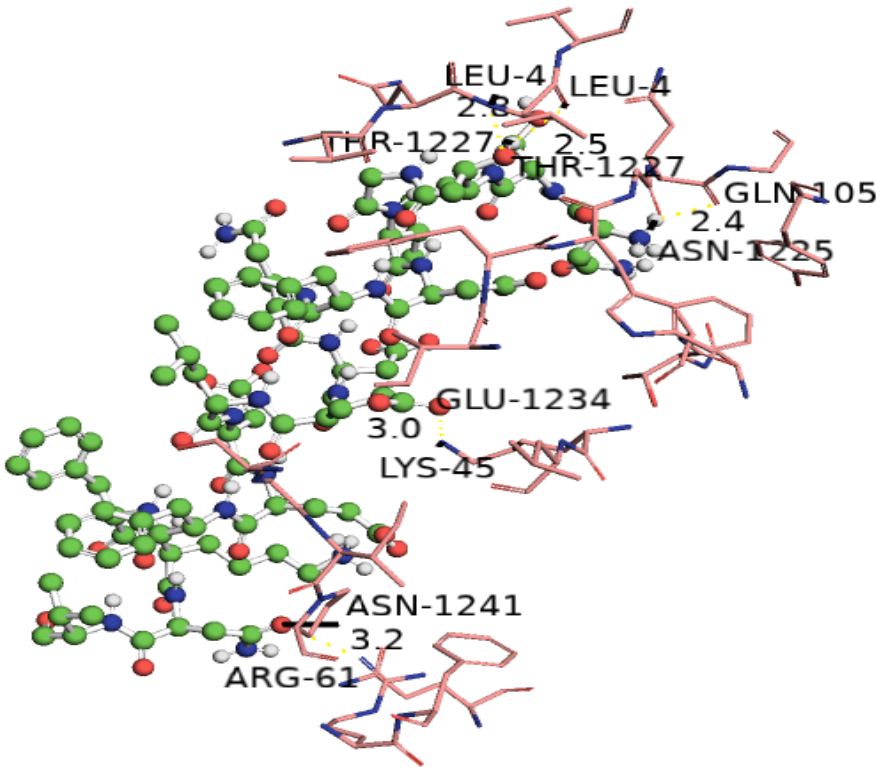

Figure III-8 CC95.108 with MERS-COV stem helix SH AutoDock Vina H_Bonds visualized by PyMOL

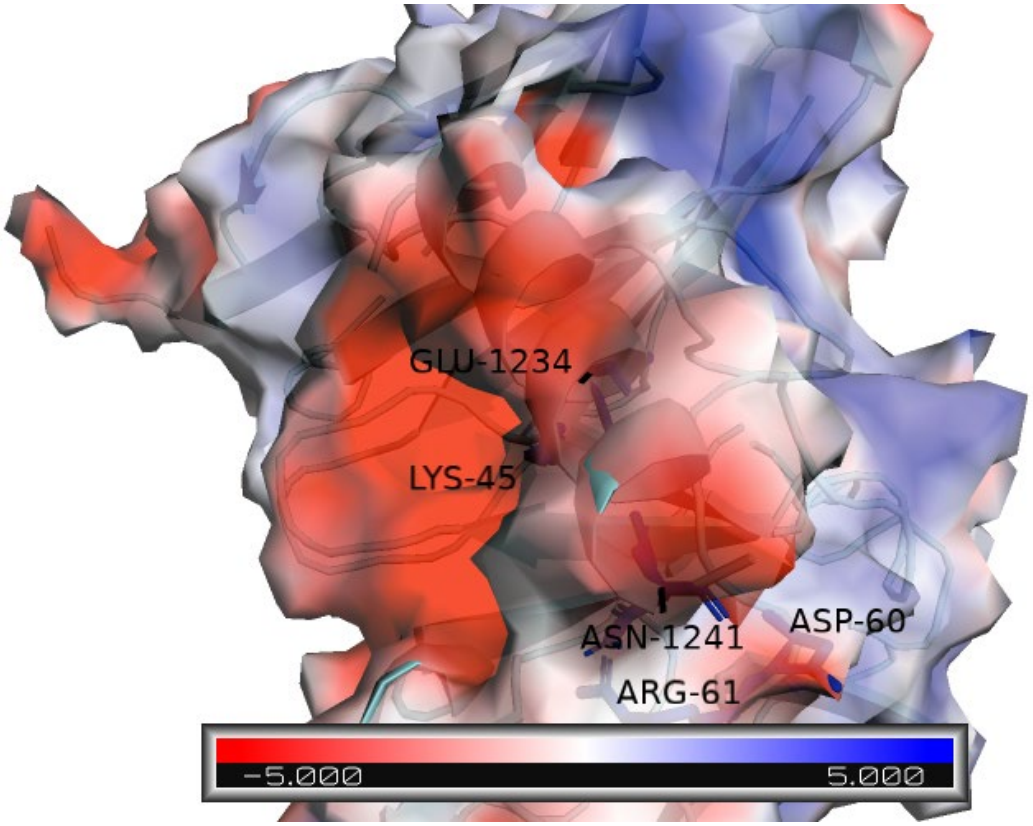

Figure III-9 CC95.108 with MERS-COV stem helix SH AutoDock Vina electrostatic interaction calculations using the APBS-PDB2PQR software suite, visualized by PyMOL

✓ CC99.103with MERS-COV stem helix SH HADDOCK results:

H_Bonds: ILE97 GLN1232 2.6A TYR233 GLU1234 2.1A

Binding site Residues: SER31 ASP32 TYR33 ILE50 ASN52 SER55 GLY56 THR57 ARG58 GLY96 ILE97 LEU98 THR99 GLY100 LEU101 ASN232 TYR233 GLY251 THR254 TYR292 GLY293 SER294 SER295 PRO296 PHE298

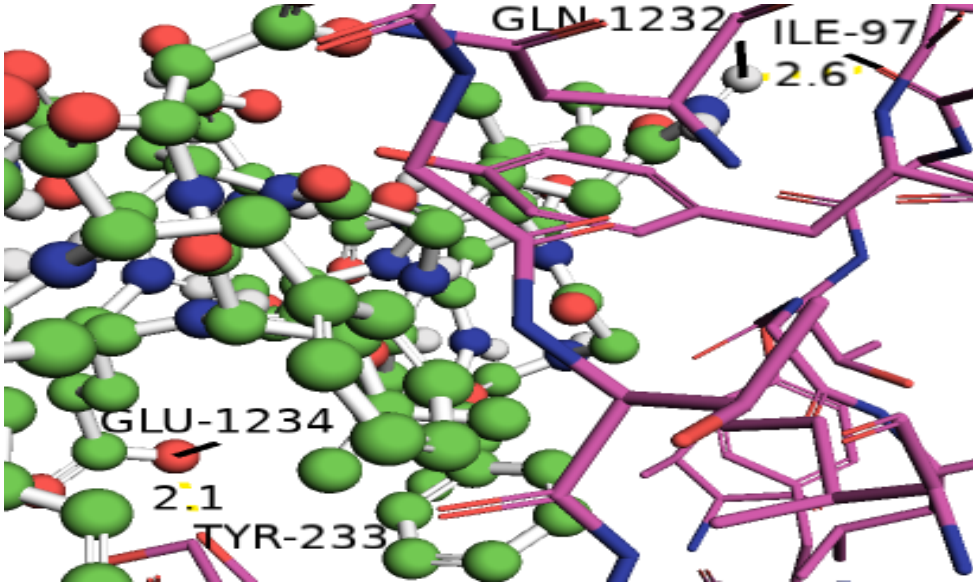

Figure III-10 CC99.103 with MERS-COV stem helix SH HADDOCK H_Bonds visualized by PyMOL

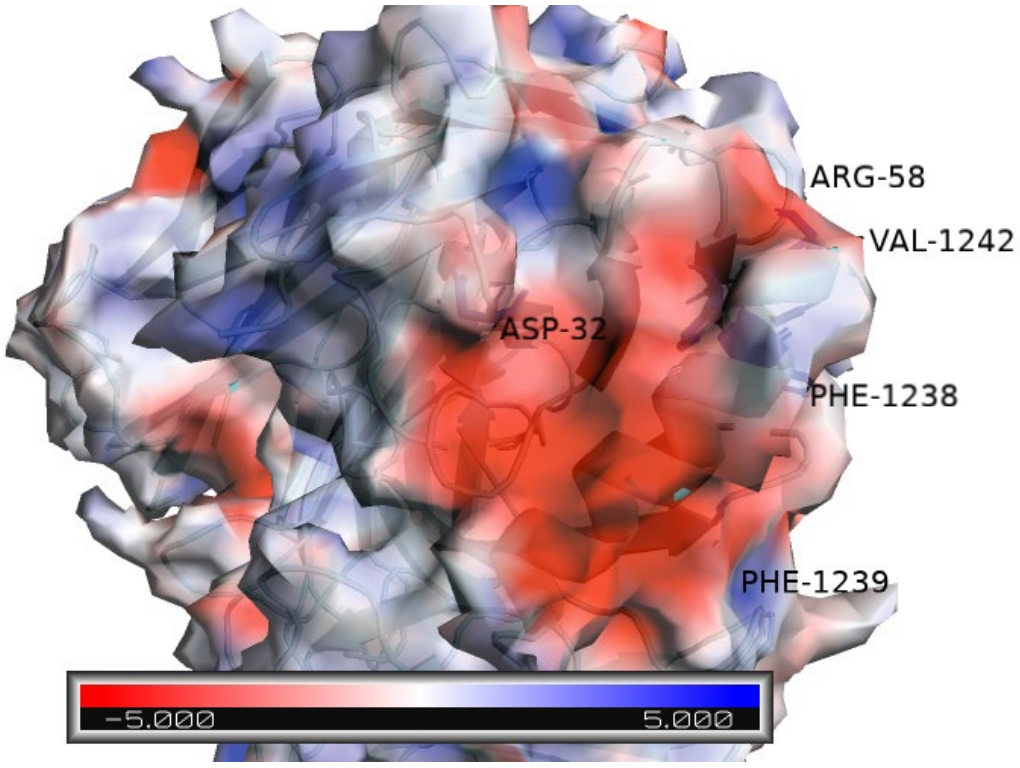

Figure III-11 CC99.103 with MERS-COV stem helix SH HADDOCK electrostatic interaction calculations using the APBS-PDB2PQR software suite, visualized by PyMOL

✓ CC99with MERS-COV stem helix SH AutoDock Vina results: H-Bonds:

TYR32 GLU1234 2.7A TYR33 ASP1236 2.5A SER_93, ILE96 GLN1232 2.7A

Binding site Residues: ASN31 ASP32 TYR33 TYR49 ILE50 ASN52 GLY56 ARG58 TYR91 GLY92 PRO95 PHE96 GLY99 LEU100

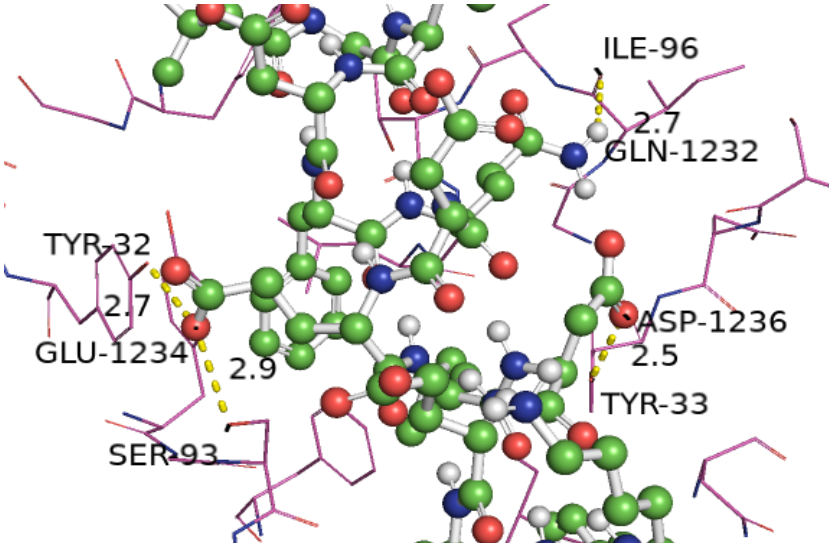

Figure III-12 CC99.103 with MERS-COV stem helix SH AutoDock Vina H_Bonds visualized by PyMOL

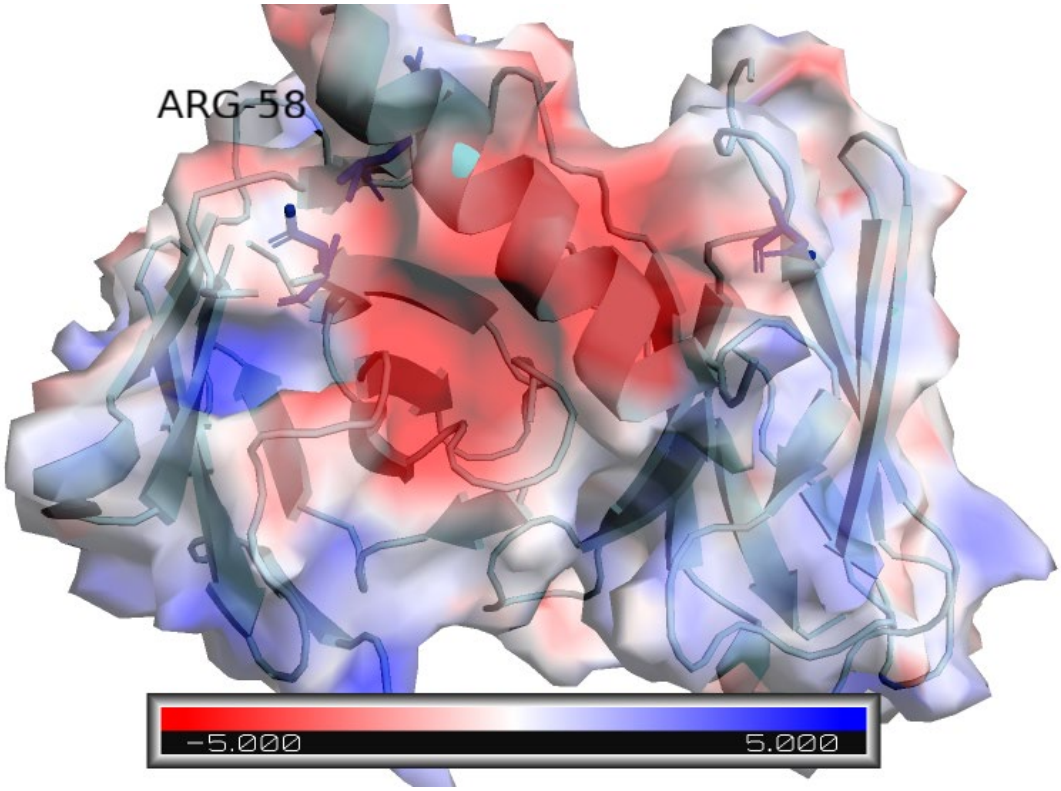

Figure III-13 CC99.103 with MERS-COV stem helix SH AutoDock Vina electrostatic interaction calculations using the APBS-PDB2PQR software suite, visualized by PyMOL

✓ CC9.113with MERS-COV stem helix SH HADDOCK results:

H-Bonds: ARG55 PHE1239 3.4A SER77 ASP1236 4.0A ARG78 GLN1232 2.0A ARG78 ASP1236 2.6A ARG211 GLN1232 3.4A ARG211 ASP1233 2.5A ARG211 ILE1229 1.8A

Binding site Residues: GLY_16, ARG_18, SER_53, ARG_55, ASP_61, ARG_62, SER_64, GLY_65, SER_66, SER_77, ARG_78, GLU_80, SER_141, TRP_157, ILE_160, SER_169, PHE_210, ARG_211, PRO_213

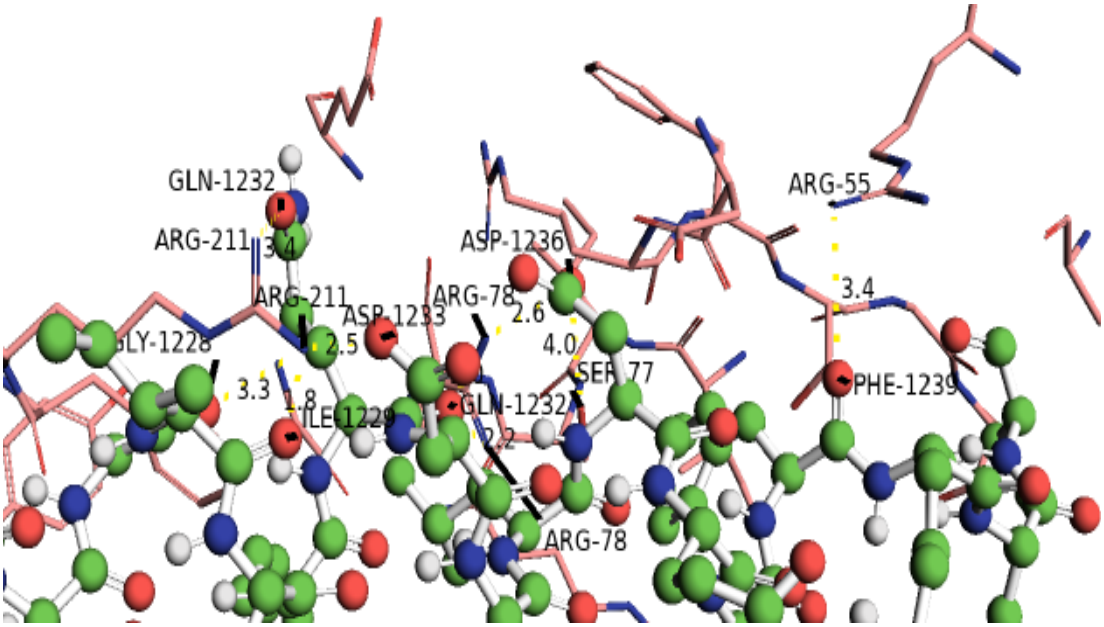

Figure III-14 CC9.113 with MERS-COV stem helix SH HADDOCK H_Bonds visualized by PyMOL

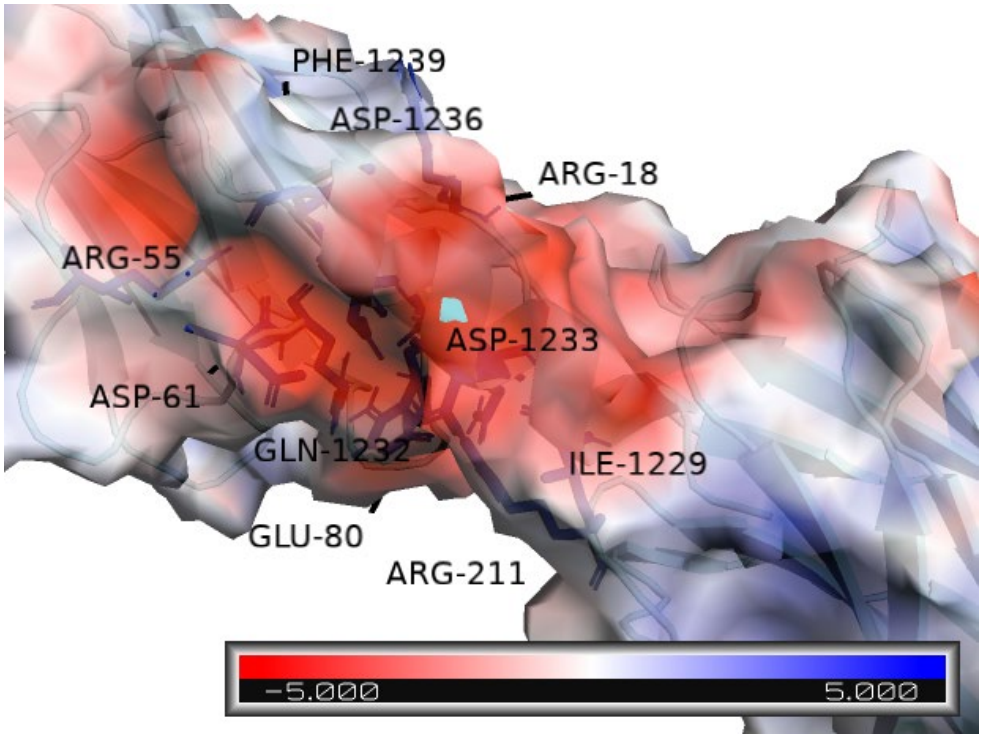

Figure III-15 CC9.113 with MERS-COV stem helix SH HADDOCK electrostatic interaction calculations using the APBS-PDB2PQR software suite, visualized by PyMOL

✓ CC9.113with MERS-COV stem helix SH AutoDock Vina results:

H_Bonds: TYR88 ASP1236 2.8A PHE101 VAL1242 3.0A

Binding site Residues: GLN39 PRO41 GLY42 PRO45 PHE84 ALA85 VAL86 TYR88 LEU99 THR100 PHE101 GLY102 PRO103 GLY104 LYS106

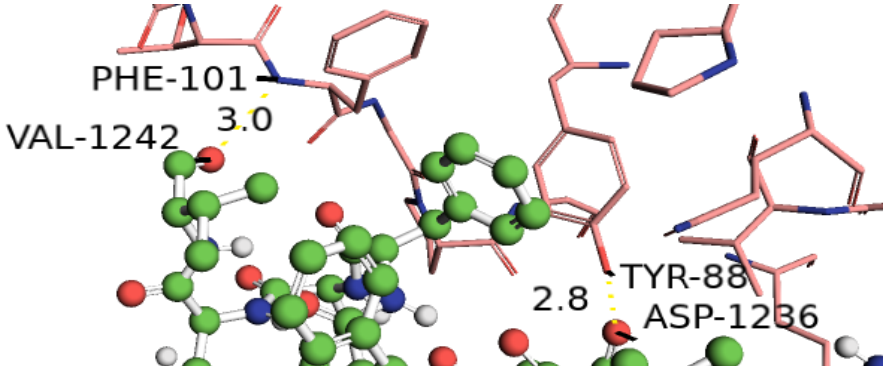

Figure III-16 CC9.113 with MERS-COV stem helix SH AutoDock Vina H_Bonds visualized by PyMOL

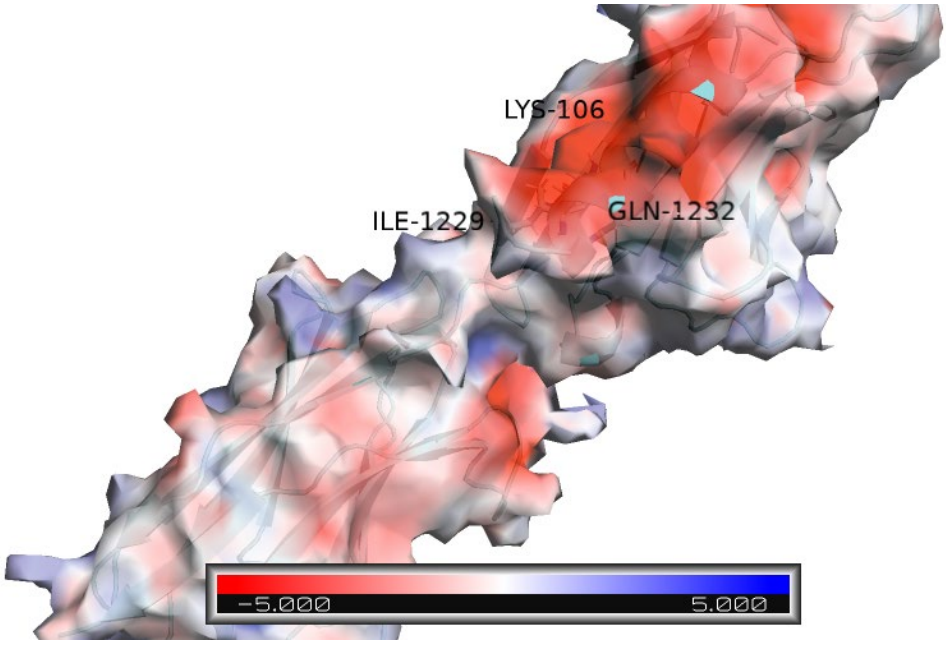

Figure III-17 CC9.113 with MERS-COV stem helix SH AutoDock Vina electrostatic interaction calculations using the APBS-PDB2PQR software suite, visualized by PyMOL

✓ C25.36 with MERS-COV stem helix SH HADDOCK results:

H_bonds: PRO14 GLN1232 1.8A ASP62 THR1227 3.8A, 4.1A THR78 GLY1228 4.3A ARG143 GLN1232 2.7A VAL211 PHE1238 2.5A TYR214 PHE1238 3.1A

Binding site Residues: ALA13 PRO14 GLY15GLN16 ARG17 PRO61 ASP62 PHE64 SER65 ILE77 THR78 GLY79 LEU80 SER142 ARG143 ASN144 TYR161 SER164 ARG208 GLY209 VAL210 VAL211 GLY212 TYR213 TYR214 ASP215 MET216 ASN223 TRP224 LEU225

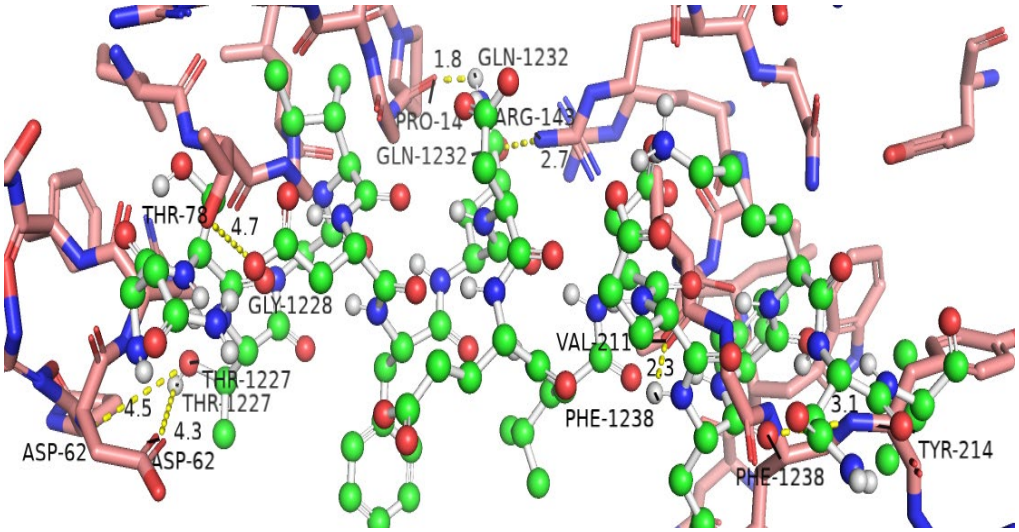

Figure III-18 CC25.36 with MERS-COV stem helix SH HADDOCK H_Bonds visualized by PyMOL

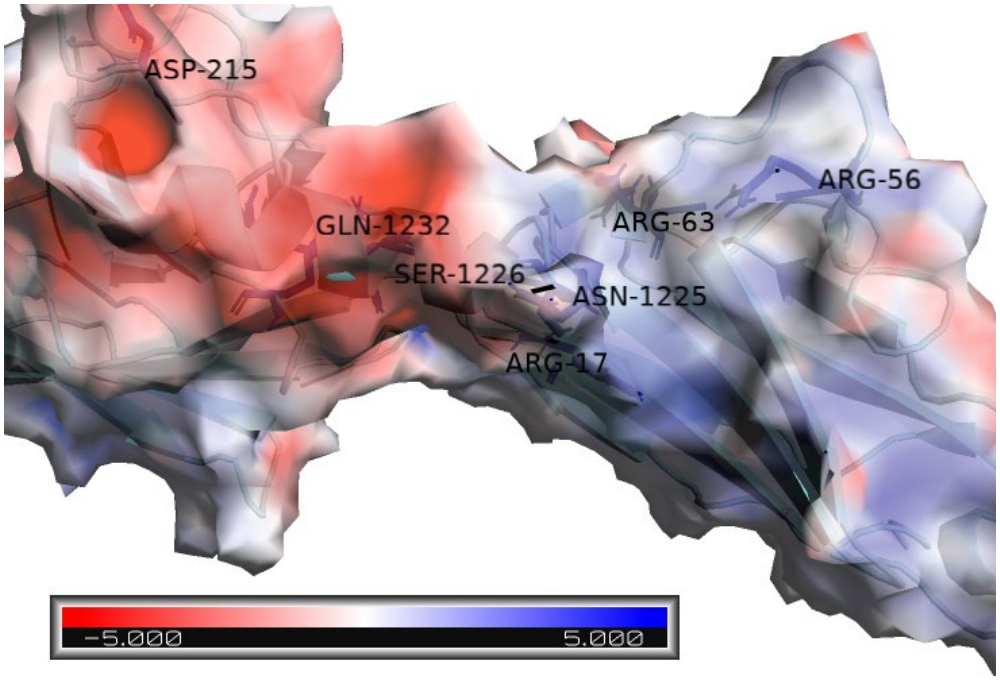

Figure III-19 CC25.36 with MERS-COV stem helix SH HADDOCK electrostatic interaction calculations using the APBS-PDB2PQR software suite, visualized by PyMOL

✓ CC25.36 with MERS-COV stem helix SH AutoDock Vina results:

H_Bonds: GLY176 LYS1240 2.3A SER181 GLU1234 2.8A ARG182 ASP1230 3.4A ASN194 GLU1237 3.2A

Binding site Residues: SER128 ARG130 ILE162 SER163 SER154 SER165 GLY166 SER167 GLY176 ARG177 PHE178 SER179 ILE180 SER181 ARG182 ASP183 ASN184 TYR190 LEU191 ASN194 SER195

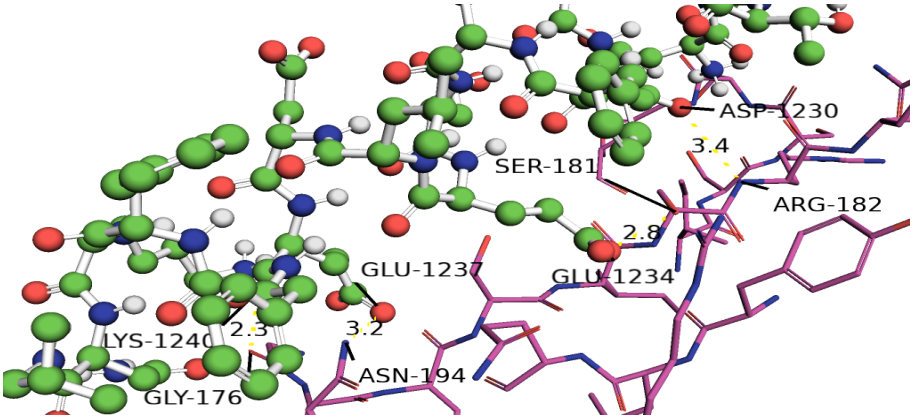

Figure III-20 CC25.36 with MERS-COV stem helix SH AutoDock Vina H_Bonds visualized by PyMOL

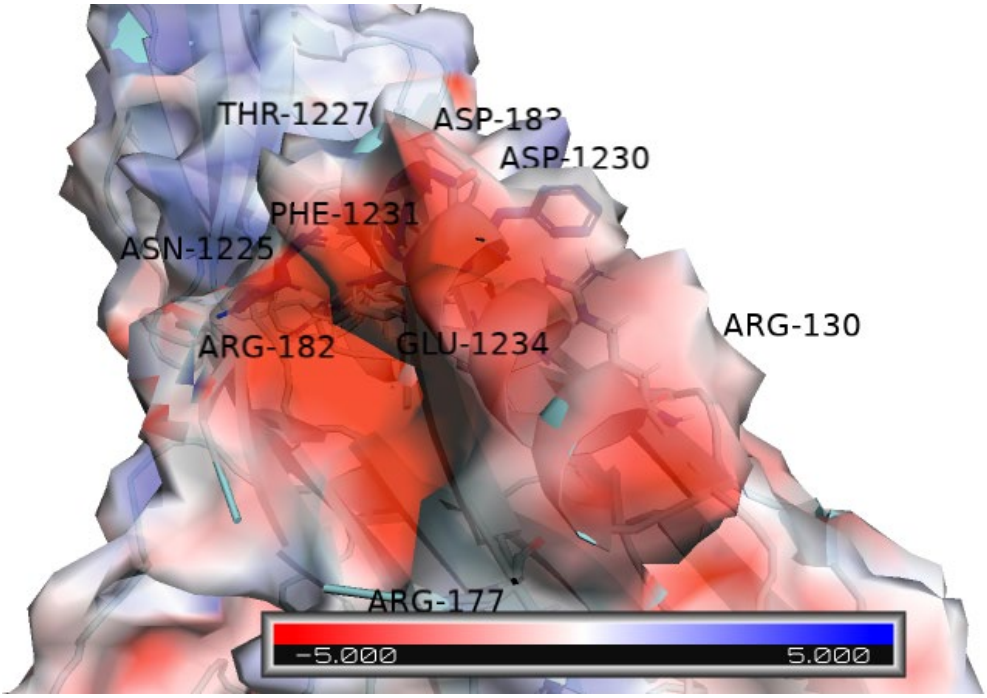

Figure III-21 CC25.36 with MERS-COV stem helix SH AutoDock Vina electrostatic interaction calculations using the APBS-PDB2PQR software suite visualized by PyMOL

Table III-4 SARS Docking residues

SARS-CoV-2		*CC25.106*	*CC95.108*	*CC99.103*	*CC9.113*	*CC25.36*
HADDOCK2.4	*H_bond Residues*	*TYR33 LYS52 ASN56 THR57 ARG58 HIS99 ASN245 ASN246 TYR247 ASN266 TRP306*	*TYR33 LYS52 ASN56 ASP96 ARG98 THR243 PHE245 LYS279 TRP304 SER306*	*ASN232 SER253*	*ARG18 SER64 SER66*	
	Binding site Residues	*TYR32 TYR3 HIS35 ILE 50 ILE51 LYS52 SER53 GLY55 ASN56 THR57 ARG58 ASN59 GLY96 GLY97 VAL98 HIS99 GLY100 GLY244 ASN245 ASN246 TYR247 VAL248 LYS281 TRP306 ASP307 THR308 LEU310 PHE312*	*TYR33 HIS35 ILE50 ILE51 LYS52 ASN56 THR57 ARG58 ASP96 SER97 ARG98 GLY99 THR243 ASN244 PHE245 LYS279 SER306 THR307 PRO308 TRP310*	*THR230 LYS231 ASN232 TYR233 VAL234 TYR250 GLY251 ALA252 SER253 THR254 GLY265 SER266 GLY267 PHE272 GLY293 SER294*	*GLY16 GLU17 ARG18 ALA19 LEU21 SER22 CYS23 LYS31 LEU34 ALA35 TRP36 ILE49 TYR50 GLY51 ALA52 SER53 SER54 ARG62 PHE63 SER64 GLY65 SER66 GLY67 SER68 ASP71 PHE72 LEU74 ILE76 SER77 ARG78 CYS89 GLY90 SER141*	*GLY_15 ARG_17 SER_54 ASP_62 SER_142 VAL_210 VAL_211 GLY_212 TYR_213 ASN_223*

AutoDock Vina	*H_bond Residues*	*ASN30 TYR32 TYR33 ASN51 LYS52 YS66 TRP91 THR93 HIS98*	*LYS45 TRP103*	*LEU4 ARG61 ASP101*	*TRP157*	*SER11 ARG17 THR19 SER67 SER*
	Binding site Residues	*ASN31 TYR33 ILE50 LYS52 ASN56 ARG58 LYS66 TRP91 THR93 PHE96 GLY99*	*VAL2 GLN3 LEU4 VAL5 THR42 ALA43 LYS45 LEU46 SER56 GLY57 ILE58 PRO59 ARG61 PHE62 GLN79 TYR91 ILE101 PHE102 TRP103 GLN105 GLY106 THR122*	*GLN1 VAL2 GLN3 LEU4 LYS39 GLN42 ALA43 PRO44 ARG45 GLY57 ILE58 PRO59 ARG61 GLU81 ASP101 TYR102 TRP103 GLY104*	*HIS145 LEU-155 GLU156 TRP157 TYR170 ALA171 PRO172 LYS173 GLY212 PRO213 PHE215*	*SER9 VAL10 SER11 ARG17 VAL18 THR19 SER65 GLY66 SER67 LYS68 SER69 SER74 LEU75*
Experimental Results	*H_bond Residues*	*VL ASN51 LYS66 VH TYR33 LYS52 GLY95 HIS97*	*VL ASN51 LYS66 VH TYR33 LYS52 GLY95 HIS97*	*VL ASN51 LYS66 VH TYR33 LYS52 GLY95 HIS97*		
	Binding site Residues	*VH ASN56 VH TYR33 ILE50 ARG98/HIS97 VL TYR32*	*VH ASN56 VH TYR33 ILE50 ARG98/H97 VL TYR32*	*VH TYR33 ILE50 VH THR57 GLY95 ILE96 VL TYR32 TYR91 PHE96 VL PRO95 PRO95a.*		

✓ CC25.106 with SARS-COV-2 stem helix SH HADDOCK results:

H-bonds: LYS52 GLU1151 1.6A,2.3A TYR33 GLU1151 2.2A ASN56 SER1147 1.8A HIS99 TYR1155 2.0A THR57 LEU11451.8A ARG58 ASP1146 1.6A,2.7A TRP306 ASP1153 1.9A ASN246 LYS1157 1.9A ASN245 ASN1158 1.8A LYS281 ASN1158 2.0A ASN-266 ASN-1158 1.8A TYR247 PHE1156 2.0A HIS99 TYR1155 2.0A [TYR33 LYS52 ASN56 THR57 ARG58 HIS99 ASN245 ASN246 TYR247 ASN266 TRP306]

Binding site Residues: TYR32 TYR33 HIS35 ILE50 ILE51 LYS52 SER53 GLY55 ASN56 THR57 ARG58 ASN59 GLY96 GLY97 VAL98 HIS99 GLY100 GLY244 ASN245 ASN_246 TYR247 VAL248 LYS281 TRP306 ASP307 THR308 LEU310 PHE312

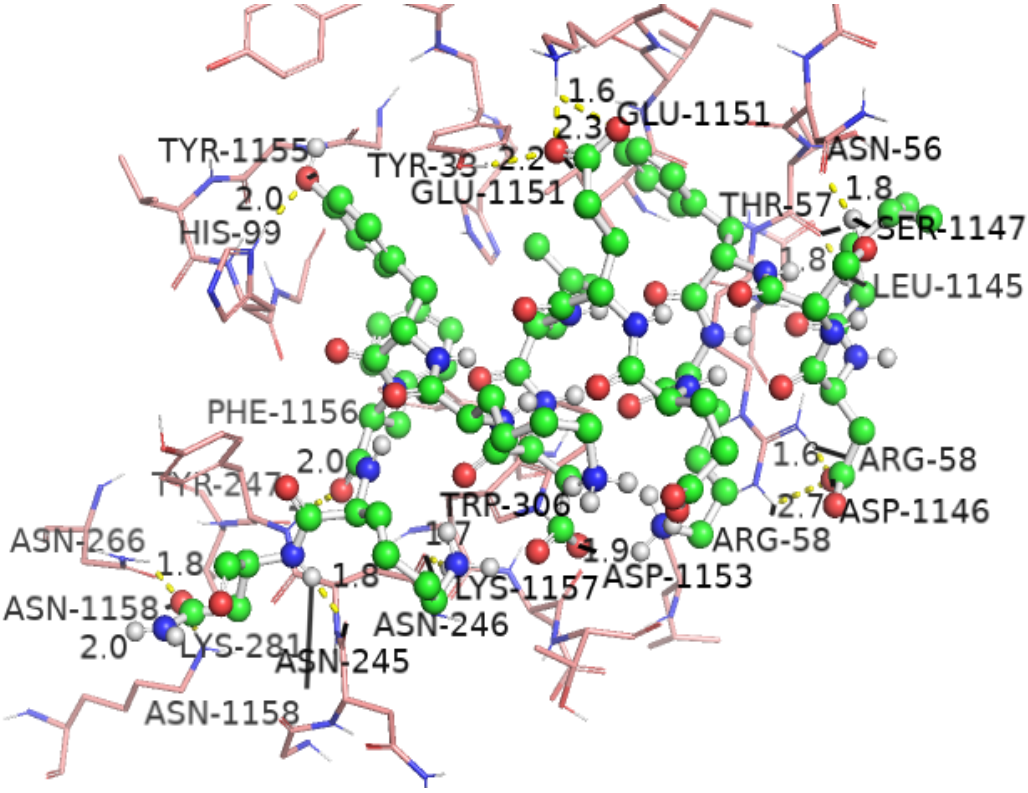

Figure III-22 CC25.106 with SARS-COV-2 stem helix SH HADDOCK H_Bonds visualized by PyMOL

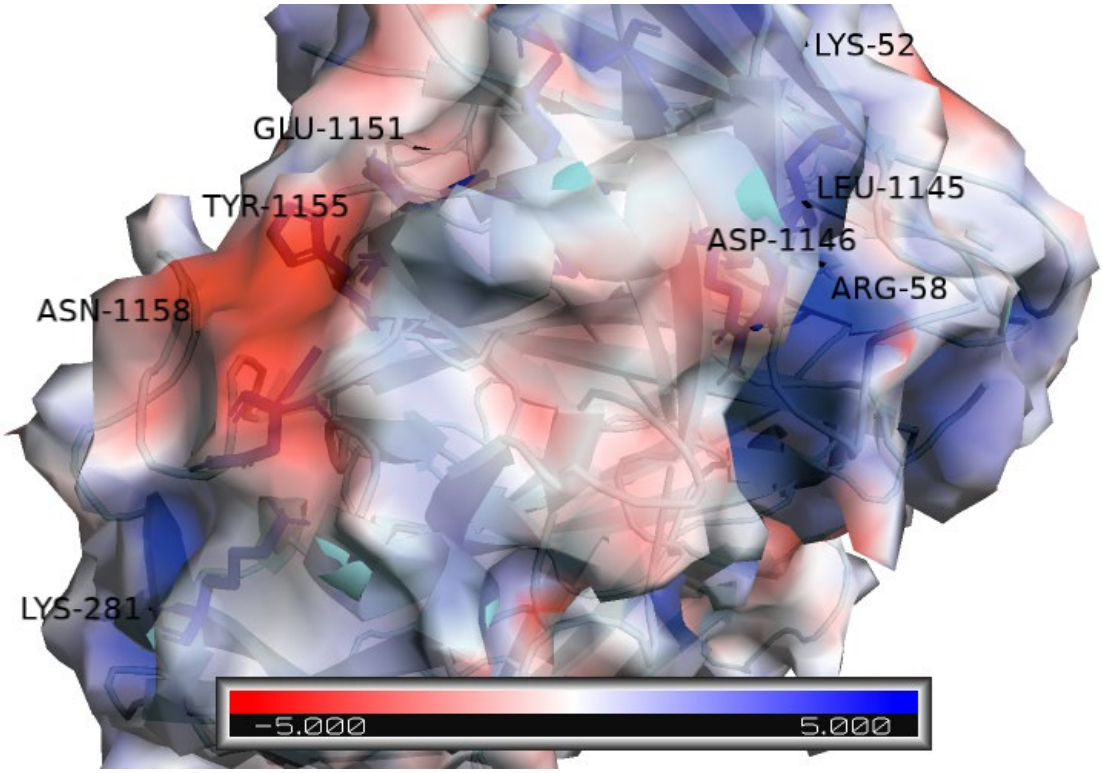

Figure III-23 CC25.106 with SARS-COV-2 stem helix SH HADDOCK electrostatic interaction calculations using the APBS-PDB2PQR software suite, visualized by PyMOL

✓ CC25.106 with SARS-COV-2 stem helix SH AutoDock Vina results:

H- bonds: LYS52 GLU1151 2.8A TYR33 GLU1151 2.7A HIS98 TYR1155 3.4A TYR32 PHE1156 3.3A ASN51 ASN1158 2.9A LYS66 ASN1158 3.2A ASN30 ASN1158 1.8A TRP91 ASP1153 2.8A THR93 LYS1149 1.9A [ASN30 TYR32 TYR33 ASN51 LYS52 LYS66 TRP91 THR93 HIS98]

Binding site Residues: ASN31 TYR33 ILE50 LYS52 ASN56 ARG58 LYS66 TRP91 THR93 PHE96 GLY99

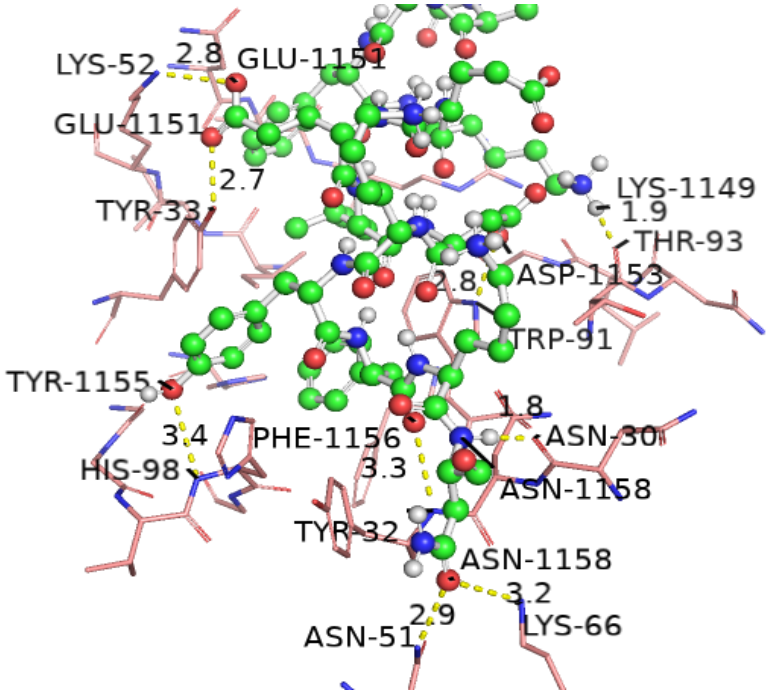

Figure III-24 CC25.106 with SARS-COV-2 stem helix SH AutoDock Vina H_Bonds visualized by PyMOL

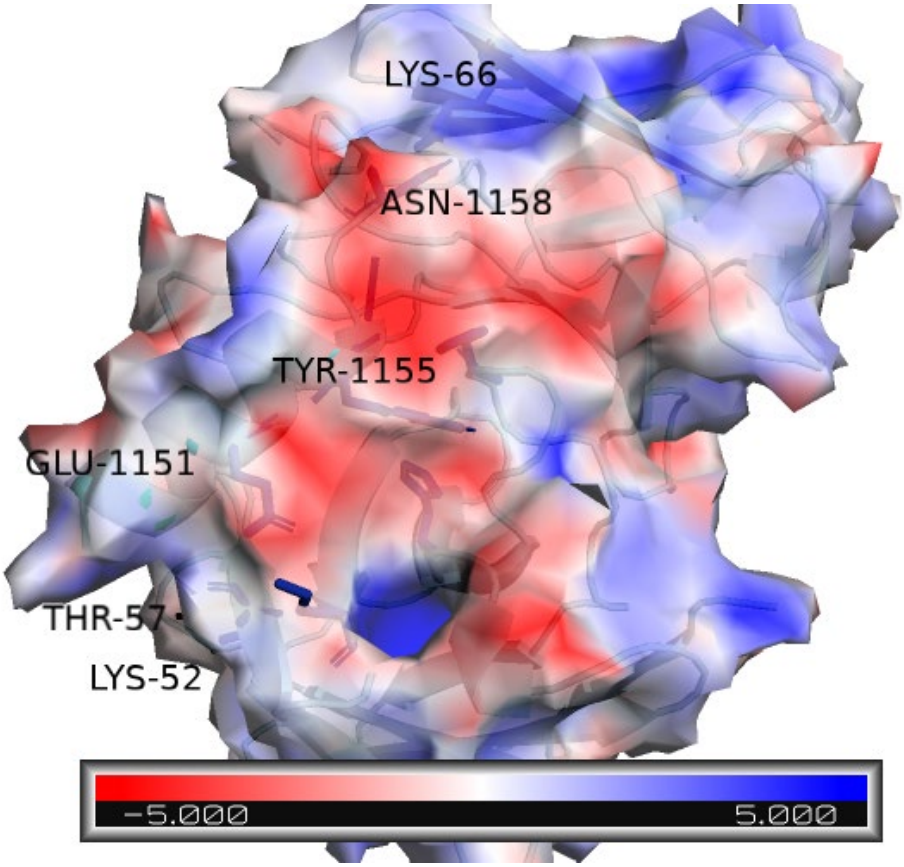

Figure III-25 CC25.106 with SARS-COV-2 stem helix SH AutoDock electrostatic interaction calculations using the APBS-PDB2PQR software suite, visualized by PyMOL

✓ CC95.108 with SARS-COV-21 stem helix SH HADDOCK results:

H_Bonds: TYR33 GLU1151 1.9A LYS52 GLU1151 3.2A ASN56 SER1147 3.4A ASP96 TYR1155 2.6A ARG98 TYR1155 2.8A,2.7A THR243 ASN1158 2.1A PHE245 PHE1156 3.1A LYS279 ASN1158 3.4A TRP304 ASP1153 2.8A SER306 LYS1149 2.6A SER306 ASP1153 3.5A

Binding site Residues: TYR33 HIS35 ILE50 ILE51 LYS52 ASN56 THR57 ARG-58 ASP96 SER97 ARG98 GLY99 THR243 ASN244 PHE245 LYS279 SER306 THR307 PRO308 TRP310

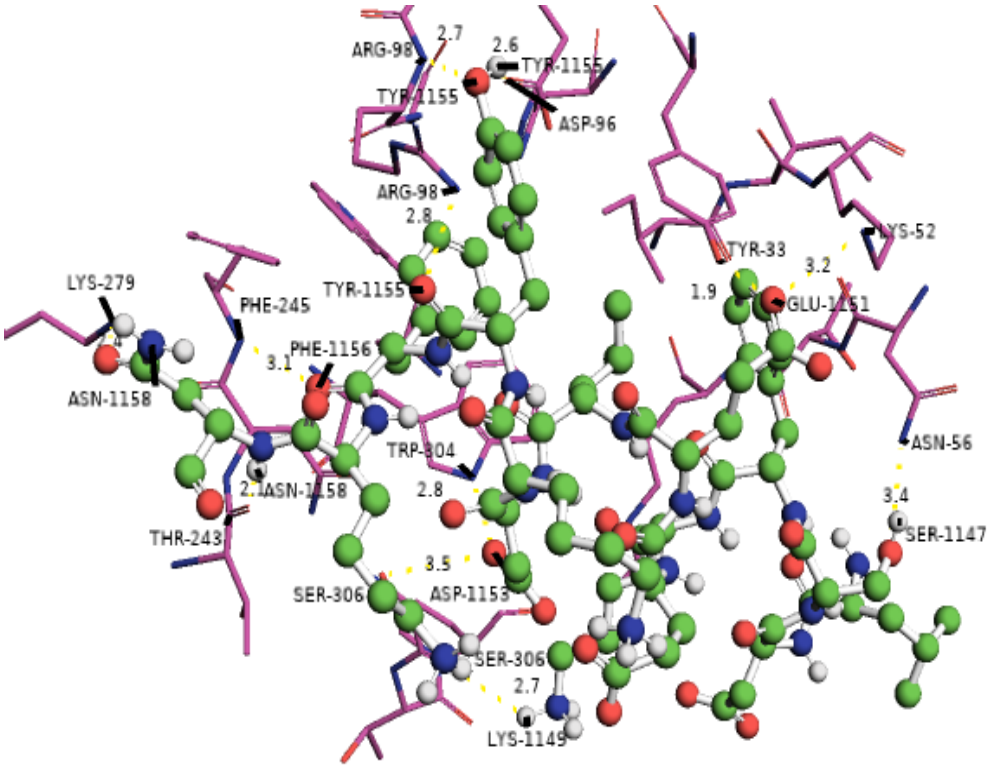

Figure III-26 CC95.108 with SARS-COV-2 stem helix SH HADDOCK H_Bonds visualized by PyMOL

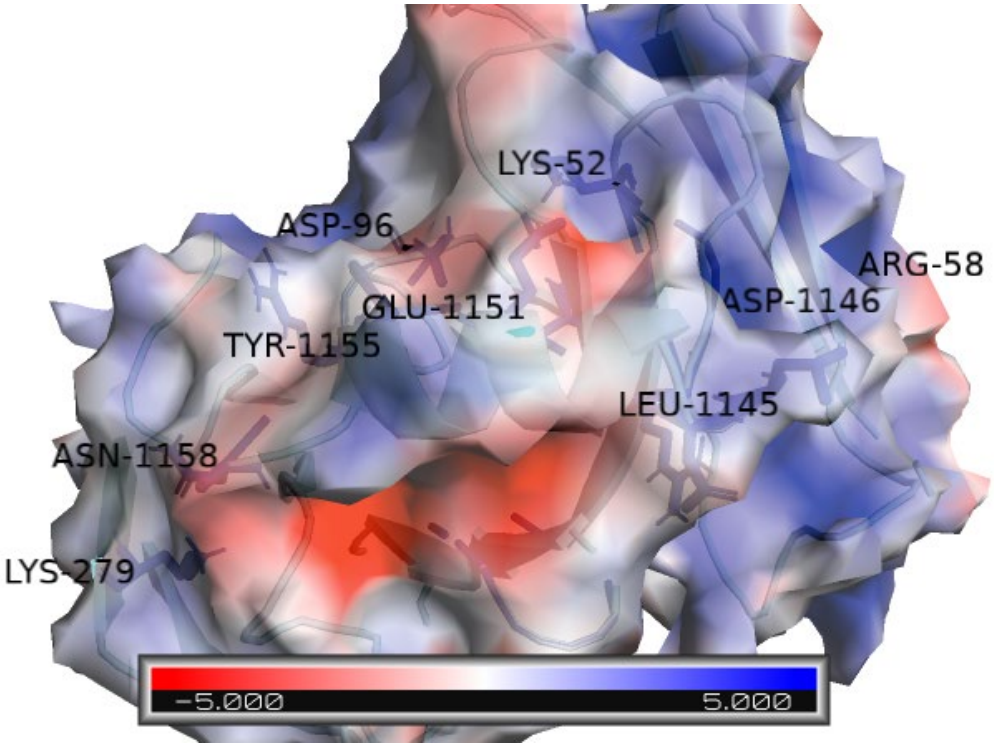

Figure III-27 CC95.108 with SARS-COV-2 stem helix SH HADDOCK electrostaticinteraction calculations using the APBS-PDB2PQR software suite, visualized by PyMOL

✓ CC95with SARS-COV-2 stem helix SH AutoDock Vina results:

H_Bonds: LYS45 LYS1149 3.5A LYS45 ASP1153 2.5A TRP103 ASP1146 2.4A

Binding site Residues: VAL-2 LEU-4 THR-42 PRO-55 SER-56 GLY-57 ILE-58 PRO-59 ARG-61 GLN-79 GLY-81 ILE-101 PHE-102 TRP-103 GLY-104 GLN-105

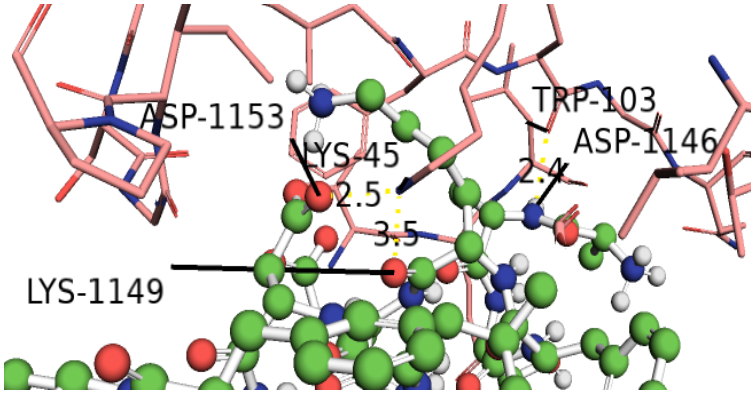

Figure III-28 CC95.108 with SARS-COV-2 stem helix SH AutoDock Vina H_Bonds visualized by PyMOL

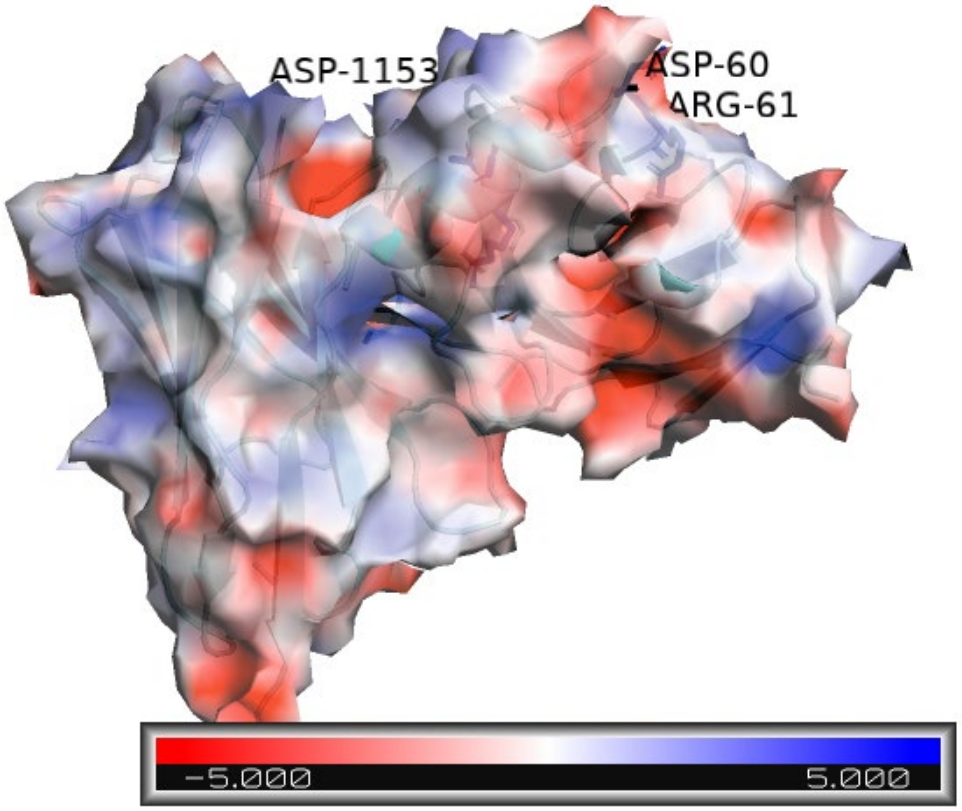

Figure III-29 CC95.108 with SARS-COV-2 stem helix SH AutoDock Vina electrostatic interaction calculations using the APBS-PDB2PQR software suite, visualized by PyMOL

✓ CC99.103with SARS-COV-2 stem helix SH HADDOCK results:

H_Bonds: ASN232 PHE1148 1.9A SER253 LEU1145 1.5A

Binding site Residues: THR230 LYS231 ASN232 TYR233 VAL234 TYR250 GLY251 ALA252 SER253 THR254 GLY265 SER266 GLY267 PHE272 GLY293 SER294

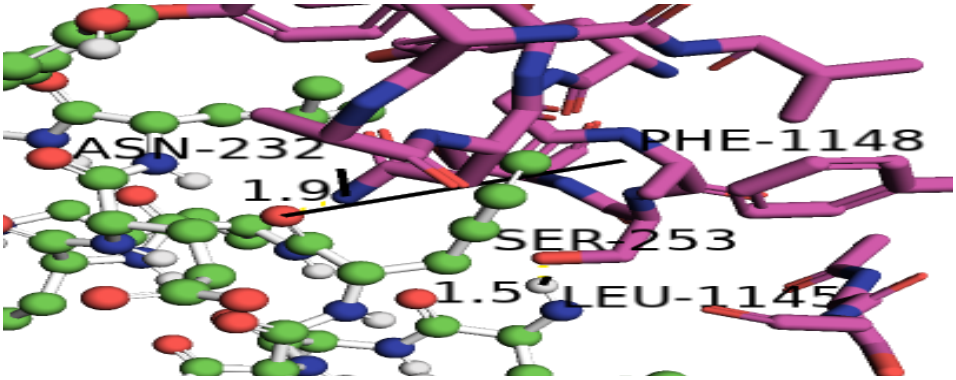

Figure III-30 CC99.103 with SARS-COV-2 stem helix SH HADDOCK H_Bonds visualized by PyMOL

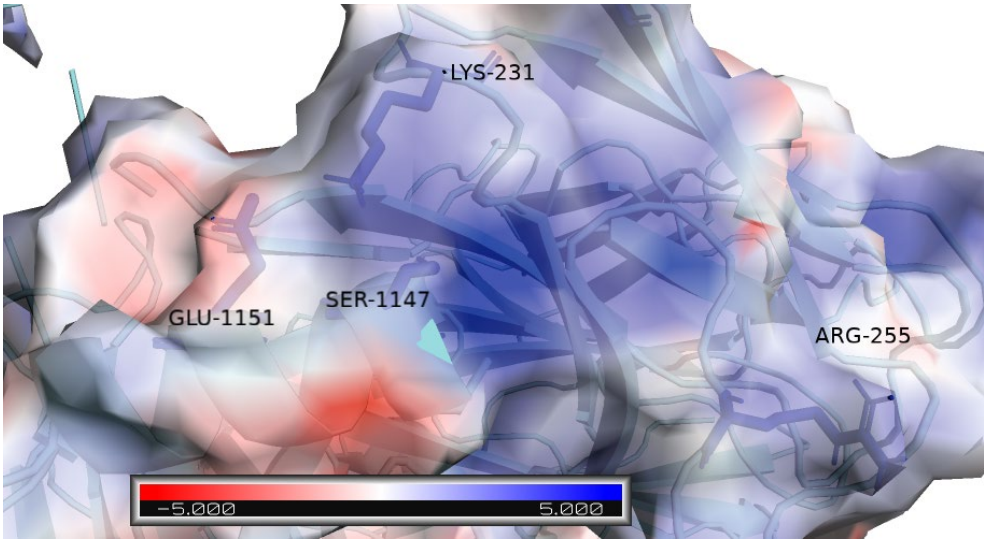

Figure III-31 CC99.103 with SARS-COV-2 stem helix SH HADDOCK electrostatic interaction calculations using the APBS-PDB2PQR software suite, visualized by PyMOL

✓ CC99with SARS-COV-2 stem helix SH AutoDock Vina results:

H_Bonds: LEU4 ASP1146 2.5A ARG61 ASN1158 3.0A ASP101 LYS1149 2.5A

Binding site Residues: GLN1 VAL2 GLN3 LEU4 LYS39 GLN42 ALA43 PRO44 AR-45 GLY-57 ILE58 PRO59 ARG61 GLU81 ASP101 TYR102 TRP103 GLY104

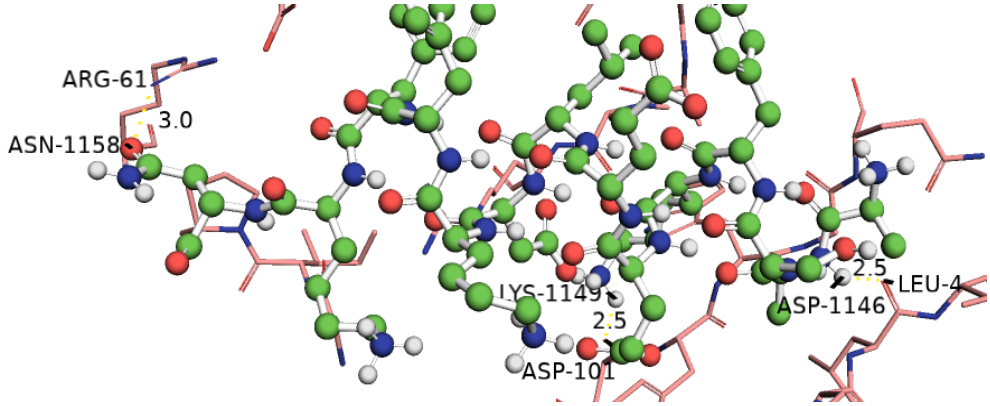

Figure III-32 CC99.103 with SARS-COV-2 stem helix SH AutoDock Vina H_Bonds visualized by PyMOL

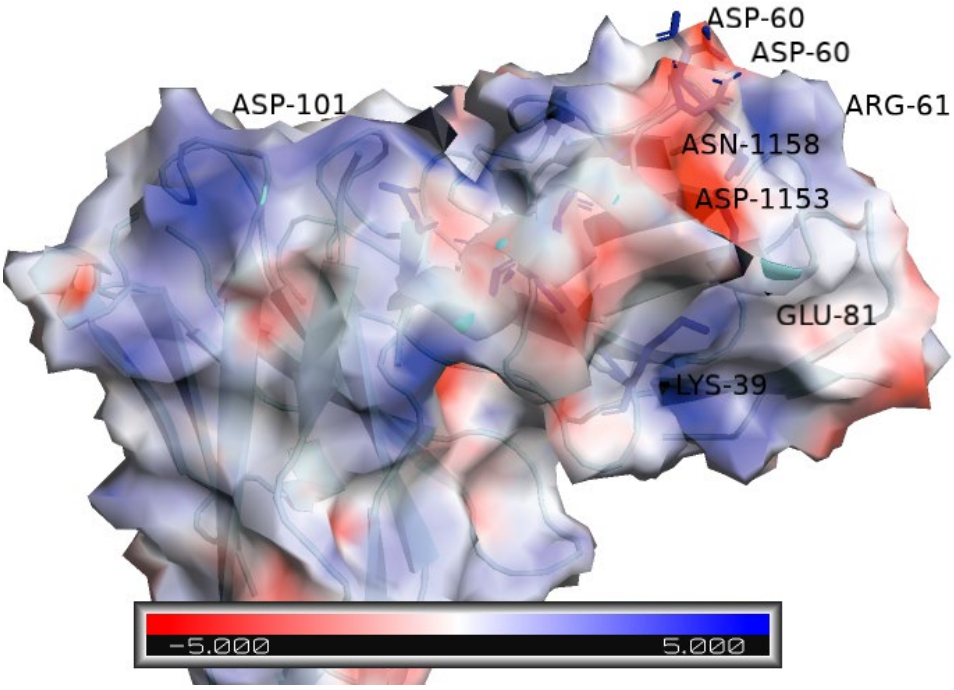

Figure III-33 CC99.103 with SARS-COV-2 stem helix SH AutoDock Vina electrostatic interaction calculations using the APBS-PDB2PQR software suite, visualized by PyMOL

CC9.113with SARS-COV-2 stem helix SH HADDOCK results:

H_Bonds: ARG18 GLU1150 2.2A ARG18 SER1147 3.2A SER-64 LYS1157 2.0A SER-64 ASP1153 2.5A, 2.9A SER-66 LYS1157 1.1A SER-66 LYS1154 3.1A

Binding site Residues: GLY16 GLU17 ARG18 ALA19 LEU21 SER22 CYS23 LYS31 LEU34 ALA35 TRP36 ILE49 TYR50 GLY51 ALA52 SER53 SER54 ARG62 PHE63 SER64 GLY65 SER66 GLY67 SER68 ASP71 PHE72 LEU-74 ILE-76 SER77 ARG78 CYS89 GLY90 SER141

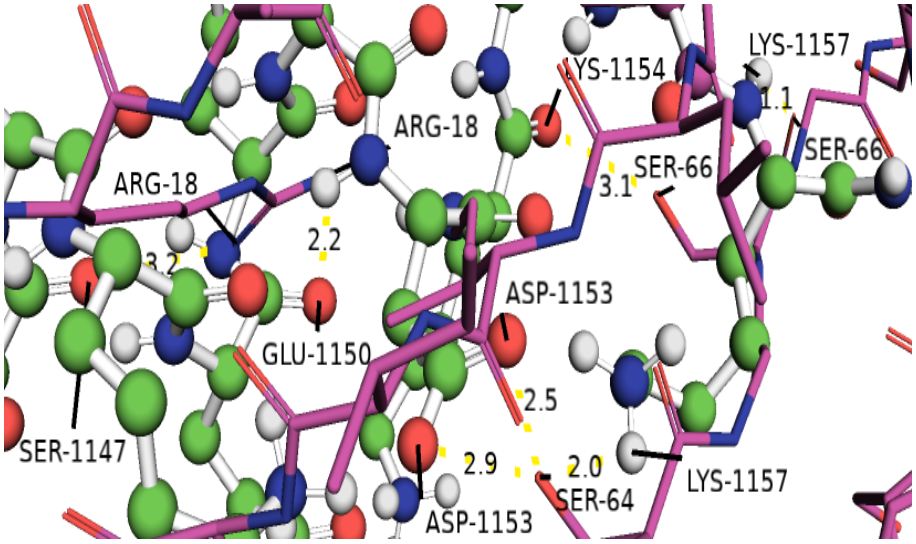

Figure III-34 CC9.113 with SARS-COV-2 stem helix SH HADDOCK H_Bonds visualized by PyMOL

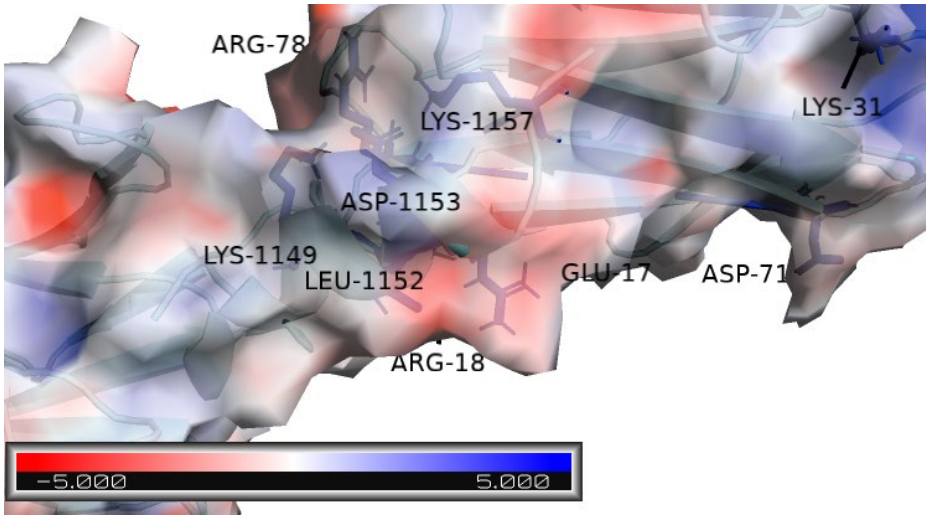

Figure III-35 CC9.113 with SARS-COV-2 stem helix SH HADDOCK electrostatic interaction calculations using the APBS-PDB2PQR software suite, visualized by PyMOL

✓ CC9.113with SARS-COV-2 stem helix SH AutoDock Vina results:

H_Bonds: TRP157 ASP1153 3.3A

Binding site Residues: HIS145 LEU155 GLU156 TRP157 TYR170 ALA171 PRO172 LYS173 GLY212 PRO213 PHE215

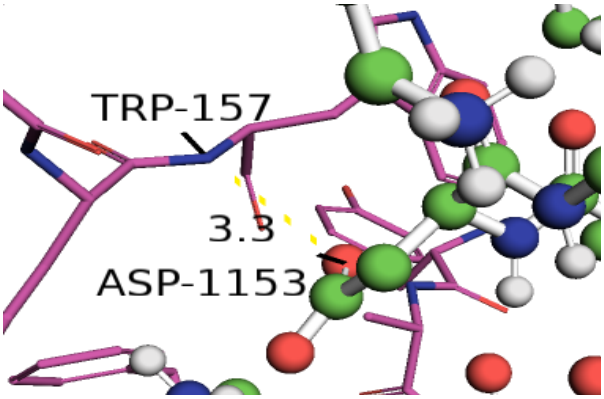

Figure III-36 CC9.113 with SARS-COV-2 stem helix SH AutoDock Vina H_Bonds visualized by PyMOL

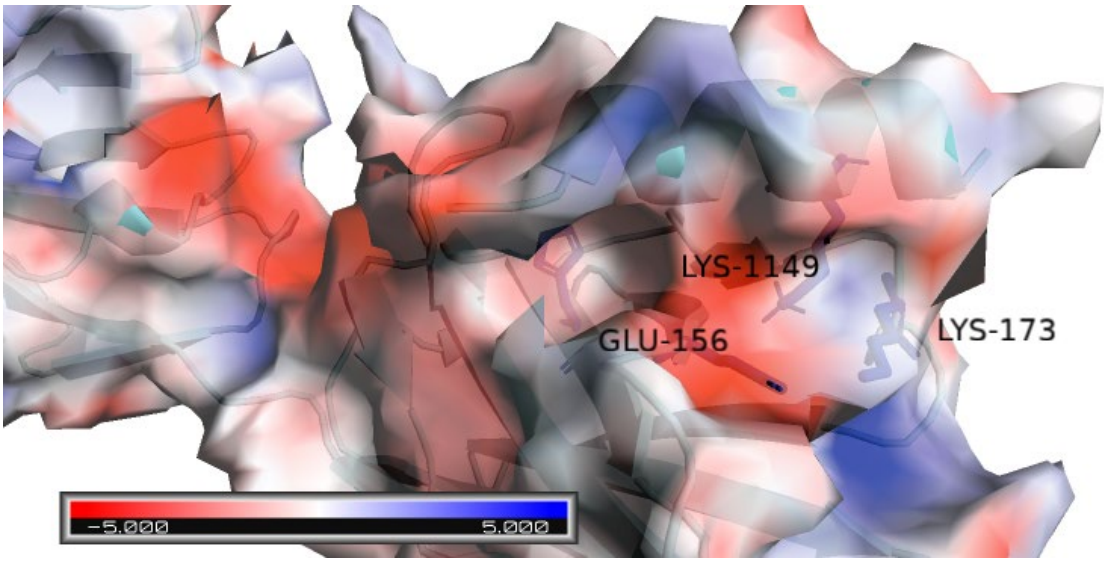

Figure III-37 CC9.113 with SARS-COV-2 stem helix SH AutoDock Vina electrostatic interaction calculations using the APBS-PDB2PQR software suite, visualized by PyMOL

✓ CC25.36 with SARS-COV-2 stem helix SH HADDOCK results:

Binding site Residues: GLY15 ARG17 SER54 ASP62 SER142 VAL210 VAL211 GLY212 TYR213 ASN223

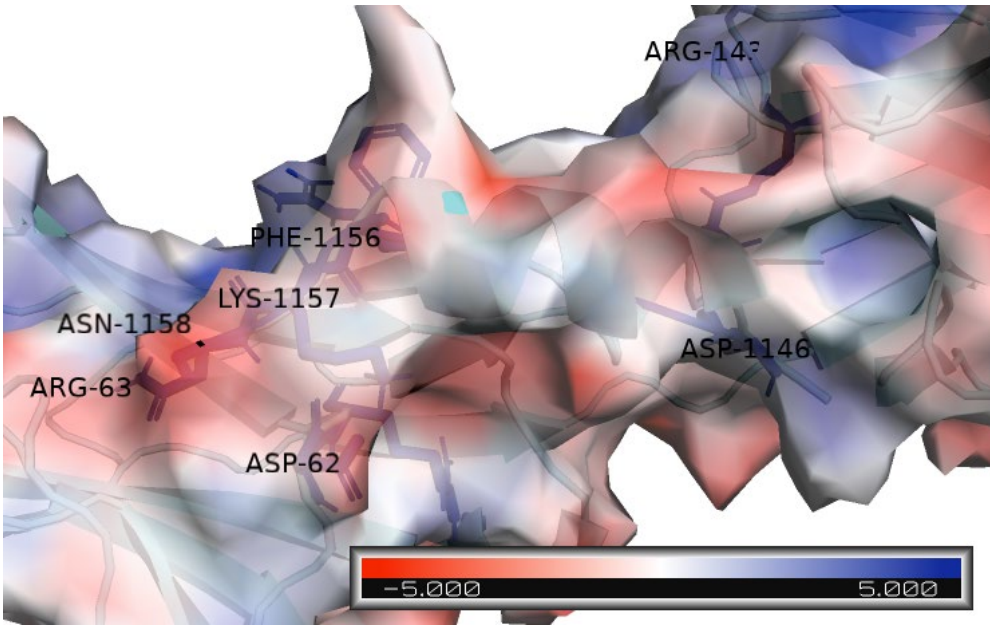

Figure III-38 CC25.36 with SARS-COV-2 stem helix SH HADDOCK electrostatic interaction calculations using the APBS-PDB2PQR software suite, visualized by PyMOL

✓ CC25.36 with SARS-COV-2 stem helix SH AutoDock Vina results:

H_Bonds: SER11 ASN1158 3.0A, 3.1A ARG17 ASP1153 2.8A THR19 ASP1153 3.2A SER67 GLU1150 3.1A SER67 LYS1149 2.3A SER74 ASP1153 2.9A

Binding site Residues: SER9 VAL10 SER11 ARG17 VAL18 THR19 SER65 GLY66 SER67 LYS68 SER69 SER74 LEU75

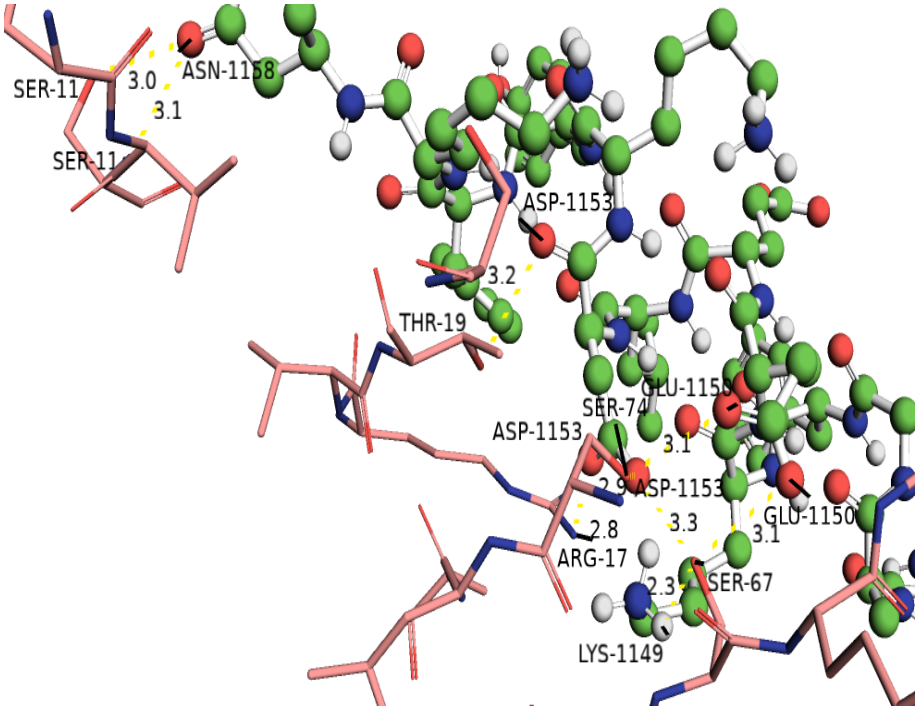

Figure III-39 CC25.36 with SARS-COV-2 stem helix SH AutoDock Vina H_Bonds visualized by PyMOL

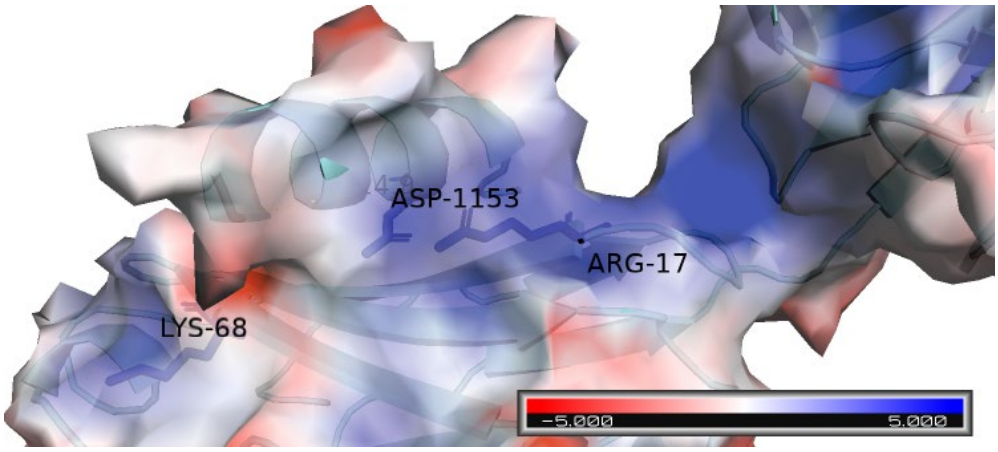

Figure III-40 CC25.36 with SARS-COV-2 stem helix SH AutoDock Vina electrostatic interaction calculations using the APBS-PDB2PQR software suite, visualized by PyMOL

IV.2. Discussion

Current research endeavors primarily focus on isolating and characterizing bnAbs from individuals previously infected with HCoVs. These efforts aim to identify and develop bnAbs capable of effectively neutralizing the virus by targeting the stem helix region, a crucial site for neutralization.

The exploration of bnAbs for coronaviruses aims to develop effective treatments by characterizing these antibodies, understanding their mechanisms of action, and evaluating their efficacy in preclinical and clinical trials.

In our referenced study, bnAbs were selected based on Zhou, P. et al.'s investigation, deriving from a collection established in Zhou's research. This assortment of β-CoV spike stem-helix bnAbs was procured using SARS-CoV-2 and MERS-CoV S proteins as bait. The approach involved isolating 40 stem-helix monoclonal antibodies (mAbs) from 10 convalescent COVID-19 donors. This targeted isolation process focused on specific single B cells responsive to the antigen. Such an approach holds substantial promise in elucidating intricate antibody-virus interactions concerning the viral stem helices.

The method's efficacy lies in its specificity, isolating antibodies finely tuned to recognize and potentially neutralize the viral stem regions. This not only broadens our understanding of viral structures but also illuminates potential therapeutic targets, offering a pathway for decoding crucial antibody-virus interactions vital in combating viral infections.

Furthermore, employing computational techniques such as HADDOCK and AutoDock Vina showcases robust methodologies for predicting and scrutinizing bnAb-virus interactions. Insights gleaned from affinity scores, RMSD values, Z-scores, and residue interactions provide substantial structural details. These insights

are instrumental in recognizing potential therapeutic targets and enhancing our comprehension of bnAb-MERS-CoV interactions.

The comprehensive analysis integrating various parameters such as HADDOCK score, affinity scores, RMSD values, Z-scores, and identification of interacting residues plays a pivotal role in prognosticating the binding efficacy of Broadly Neutralizing Antibodies (bnAbs) with the Human Coronavirus (HCoV) stem helix. This detailed assessment provides crucial insights into potential high-affinity binding locales, the precision of predicted structural conformations, the reliability of docking predictions, and the pivotal amino acid residues engaged in the interaction. Such a comprehensive approach facilitates an in-depth understanding of the binding efficacy and structural configurations of bnAbs with the HCoV stem helix. Moreover, it aids in identifying potential therapeutic targets and guides further experimental investigations.

* HADDOCK score operates in two phases:

Calculation of a weighted sum for each docking stage within the HADDOCK protocol.

New 1000 Standard settings

$$Rigid\ body\ HADDOCK\ Score = 1.0E_{vdw} + 1.0E_{elec} + 1.0E_{desolv} + 0.01E_{air} \cdot 0.01BSA$$

$$Semi - flexible\ HADDOCK\ Score = 1.0E_{vdw} + 1.0E_{elec} + 1.0E_{desolv} + 0.1E_{air} \cdot 0.01BSA$$

$$Water\ refienement\ HADDOCK\ Score = 1.0E_{vdw} + 0.1E_{elec} + 1.0E_{desolv} + 0.1E_{air} \cdot 0.0BSA$$

The sum for each stage is computed by combining the weighted energies of van der Waals, electrostatics, desolvation, and restraint violation energies specific to that stage.

New 1000 Buried settings

$$Rigid\ body\ HADDOCK\ Score = 0.0E_{vdw} + 1.0E_{elec} + 1.0E_{desolv} + 0.01E_{air} \cdot 0.01BSA$$

$$Semi - flexible\ HADDOCK\ Score = 1.0E_{vdw} + 1.0E_{elec} + 1.0E_{desolv} + 0.1E_{air} \cdot 0.01BSA$$

$$Water\ refienement\ HADDOCK\ Score = 1.0E_{vdw} + 0.1E_{elec} + 1.0E_{desolv} + 0.1E_{air} \cdot 0.0BSA$$

HADDOCK 2.2 @BonvinLab. HADDOCK2.2 manual: Analysis. http://www.bonvinlab.org/software/haddock2.2/introduction/ (accessed Feb 4, 2020).

These HADDOCK results display the following energy values for interactions between bnAbs and specific coronavirus Stem Helices:

SARS-CoV-2 Stem Helix (SH):

-164.2 +/- 1.4 CC25.106 bnAb

-79.9+/-3.0 CC95.108 bnAb

-91.1 +/- 4.7 CC99.103 bnAb

-15.0 +/-7.1 CC9.113 bnAb

MERS-CoV Stem Helix (SH):

-120.6 +/- 1.2 CC95.108 bnAb

-107.8 +/- 2.7 CC99.103 bnAb

-23.2 +/- 9.1 CC9.113 bnAb

-19.0 +/- 6.7 CC25.36 bnAb

Based on studies CC25.106, CC95.108, and CC99.103, the stem-helix bnAbs displayed comparable neutralization IC50s for SARS-CoV-

2 in two assay formats. When tested against replication-competent MERS-CoV, they exhibited higher titers (lower IC50 values) in contrast to the pseudovirus format. All three stem-helix bnAbs showed protection against severe beta-coronavirus disease, with CC25.106 demonstrating superior efficacy compared to the other two bnAbs.

In Song.G.'s research, CC25.36, part of the bnAb panel exclusively tested against the RBD, unveiled that various antibody germline solutions within group 1 bnAbs converge to identify a shared conserved RBD bnAb site. This site is exemplified by the class 4 epitope-targeting monoclonal antibody, CR3022. However, this particular study aims to explore the efficacy of CC25.36 against the stem helix of human coronavirus (HCoV).

Drawing from the prior study and considering the HADDOCK score values, it's evident that the interaction of C25.106 with the stem helix exhibits the highest potency. Additionally, when tested against MERS-CoV, this particular bnAb demonstrates more robust neutralization. The lower HADDOCK scores observed against MERS suggest a more stable interaction between the bnAb and the virus.

Furthermore, based on the HADDOCK score findings, there's a suggestion that CC9.113 holds promise as a therapeutic candidate.

* As energy values signify the energetic stability of the respective bnAb interactions with the SARS-CoV-2 and MERS-CoV Stem Helices, lower energy values typically suggest more favorable and stable interactions between the bnAbs and their target viral components.

The evaluation of affinity scores, measured in kcal/mol, serves as an indicator of the strength of interactions between bnAbs and the HCoV stem helix. Lower scores signify robust binding interactions, illuminating potential crucial sites for high-affinity binding. Conversely, higher scores may denote weaker or non-specific interactions.

The AutoDock Vina results revealed notable affinity scores for interactions between bnAbs and HCoV stem helices:

For SARS-CoV-2 Stem Helix (SH):

The best affinity score was -21.8 kcal/mol observed with CC25.106 bnAb

For MERS-CoV Stem Helix (SH):

The most favorable affinity scores were -17.2 kcal/mol with CC99.103 bnAb, -12.5 kcal/mol with CC95.108 bnAb, and -12.3 kcal/mol with CC9.113 bnAb.

Comparing these results with experimental data, CC25.106 demonstrated the most efficient neutralization of HCoV SH.

Considering CC9.113 lacks available experimental data for comparison, its affinity scores of -12.0 kcal/mol for SARS-CoV-2 Stem Helix (SH) and -12.3 kcal/mol for MERS-CoV SH, within the context of AutoDock Vina results, demonstrate promising interactions. These scores indicate a substantial binding affinity between CC9.113 and the respective stem helices of both coronaviruses.

* Root Mean Square Deviation (RMSD) measurements quantify the structural differences between predicted and experimental structures. Lower RMSD values signify a closer alignment between the docked and actual conformations, signifying accuracy in prediction. Conversely, higher RMSD values indicate potential inaccuracies in the predicted docking poses.

To assess the AutoDock Vina results, we selected the initial ligand conformation from each bnAb-Human Coronavirus Stem Helix (HCoV SH) complex with RMSD values equal to 0 for both lower and upper bounds.

In the case of HADDOCK results, we considered the best RMSD derived from the structure with the lowest overall energy:

CC25.106 with SARS-CoV-2 Stem Helix (SH): RMSD of 2.3 +/- 1.9 Å

CC99.103 with MERS-CoV Stem Helix (SH): RMSD of 2.4 +/- 1.7 Å

CC9.113 with MERS-CoV Stem Helix (SH): RMSD of 1.1 +/- 0.6 Å

CC9.113 with SARS-CoV-2 Stem Helix (SH): RMSD of 0.9 +/- 0.6 Å

Comparing these RMSD values with experimental data, CC25.106 demonstrated effectiveness in neutralizing HCoV SH. Interestingly, despite lacking available experimental data, the RMSD values indicate that CC9.113 could potentially serve as a promising therapeutic candidate.

* Z-scores, evaluating the quality and significance of docking predictions, also play a pivotal role. Lower Z-scores validate the reliability and accuracy of predictions, thereby enhancing confidence in the forecasted binding modes by aligning more closely with experimental or expected binding conformations.

The HADDOCK results exhibit Z-scores as outlined below for different bnAb interactions with SARS-CoV-2 and MERS-CoV Stem Helices:

SARS-CoV-2 Stem Helix (SH): -1.0 CC25.106, -1.3 C25.36, -1.7 CC95.108, -1.9 CC9.113, -2.8 CC99.103

MERS-CoV Stem Helix (SH): -1.4 CC9.113, -2.2 CC25.106, -2.2 CC99.103, -2.2 C25.36, -2.7 CC95.108

Lower Z-scores indicate better agreement with experimental data or expected binding conformations, providing higher confidence in the predicted binding modes. Given that CC25.106 has demonstrated experimental broad neutralization against the HCoV stem helix, a comparison of the z scores between CC9.113 and CC25.106 suggests the potential of CC9.113 as a promising therapeutic candidate.

* Identifying interacting residues on both bnAbs and the HCoV stem helix aids in confirming the reliability of predicted binding sites. Residues conserved or critical in binding interactions highlight functional regions crucial for the interaction between bnAbs and the HCoV.

Our findings, focusing on the residues engaged in hydrogen bond formation and electrostatic interactions with the epitope identified in Zhou.p.'s study, reveal a substantial presence of residues within a 5-angstrom cutoff distance for the interaction between CC9.113 and HCoV. The APBS results reveal distinct electrostatic interactions between the MERS stem helix and the CC9.113 bnAb. Notably, the MERS stem helix shows a negatively charged surface, shown in red, while it is located in close proximity to regions on the CC9.113 bnAb represented in blue. This observation indicates that there is a significant electrostatic interaction between negatively charged residues on the MERS stem helix and positively charged residues on the CC9.113 bnAb. The generative view strongly suggests that the MERS stem helix possesses a negatively charged complementary surface region. Importantly, the binding mechanism between these two proteins is mostly influenced by charge attraction, highlighting electrostatic forces as a key driving factor in their interaction. The SARS stem helix also displays blue and red regions, with a slight prevalence of negative charges. The proximity of blue and red regions in both the stem helix and bnAbs indicates that electrostatic interactions predominantly govern their binding. This observation potentially signifies a more robust and enduring interaction, suggesting that CC9.113 holds promise as a potent and stable candidate for further consideration.

In summary, while C25.106 demonstrates strong performance across multiple parameters, including neutralization and stability in interactions, CC9.113 as mAb tested for broad neutralization efficacy against H-CoV SH, exhibits promising characteristics in binding affinity, molecular interaction, and residue engagement, suggesting its potential as a potent therapeutic candidate against coronaviruses. Further experimental validation is warranted to confirm and leverage these findings

for therapeutic development. Considering that HADDOCK2.4 harness the power of CNS (Crystallography and NMR System) for structure calculation of molecular complexes., it becomes crucial to emphasize that the results obtained for broadly neutralizing antibodies (bnAbs) with predicted 3D structures require further investigation and comprehensive studies. More in-depth research is recommended to ensure the robustness and reliability of the results, and to align them more closely with the standards set by experimental techniques such as NMR and crystallography. This careful approach is essential to harness the full potential of the predicted structures and derive meaningful insights to advance this work. Given the superior efficacy of broadly neutralizing antibodies (bnAbs) targeting the receptor binding domain (RBD) compared to those directed to the stem-helix region, future research is recommended to build on these findings. A suggested course of action involves conducting in-depth studies using two distinct bnAbs specifically designed against the stem helix. This approach aims to delve into the complexities of their affinity, elucidate their precise binding properties, and comprehensively understand their potential impact. Such detailed investigations could contribute valuable insights for therapeutic development and further refine our understanding of the stem-helix region's role in antibody-mediated responses against coronaviruses.

IV.3. Limitaions:

Our study is constrained by certain limitations. Primarily, we focused solely on investigating two bnAbs against the stem helices of SARS-CoV-2 and MERS-CoV due to time constraints, limiting the breadth of our analysis. Moreover, the existing sanctions have led to a restricted availability of open-source docking programs in our region, significantly limiting our access to these essential tools for conducting research and advancing scientific investigations.

IV.4. Conclusions:

Our study aimed to explore the broad neutralization capabilities of two monoclonal antibodies CC9.113 and CC25.36 against the stem helices of SARS-CoV-2 and MERS-CoV. To achieve this, we utilized the HADDOCK2.4 Webserver and AutoDock Vina program for docking simulations and employed PyMOL for visualizing and determining the binding interfaces. Our analysis incorporated parameters such as HADDOCK score, affinity score, z score, and residues involved in the interaction interface.

Upon assessing these docking results and comparing them with the corresponding outcomes of three tested bnAbs known for their broad neutralization effects against HCoV, our findings suggest the potential of CC9.113 as a promising therapeutic agent. The comprehensive evaluation of various parameters, including molecular interactions and binding characteristics, supports the candidacy of CC9.113 for therapeutic development against coronaviruses.

For future investigations, expanding the comparison to include a broader spectrum of bnAbs would enhance the accuracy and value of our conclusions. This approach aims to leverage comprehensive comparative analyses to streamline experimental work, minimize resource investment, and reduce both time and costs associated with therapeutic development endeavors.

Extract Conclusions

The Middle East Respiratory Syndrome Coronavirus (MERS-CoV), a member of the coronavirus family akin to SARS-CoV and SARS-CoV-2, is characterized by its crown-like appearance due to spike proteins on its surface. This pathogen has garnered attention for causing severe respiratory illness, leading to outbreaks with considerable morbidity and high mortality rates reaching up to 35%. Despite its relatively low reported cases compared to other respiratory diseases, the potential for large-scale outbreaks remains a global concern due to its substantial fatality rate.

Primarily transmitted through zoonotic origins, with dromedary camels serving as the primary reservoir, human infections often arise from direct or indirect contact with infected camels or through person-to-person transmission, especially within healthcare settings.

The significance of MERS-CoV lies in its pathogenicity, the potential for outbreaks, zoonotic origins, and the limited treatment options available. Addressing the threat posed by MERS-CoV necessitates effective therapeutic interventions, making the exploration of treatments like Broadly Neutralizing Antibodies (bnAbs) a crucial area of study in combatting this and similar coronaviruses.

In the pursuit of effective treatments for MERS-CoV, a diverse array of agents has been evaluated. Among these candidates, bnAbs have emerged as highly promising therapeutic options due to their capacity to effectively target and neutralize various strains or variants of a specific virus, making them invaluable in combating viral infections like MERS and other coronaviruses.

BnAbs possess the unique ability to recognize conserved epitopes, such as the Stem Helix peptide, on viral antigens. This exceptional trait enables them to neutralize

different strains or subtypes of Human Coronaviruses (HCoVs), rendering bnAbs potent candidates for therapeutic agents against MERS-CoV.

The investigation delineates a comprehensive analysis of monoclonal antibodies' (bnAbs) efficacy against severe acute respiratory syndrome coronavirus 2 (SARS-CoV-2) and Middle East respiratory syndrome coronavirus (MERS-CoV). Our exploration incorporates computational methodologies, specifically molecular docking, as an expedient approach to elucidate antibody-antigen complex structures. The study centers on five distinct bnAbs and their interactions with the stem helices of SARS-CoV-2 and MERS-CoV employing HADDOCK and AutoDock Vina.

The findings highlight the comparability in neutralization effectiveness of stem-helix bnAbs for SARS-CoV-2 in two assay formats. Notably, these bnAbs demonstrated heightened titers against replication-competent MERS-CoV compared to the pseudo-virus format. Of particular significance is CC25.106, displaying superior efficacy among the three stem-helix bnAbs in safeguarding against severe beta-coronavirus disease. Additionally, CC25.36's and cc9.113 assessment against the stem helix of human coronaviruses (HCoV) aims to shed light on their therapeutic potential.

Molecular docking analysis, facilitated by HADDOCK and AutoDock Vina, enriched our understanding of bnAb-MERS-CoV interactions through metrics such as affinity scores, RMSD values, Z-scores, and residue interactions. While CC25.106 exhibits robust performance across multiple parameters, CC9.113 emerges as a compelling therapeutic candidate due to its promising characteristics in binding affinity, molecular interaction, and residue engagement against coronaviruses, especially H-CoV SH.

However, the study has limitations, primarily stemming from a narrowed focus on only two bnAbs against SARS-CoV-2 and MERS-CoV due to time constraints. Furthermore, limited access to open-source docking programs due to existing sanctions constrained the breadth of the analysis.

In summary, our study highlights CC9.113 as a promising therapeutic solution against coronaviruses, leveraging a thorough assessment of molecular interactions and binding traits. Using bioinformatics tools aligned with a reference study, our results and models serve as a foundational resource, offering insights into interactions among various human respiratory viruses. To fortify these findings, future research should broaden the comparison to encompass a broader spectrum of bnAbs. This expansion aims to strengthen the depth and credibility of conclusions, ultimately facilitating more efficient therapeutic development endeavors.

References

[1]. Li, Y. H., Hu, C. Y., Wu, N. P., Yao, H. P., & Li, L. J. (2019). Molecular Characteristics, Functions, and Related Pathogenicity of MERS-CoV Proteins. *Engineering (Beijing, China)*, *5*(5), 940–947. https://doi.org/10.1016/j.eng.2018.11.035

[2]. Gulfaraz Khan, Mohamud Sheek-Hussein, Chapter 8 - The Middle East Respiratory Syndrome Coronavirus: An Emerging Virus of Global Threat, Editor(s): Moulay Mustapha Ennaji, Emerging and Reemerging Viral Pathogens, Academic Press, 2020, Pages 151-167, https://doi.org/10.1016/B978-0-12-819400-3.00008-9.

[3]. Yassine Kasmi, Khadija Khataby, Amal Souiri, Moulay Mustapha Ennaji, Chapter 7 - Coronaviridae: 100,000 Years of Emergence and Reemergence, Editor(s): Moulay Mustapha Ennaji, Emerging and Reemerging Viral Pathogens, Academic Press, 2020, Pages 127-149, https://doi.org/10.1016/B978-0-12-819400-3.00007-7.

[4]. Shuai Xia et al., A pan-coronavirus fusion inhibitor targeting the HR1 domain of human coronavirus spike. Sci. Adv.5, eaav4580 (2019). https://doi.org/10.1126/sciadv.aav4580

[5]. Deshpande, A., Schormann, N., Piepenbrink, M.S., Martinez Sobrido, L., Kobie, J.J. and Walter, M.R. (2023), Structure and epitope of a neutralizing monoclonal antibody that targets the stem helix of β coronaviruses. FEBS J, 290: 3422-3435. https://doi.org/10.1111/febs.16777

[6]. Yu, X., Zhang, S., Jiang, L., Cui, Y., Li, D., Wang, D., Wang, N., Fu, L., Shi, X., Li, Z., Zhang, L., & Wang, X. (2015). Structural basis for the

neutralization of MERS-CoV by a human monoclonal antibody MERS-27. Scientific reports,5, 13133. https://doi.org/10.1038/srep13133

[7]. Li, F., & Du, L. (2019). MERS Coronavirus: An Emerging Zoonotic Virus. Viruses,11(7), 663. https://doi.org/10.3390/v11070663

[8]. Tang Mingxing, Zhang Xin, Huang Yanhong, Cheng Wenxiang, Qu Jing, Gui Shuiqing, Li Liang, Li Shuo. (2023). Peptide-based inhibitors hold great promise as the broad-spectrum agents against coronavirus, Frontiers in Microbiology, V=13. https://doi.org/10.3389/fmicb.2022.1093646

[9]. Wang, X., Sun, L., Liu, Z., Xing, L., Zhu, Y., Xu, W., Xia, S., Lu, L., & Jiang, S. (2023). An engineered recombinant protein containing three structural domains in SARS-CoV-2 S2 protein has potential to act as a pan-human coronavirus entry inhibitor or vaccine antigen. Emerging microbes & infections, 12(2), 2244084. https://doi.org/10.1080/22221751.2023.2244084

[10]. Khalafalla Abdelmalik Ibrahim. (2023). Zoonotic diseases transmitted from the camels. Frontiers in Microbiology, V=10. https://doi.org/10.3389/fvets.2023.1244833

[11]. Widagdo, W., Sooksawasdi Na Ayudhya, S., Hundie, G. B., & Haagmans, B. L. (2019). Host Determinants of MERS-CoV Transmission and Pathogenesis. Viruses, 11(3), 280. https://doi.org/10.3390/v11030280

[12]. World Health Organization (29 August 2023). Disease Outbreak News; Middle East respiratory syndrome coronavirus (MERS-CoV) – Saudi Arabia. Available at: https://www.who.int/emergencies/disease-outbreak-news/item/2023-DON484

[13]. Conzade, R., Grant, R., Malik, M. R., Elkholy, A., Elhakim, M., Samhouri, D., Ben Embarek, P. K., & Van Kerkhove, M. D. (2018). Reported Direct and

Indirect Contact with Dromedary Camels among Laboratory-Confirmed MERS-CoV Cases. Viruses, 10(8), 425. https://doi.org/10.3390/v10080425

[14]. Khalafalla, A. I., Lu, X., Al-Mubarak, A. I., Dalab, A. H., Al-Busadah, K. A., & Erdman, D. D. (2015). MERS-CoV in Upper Respiratory Tract and Lungs of Dromedary Camels, Saudi Arabia, 2013-2014. Emerging infectious diseases, 21(7), 1153–1158. https://doi.org/10.3201/eid2107.150070

[15]. https://www.who.int/news-room/fact-sheets/detail/middle-east-respiratory-syndrome-coronavirus-(mers-cov)

[16]. Hui, D. S., Azhar, E. I., Kim, Y. J., Memish, Z. A., Oh, M. D., & Zumla, A. (2018). Middle East respiratory syndrome coronavirus: risk factors and determinants of primary, household, and nosocomial transmission. The Lancet. Infectious diseases, 18(8), e217–e227. https://doi.org/10.1016/S1473-3099(18)30127-0

[17]. Xiao, S., Li, Y., Sung, M., Wei, J., & Yang, Z. (2018). A study of the probable transmission routes of MERS-CoV during the first hospital outbreak in the Republic of Korea. Indoor air, 28(1), 51–63. https://doi.org/10.1111/ina.12430

[18]. Zeidler A, Karpinski T M. SARS-CoV, MERS-CoV, SARS-CoV-2 Comparison of Three Emerging Coronaviruses. Jundishapur J Microbiol. 2020;13(6):e103744. https://doi.org/10.5812/jjm.103744.

[19]. Zumla, A., Chan, J. F., Azhar, E. I., Hui, D. S., & Yuen, K. Y. (2016). Coronaviruses - drug discovery and therapeutic options. Nature reviews. Drug discovery, 15(5), 327–347. https://doi.org/10.1038/nrd.2015.37

[20]. Sabeena Mustafa, Hanan Balkhy, Musa N. Gabere, Current treatment options and the role of peptides as potential therapeutic components for Middle East Respiratory Syndrome (MERS): A review, Journal of Infection and Public

Health, Volume 11, Issue 1, 2018, Pages 9-17, ISSN 1876-0341, https://doi.org/10.1016/j.jiph.2017.08.009.

[21]. Xia, S., Yan, L., Xu, W., Agrawal, A. S., Algaissi, A., Tseng, C. K., Wang, Q., Du, L., Tan, W., Wilson, I. A., Jiang, S., Yang, B., & Lu, L. (2019). A pan-coronavirus fusion inhibitor targeting the HR1 domain of human coronavirus spike. Science advances, 5(4), eaav4580. https://doi.org/10.1126/sciadv.aav4580

[22]. Tiffany Tang, Miya Bidon, Javier A. Jaimes, Gary R. Whittaker, Susan Daniel, Coronavirus membrane fusion mechanism offers a potential target for antiviral development, Antiviral Research, Volume 178, (2020), 104792, ISSN 0166-3542, https://doi.org/10.1016/j.antiviral.2020.104792.

[23]. Jurrus E, Engel D, Star K, Monson K, Brandi J, Felberg LE, Brookes DH, Wilson L, Chen J, Liles K, Chun M, Li P, Gohara DW, Dolinsky T, Konecny R, Koes DR, Nielsen JE, Head-Gordon T, Geng W, Krasny R, Wei GW, Holst MJ, McCammon JA, Baker NA. Improvements to the APBS biomolecular solvation software suite. Protein Sci. 2018 Jan;27(1):112-128. doi: 10.1002/pro.3280. Epub 2017 Oct 24. PMID: 28836357; PMCID: PMC5734301.

[24]. Mou, H., Raj, V. S., van Kuppeveld, F. J., Rottier, P. J., Haagmans, B. L., & Bosch, B. J. (2013). The receptor binding domain of the new Middle East respiratory syndrome coronavirus maps to a 231-residue region in the spike protein that efficiently elicits neutralizing antibodies. Journal of virology, 87(16), 9379–9383. https://doi.org/10.1128/JVI.01277-13

[25]. Naru Zhang, Jian Shang, Chaoqun Li, Kehui Zhou & Lanying Du (2020) An overview of Middle East respiratory syndrome coronavirus vaccines in preclinical

studies, Expert Review of Vaccines, 19:9, 817-829, DOI: 10.1080/14760584.2020.1813574

[26]. Du, L., Kou, Z., Ma, C., Tao, X., Wang, L., Zhao, G., Chen, Y., Yu, F., Tseng, C. T., Zhou, Y., & Jiang, S. (2013). A truncated receptor-binding domain of MERS-CoV spike protein potently inhibits MERS-CoV infection and induces strong neutralizing antibody responses: implication for developing therapeutics and vaccines. PloS one, 8(12), e81587. https://doi.org/10.1371/journal.pone.0081587

[27]. Lu, G., Hu, Y., Wang, Q., Qi, J., Gao, F., Li, Y., Zhang, Y., Zhang, W., Yuan, Y., Bao, J., Zhang, B., Shi, Y., Yan, J., & Gao, G. F. (2013). Molecular basis of binding between novel human coronavirus MERS-CoV and its receptor CD26. Nature, 500(7461), 227–231. https://doi.org/10.1038/nature12328

[28]. Guo, L., Lin, S., Chen, Z. et al. Targetable elements in SARS-CoV-2 S2 subunit for the design of pan-coronavirus fusion inhibitors and vaccines. Sig Transduct Target Ther 8, 197 (2023). https://doi.org/10.1038/s41392-023-01472-x

[29]. Cai, Y., Zhang, J., Xiao, T., Peng, H., Sterling, S. M., Walsh, R. M., Jr, Rawson, S., Rits-Volloch, S., & Chen, B. (2020). Distinct conformational states of SARS-CoV-2 spike protein. Science (New York, N.Y.), 369(6511), 1586–1592. https://doi.org/10.1126/science.abd4251

[30]. Yuan, Y., Cao, D., Zhang, Y. et al. Cryo-EM structures of MERS-CoV and SARS-CoV spike glycoproteins reveal the dynamic receptor binding domains. Nat Commun 8, 15092 (2017). https://doi.org/10.1038/ncomms15092

[31]. Wang, N., Shi, X., Jiang, L., Zhang, S., Wang, D., Tong, P., Guo, D., Fu, L., Cui, Y., Liu, X., Arledge, K. C., Chen, Y. H., Zhang, L., & Wang, X. (2013).

Structure of MERS-CoV spike receptor-binding domain complexed with human receptor DPP4. Cell research, 23(8), 986–993. https://doi.org/10.1038/cr.2013.92

[32]. Piepenbrink, M. S., Park, J. G., Deshpande, A., Loos, A., Ye, C., Basu, M., Sarkar, S., Khalil, A. M., Chauvin, D., Woo, J., Lovalenti, P., Erdmann, N. B., Goepfert, P. A., Truong, V. L., Bowen, R. A., Walter, M. R., Martinez-Sobrido, L., & Kobie, J. J. (2022). Potent universal beta-coronavirus therapeutic activity mediated by direct respiratory administration of a Spike S2 domain-specific human neutralizing monoclonal antibody. PLoS pathogens, 18(7), e1010691. https://doi.org/10.1371/journal.ppat.1010691

[33]. A. Bleibtreu, M. Bertine, C. Bertin, N. Houhou-Fidouh, B. Visseaux, (2020), Focus on Middle East respiratory syndrome coronavirus (MERS-CoV), Médecine et Maladies Infectieuses, Volume 50, Issue 3, Pages 243-251, ISSN 0399-077X, https://doi.org/10.1016/j.medmal.2019.10.004.

[34]. Al-Tawfiq, J. A., Hinedi, K., Ghandour, J., Khairalla, H., Musleh, S., Ujayli, A., & Memish, Z. A. (2014). Middle East respiratory syndrome coronavirus: a case-control study of hospitalized patients. Clinical infectious diseases: an official publication of the Infectious Diseases Society of America, 59(2), 160–165. https://doi.org/10.1093/cid/ciu226

[35]. Wang, Q., Wong, G., Lu, G., Yan, J., & Gao, G. F. (2016). MERS-CoV spike protein: Targets for vaccines and therapeutics. Antiviral research, 133, 165–177. https://doi.org/10.1016/j.antiviral.2016.07.015

[36]. Arabi, Y. M., Arifi, A. A., Balkhy, H. H., Najm, H., Aldawood, A. S., Ghabashi, A., Hawa, H., Alothman, A., Khaldi, A., & Al Raiy, B. (2014). Clinical course and outcomes of critically ill patients with Middle East

respiratory syndrome coronavirus infection. Annals of internal medicine, 160(6), 389–397. https://doi.org/10.7326/M13-2486

[37]. https://doi.org/10.1016/j.xcrm.2022.100893

[38]. Hu, Y., Li, W., Gao, T., Cui, Y., Jin, Y., Li, P., Ma, Q., Liu, X., & Cao, C. (2017). The Severe Acute Respiratory Syndrome Coronavirus Nucleocapsid Inhibits Type I Interferon Production by Interfering with TRIM25-Mediated RIG-I Ubiquitination. Journal of virology, 91(8), e02143-16. https://doi.org/10.1128/JVI.02143-16

[39]. Mubarak, A., Alturaiki, W., & Hemida, M. G. (2019). Middle East Respiratory Syndrome Coronavirus (MERS-CoV): Infection, Immunological Response, and Vaccine Development. Journal of immunology research, 2019, 6491738. https://doi.org/10.1155/2019/6491738

[40]. Marshall, J.S., Warrington, R., Watson, W. et al. An introduction to immunology and immunopathology. Allergy Asthma Clin Immunol 14 (Suppl 2), 49 (2018). https://doi.org/10.1186/s13223-018-0278-1

[41].Nimmerjahn, F., Vidarsson, G. & Cragg, M.S. Effect of posttranslational modifications and subclass on IgG activity: from immunity to immunotherapy. Nat Immunol 24, 1244–1255 (2023). https://doi.org/10.1038/s41590-023-01544-8

[42]. Wang, N., Rosen, O., Wang, L., Turner, H. L., Stevens, L. J., Corbett, K. S., Bowman, C. A., Pallesen, J., Shi, W., Zhang, Y., Leung, K., Kirchdoerfer, R. N., Becker, M. M., Denison, M. R., Chappell, J. D., Ward, A. B., Graham, B. S., & McLellan, J. S. (2019). Structural Definition of a Neutralization-Sensitive

Epitope on the MERS-CoV S1-NTD. Cell reports, 28(13), 3395–3405.e6. https://doi.org/10.1016/j.celrep.2019.08.052

[43]. Panpan Zhou, Ge Song, Hejun Liu, Meng Yuan, Wan-ting He, Nathan Beutler, Xueyong Zhu, Longping V. Tse, David R. Martinez, Alexandra Schäfer, Fabio Anzanello, Peter Yong, Linghang Peng, Katharina Dueker, Rami Musharrafieh, Sean Callaghan, Tazio Capozzola, Oliver Limbo, Mara Parren, Elijah Garcia, Stephen A. Rawlings, Davey M. Smith, David Nemazee, Joseph G. Jardine, Yana Safonova, Bryan Briney, Thomas F. Rogers, Ian A. Wilson, Ralph S. Baric, Lisa E. Gralinski, Dennis R. Burton, Raiees Andrabi, Broadly neutralizing anti-S2 antibodies protect against all three human betacoronaviruses that cause deadly disease, Immunity, Volume 56, Issue 3, 2023, Pages 669-686.e7, ISSN 1074-7613, https://doi.org/10.1016/j.immuni.2023.02.005.

[44]. Keitany, G. J., Rubin, B. E. R., Garrett, M. E., Musa, A., Tracy, J., Liang, Y., Ebert, P., Moore, A. J., Guan, J., Eggers, E., Lescano, N., Brown, R., Carbo, A., Al-Asadi, H., Ching, T., Day, A., Harris, R., Linkem, C., Popov, D., Wilkins, C., Gilbert, A. E. (2023). Multimodal, broadly neutralizing antibodies against SARS-CoV-2 identified by high-throughput native pairing of BCRs from bulk B cells. Cell chemical biology, 30(11), 1377–1389.e8. https://doi.org/10.1016/j.chembiol.2023.07.011

[45]. He, Wt., Musharrafieh, R., Song, G. et al. Targeted isolation of diverse human protective broadly neutralizing antibodies against SARS-like viruses. Nat Immunol 23, 960–970 (2022). https://doi.org/10.1038/s41590-022-01222-1

[46]. Zhang, S., Zhou, P., Wang, P., Li, Y., Jiang, L., Jia, W., Wang, H., Fan, A., Wang, D., Shi, X., Fang, X., Hammel, M., Wang, S., Wang, X., & Zhang, L.

(2018). Structural Definition of a Unique Neutralization Epitope on the Receptor-Binding Domain of MERS-CoV Spike Glycoprotein. Cell reports, 24(2), 441–452. https://doi.org/10.1016/j.celrep.2018.06.041

[47]. Jiang, L., Wang, N., Zuo, T., Shi, X., Poon, K. M., Wu, Y., Gao, F., Li, D., Wang, R., Guo, J., Fu, L., Yuen, K. Y., Zheng, B. J., Wang, X., & Zhang, L. (2014). Potent neutralization of MERS-CoV by human neutralizing monoclonal antibodies to the viral spike glycoprotein. Science translational medicine, 6(234), 234ra59. https://doi.org/10.1126/scitranslmed.3008140

[48]. Roy, A. N., Gupta, A. M., Banerjee, D., Chakrabarti, J., & Raghavendra, P. B. (2023). Unraveling DPP4 Receptor Interactions with SARS-CoV-2 Variants and MERS-CoV: Insights into Pulmonary Disorders via Immunoinformatics and Molecular Dynamics. Viruses, 15(10), 2056. https://doi.org/10.3390/v15102056

[49]. Joshi, A., Akhtar, N., Sharma, N. R., Kaushik, V., & Borkotoky, S. (2023). MERS virus spike protein HTL-epitopes selection and multi-epitope vaccine design using computational biology. Journal of biomolecular structure & dynamics, 41(22), 12464–12479. https://doi.org/10.1080/07391102.2023.2191137

[50]. Corti, D., Purcell, L. A., Snell, G., & Veesler, D. (2021). Tackling COVID-19 with neutralizing monoclonal antibodies. Cell, 184(12), 3086–3108. https://doi.org/10.1016/j.cell.2021.05.005

[51]. Glassman, P. M., & Balthasar, J. P. (2019). Physiologically-based modeling of monoclonal antibody pharmacokinetics in drug discovery and development. Drug metabolism and pharmacokinetics, 34(1), 3–13. https://doi.org/10.1016/j.dmpk.2018.11.002

[52]. Ambrosetti, F., Jiménez-García, B., Roel-Touris, J., & Bonvin, A. M. J. J. (2020). Modeling Antibody-Antigen Complexes by Information-Driven Docking. Structure (London, England : 1993), 28(1), 119–129.e2. https://doi.org/10.1016/j.str.2019.10.011

[53]. Guest, J. D., Vreven, T., Zhou, J., Moal, I., Jeliazkov, J. R., Gray, J. J., Weng, Z., & Pierce, B. G. (2021). An expanded benchmark for antibody-antigen docking and affinity prediction reveals insights into antibody recognition determinants. Structure (London, England : 1993), 29(6), 606–621.e5. https://doi.org/10.1016/j.str.2021.01.005

[54]. Ko, H. L., Lee, D. K., Kim, Y., Jang, H. J., Lee, Y. W., Lee, H. Y., Seok, S. H., Park, J. W., Limb, J. K., On, D. I., Yun, J. W., Lyoo, K. S., Song, D., Yeom, M., Lee, H., Seong, J. K., & Lee, S. (2023). Development of a neutralization monoclonal antibody with a broad neutralizing effect against SARS-CoV-2 variants. Virology journal, 20(1), 285. https://doi.org/10.1186/s12985-023-02230-9

[55]. Meng, X. Y., Zhang, H. X., Mezei, M., & Cui, M. (2011). Molecular docking: a powerful approach for structure-based drug discovery. Current computer-aided drug design, 7(2), 146–157. https://doi.org/10.2174/157340911795677602

[56]. Durai, P., Batool, M., Shah, M. et al. Middle East respiratory syndrome coronavirus: transmission, virology and therapeutic targeting to aid in outbreak control. Exp Mol Med 47, e181 (2015). https://doi.org/10.1038/emm.2015.76

[57]. Alnuqaydan, A.M., Almutary, A.G., Sukamaran, A. et al. Middle East Respiratory Syndrome (MERS) Virus—Pathophysiological Axis and the

Current Treatment Strategies. AAPS PharmSciTech 22, 173 (2021). https://doi.org/10.1208/s12249-021-02062-2

[58]. A. Bleibtreu, M. Bertine, C. Bertin, N. Houhou-Fidouh, B. Visseaux, Focus on Middle East respiratory syndrome coronavirus (MERS-CoV), Médecine et Maladies Infectieuses, Volume 50, Issue 3, 2020, Pages 243-251, ISSN 0399-077X, https://doi.org/10.1016/j.medmal.2019.10.004.

[59]. Mubarak, A., Alturaiki, W., & Hemida, M.G. (2019). Middle East Respiratory Syndrome Coronavirus (MERS-CoV): Infection, Immunological Response, and Vaccine Development. *Journal of Immunology Research, 2019*.

[60]. Mubarak, A., Alturaiki, W., & Hemida, M.G. (2019). Middle East Respiratory Syndrome Coronavirus (MERS-CoV): Infection, Immunological Response, and Vaccine Development. *Journal of Immunology Research, 2019*.

[61]. Rabaan, A.A., Al-Ahmed, S.H., Sah, R. et al. MERS-CoV: epidemiology, molecular dynamics, therapeutics, and future challenges. Ann Clin Microbiol Antimicrob 20, 8 (2021). https://doi.org/10.1186/s12941-020-00414-7

[62]. Tianlei Ying, Haoyang Li, Lu Lu, Dimiter S. Dimitrov, Shibo Jiang, Development of human neutralizing monoclonal antibodies for prevention and therapy of MERS-CoV infections, Microbes and Infection, Volume 17, Issue 2, 2015, Pages 142-148, ISSN 1286-4579, https://doi.org/10.1016/j.micinf.2014.11.008.

[63]. Xu, J., Jia, W., Wang, P., Zhang, S., Shi, X., Wang, X., & Zhang, L. (2019). Antibodies and vaccines against Middle East respiratory syndrome coronavirus. Emerging microbes & infections, 8(1), 841–856. https://doi.org/10.1080/22221751.2019.1624482

[64]. Cherrelle Dacon, Linghang Peng, Ting-Hui Lin, Courtney Tucker, Chang-Chun D. Lee, Yu Cong, Lingshu Wang, Lauren Purser, Andrew J.R. Cooper, Jazmean K. Williams, Chul-Woo Pyo, Meng Yuan, Ivan Kosik, Zhe Hu, Ming Zhao, Divya Mohan, Mary Peterson, Jeff Skinner, Saurabh Dixit, Erin Kollins, Louis Huzella, Donna Perry, Russell Byrum, Sanae Lembirik, Michael Murphy, Yi Zhang, Eun Sung Yang, Man Chen, Kwanyee Leung, Rona S. Weinberg, Amarendra Pegu, Daniel E. Geraghty, Edgar Davidson, Benjamin J. Doranz, Iyadh Douagi, Susan Moir, Jonathan W. Yewdell, Connie Schmaljohn, Peter D. Crompton, John R. Mascola, Michael R. Holbrook, David Nemazee, Ian A. Wilson, Joshua Tan, Rare, convergent antibodies targeting the stem helix broadly neutralize diverse betacoronaviruses, Cell Host & Microbe, Volume 31, Issue 1, 2023, Pages 97-111.e12, ISSN 1931-3128, https://doi.org/10.1016/j.chom.2022.10.010.

[65]. Zhao, J.; Nussinov, R.; Wu, W.-J.; Ma, B. In Silico Methods in Antibody Design. *Antibodies* 2018, *7*, 22. https://doi.org/10.3390/antib7030022

[66]. https://wenmr.science.uu.nl/haddock2.4/#:~:text=HADDOCK%20(High%20Ambiguity%20Driven%20protein,the%20modeling%20of%20biomolecular%20complexes

[67]. https://www.technologyreview.com/2020/11/30/1012712/deepmind-protein-folding-ai-solved-biology-science-drugs-disease/

[68]. https://pymol.org/2/

[69]. Francesco Ambrosetti, Tobias Hegelund Olsen, Pier Paolo Olimpieri, Brian Jiménez-García, Edoardo Milanetti, Paolo Marcatilli, Alexandre M J J Bonvin, proABC-2: PRediction of AntiBody contacts v2 and its application to

information-driven docking, *Bioinformatics*, Volume 36, Issue 20, October 2020, Pages 5107–5108, https://doi.org/10.1093/bioinformatics/btaa644

[70]. Honorato Rodrigo V., Koukos Panagiotis I., Jiménez-García Brian, Tsaregorodtsev Andrei, Verlato Marco, Giachetti Andrea, Rosato Antonio, Bonvin Alexandre M. J. J., Structural Biology in the Clouds: The WeNMR-EOSC Ecosystem, (2021), Frontiers in Molecular Biosciences, VOLUME=8, https://www.frontiersin.org/articles/10.3389/fmolb.2021.729513, DOI=10.3389/fmolb.2021.729513